RESISTIVITY METHODS WITH APPLICATION TO PLANILLAS GEOTHERMAL FIELD, MEXICO

Pablo Reyes Vermot

UNU Geothermal Training Programme
Reykjavík, Iceland
Report 9, 1989

Report 9, 1989

RESISTIVITY METHODS WITH APPLICATION TO PLANILLAS GEOTHERMAL FIELD, MEXICO

Pablo Reyes Vermot
UNU Geothermal Training Programme
National Energy Authority
Grensásvegur 9
108 Reykkjavík
ICELAND

Permanent Adress:
Comision Federal de Electricidad
Superintendencia General La Primavera
Km. 21+460 Periferico Norte Cd. Granja
Zapopan, Jalisco
MEXICO

ABSTRACT

The depth of penetration of Schlumberger soundings is controlled by the shortest distance between the current electrode and the potential electrode (S-P). This together with the application of the finite potential electrodes separation over a resistivity distribution with high contrasts between layers and lateral resistivity variations near the surface at the sounding site, causes converging and constant shifts of the different segments of the apparent resistivity curve. These shifts, if not correctly treated, will lead the interpretation astray. Therefore the theory of one-dimensional interpretation of Schlumberger soundings is presented in this report in some details in order to understand the reasons for these shifts and to make an appropriate use of two computer programs for one-dimensional interpretation. A two-dimensional interpretation program, which takes the topography into account, is also discussed.

Schlumberger soundings from Planillas Geothermal Field, Mexico were interpreted one- and two-dimensionally. This resulted in the delineation of a low resistivity anomaly (resistivity less than 40 Ωm). At 1.500 m a.s.l. the anomaly presents a NW-SE trend. It continues at greater depths (1.000 m a.s.l.) with the same NW-SE trend together with a mixed N-S trend having lower resistivity values (less than 20 Ωm).

The geothermal fluids associated with Primavera Geothermal Area are stored in extensional strike slip faults with NW-SE orientation, within the lower Cordilleran volcanics (andesites), reactivated and opened by a vertical stress field. Primavera Geothermal Area is located 7 km north of Planillas Geothermal Field. The same geological formations, i.e. lower Cordilleran volcanics are located beneath Planillas Geothermal Field. Two-dimensional interpretation of a profile perpendicular to the low resistivity anomaly is characterized by a less than 15 Ωm anomaly, 3.5 km wide in the southwestern slopes of Cerros Las Planillas, flanked by two relatively resistive structures, reaching towards the surface. At the NE flank there are steam vents and near the SW flank hot springs are found, at a relatively low elevation. Inside this main anomaly there is a narrower anomaly, 1.2 km wide having a resistivity of 7 Ωm. This suggests a possible vertical flow of geothermal fluids in the middle of the low resistivity anomaly probably convecting along an open fault oriented NW-SE within the lower Cordilleran volcanics and leaking laterally SW and NE into the upper Cordilleran volcanics (lithic tuffs).

TABLE OF CONTENTS

LIST OF FIGURES

LIST OF TABLES

1. INTRODUCTION

This report is a result of six months work under the United Nations University Geothermal Training Programme at Orkustofnun (National Energy Authority, NEA) in Iceland.

At the beginning of the training programme the author attended seminars and lectures on geology, general explorational geophysics, borehole geophysics, geochemistry, groundwater hydrology, reservoir engineering, drilling, wastes disposal and low/high geothermal utilization.

As a specialized field the author received training in the advanced techniques of one- and two-dimensional computer aided interpretation of Schlumberger resistivity soundings utilizing Orkustofnun's computer facilities, both PC-computer and a Hewlett Packard-9000/840 mainframe running under UNIX operating system.

As an integral part of the author's training, Schlumberger resistivity soundings from Planillas Geothermal Field in Mexico, previously collected with the author's participation, were interpreted using one-and two-dimensional models.

With the aim of placing the Schlumberger method among other resistivity methods, chapter 2 gives a brief description of the resistivity methods most commonly used in geothermal exploration i.e. Head-on, Magnetotellurics and the more recently developed Transient Electromagnetics.

In order to understand the mathematical algorithms utilized in the computer programs, the theory of one-dimensional interpretation over a horizontally stratified earth is presented in chapter 3. From the divergence theorem and the solution of Laplace equation, the Stefanescu's integral is established. The integral is solved with the help of the linear filter method using two different methods. The depth of penetration in Schlumberger soundings is also discussed in order to understand the shifting presented in soundings carried out over high resistivity vertical contrast using a finite potential electrode separation.

Chapter 4 gives a description of the computer programs SLINV, ELLIPSE and FELIX. The first one is a one-dimensional interpretation program, assuming that the distance between the potential electrodes is much smaller than the distance between the current electrodes (gradient approach). ELLIPSE is a one-dimensional interpretation program too, but it simulates the actual electrode position. Both SLINV and ELLIPSE are automatic inversion programs. The third one is a two-dimensional finite element interpretation program, where the resistivity besides from changing vertically, also can change in one horizontal direction. The topography is also modeled in FELIX. SLINV is run on a PC-computer, but ELLIPSE and FELIX on the Hewlett Packard mainframe.

Finally, chapter 5 describes the results of the interpretation of Schlumberger resistivity soundings from Planillas Geothermal Field applying and comparing all three computer programs. Based on the results from the Schlumberger soundings, a conceptual model for the geothermal field is put forward.

2. RESISTIVITY METHODS

2.1 Introduction

Among all geophysical methods, resistivity methods are the only one's where the measured parameter, i.e. **RESISTIVITY** has a direct relationship with the physical properties of a geothermal reservoir such as **TEMPERATURE, EFFECTIVE POROSITY** and **WATER CONTENT**. It is therefore easy to understand the importance of resistivity methods in geothermal exploration (see e.g. Hersir, 1989).

In chapter 2.2 a definition of the resistivity is presented together with its relation to the important physical properties mentioned above. Chapter 2.3 discusses the application of Direct Current methods (DC-methods) and how different DC-methods can be used for different purposes.

In chapter 2.4 two Alternate Current methods (AC-methods) are discussed with a practical approach of the basic principles involved. These methods and their application is compared with the DC-methods.

2.2 Resistivity

It is well known that the electrical resistance R of a body against the current flow, is directly proportional to it's length L and inversely proportional to it's cross sectional area A. This can be expressed as:

$$R \propto \frac{L}{A} \tag{2.1}$$

where:

R : Electrical resistance [Ω]

L : Longitudinal dimension of the body [m]

A : Area perpendicular to the current flow [m^2]

Electrical resistivity, ρ, can be defined as the electrical resistance of a cylinder of unit length [1 m] and unit cross sectional area [1 m^2].

$$\rho = R \frac{A}{L} \tag{2.2}$$

The electrical resistivity, ρ, is measured in [Ωm].

The rocks found in nature present a bulk resistivity ρ, which is a rather complex one, being a function of several variables. These variables are related to the rock composition itself. Archie's law is often used to relate the porosity and the resistivity of the water saturating in the rock. This relation (Archie, 1942) has the following form for a completely saturated sample:

$$F = \frac{\rho}{\rho_w} = a \cdot \phi^{-m} \tag{2.3}$$

where:

F : Formation factor

ρ : Bulk resistivity [Ωm]

ρ_w : Resistivity of the pore fluid [Ωm]

ϕ : Porosity

a : An empirical parameter, varies from less than 1 for intergranular porosity to over 1 for joint porosity, usually around 1

m : Cementing factor, an empirical parameter, varies from 1.2 for unconsolidated sediments to 3.5 for crystalline rocks, usually around 2

Equation (2.3) only applies when the fluid conduction dominates the interface conduction (Flóvenz et al., 1985). Archie's equation is valid if the resistivity of the pore fluid is 2 Ωm or less, but doubts are raised if the resistivity is higher (Flóvenz et al., 1985).

Resistivity depends also on temperature. Equation (2.4) relates the pore fluid resistivity to temperatures of up to 150°-200°C (Dakhnov, 1962).

$$\rho_w = \frac{\rho_{w_0}}{1 + \alpha (T - T_0)} \tag{2.4}$$

where:

ρ_w : Pore fluid resistivity [Ωm]

ρ_{w_0} : Pore fluid resistivity at temperature T_0 [Ωm]

T_0 : Temperature [°C]

α : Temperature coefficient of resistivity, close to 0.023 [$°C^{-1}$] for T_0 = 23 °C, and 0.025 [$°C^{-1}$] for T_0 = 0 °C

Since equation (2.3) only applies for relatively low resistivity values of the pore fluid as mentioned above, several relations have been developed where interface conduction dominates both matrix and ionic conduction. Flóvenz et al. (1985) established the following equation relating the bulk resistivity ρ, to the fracture porosity ϕ_f, the temperature T and the pore fluid resistivity ρ_{w_0}, for T_0 = 23 °C. This equation applies for the uppermost 1 kilometer of the Icelandic basaltic crust for temperatures of up to at least 100 °C.

$$\frac{1}{\rho} = \frac{0.22}{\rho_w}\left[1 - (1 - \phi_f)^{2/3} + \frac{(1 - \phi_f)^{2/3}}{1 + (1 - \phi_f)^{1/3} + (1 - \phi_f)^{1/3}\, 4.9 \cdot 10^{-3}}\right] + \frac{\phi_f^{1.06}}{b} \tag{2.5}$$

where:

$$\rho_w = \rho_{w_0}/[1+0.023(T - 23)] \quad \text{and} \quad b = 8.7/[1 + 0.023(T - 23)][1 + 0.018(T - 23)]$$

Equation (2.5) is an extension of a double-porosity model put forward by Stefansson et al. (1982). Equation (2.5) demonstrates that interface conduction is the most important conduction mechanism in the uppermost 1 km of the basaltic crust in Iceland.

Caldwell et al. (1986) made laboratory resistivity measurements on core samples from several geothermal fields. Their experiments lead to the relation:

$$\rho = a\ \rho_w^m\ \phi^n\ e^{bc}\ \frac{e^{E/kT}}{e^{E/k\,300}} \tag{2.6}$$

where:

ρ : Bulk resistivity of the rock [Ωm]

ρ_w : Pore fluid resistivity [Ωm]

c : Clay content

ϕ : Total porosity

T : Temperature [°K]

k : Boltzman constant, 1.38×10^{-23}[J/°K]

a, m, n, E and b : Empirical constants

In order to apply these relations, the interpreter must know which kind of conduction he is dealing with; ionic, interface or even rock matrix conduction. This can be achieved by means of additional information revealed from for instance, direct conductivity measurements of fluid conductivity in geothermal wells or springs, independent measurements of clay contents in the rock, etc.

None of the above mentioned relations for the bulk resistivity can be stated to be of general validity. Which relation should be used in each particular case can be a matter of dispute. Nevertheless, it can be said, that the resistivity of rocks, is a function strongly dependent on temperature, porosity, clay content and pore fluid resistivity. A fact, that must be noticed when interpreting resistivity data.

2.3 DC-methods

Direct Current methods (DC-methods) make use of a constant current independent of time, to build a potential field in the earth. Here, two types are discussed,

Schlumberger soundings and Head-on profiling. The term sounding means that the method searches for vertical resistivity changes, whereas the term profiling means searching for lateral resistivity changes.

2.3.1 Schlumberger soundings

In the Schlumberger array two potential and two current electrodes are placed along a straight line. The array is symmetrical around the midpoint O. The set-up is shown in figure 1, where the current electrodes are placed at A and B and the potential electrodes are placed at N and M. The distances are given as, AO=OB=S and NO=MO=P.

By applying Schlumberger soundings, it is possible to get a picture of the earth's vertical resistivity distribution. Generally there are some lateral influences. They will be discussed later, together with two-dimensional interpretation (chapter 4.2).

A current I is injected into the earth, through A for instance, and the circuit is closed at B. The resulting potential difference between M and N, ΔV, is measured. The measured values I and ΔV together with the geometrical constants S and P are used to calculate the socalled apparent resistivity, ρ_a, according to the formula:

$$\rho_a = \frac{\pi}{2} \frac{S^2 - P^2}{P} \frac{\Delta V}{I}$$

The apparent resistivity is plotted on a bi-logarithmic paper as a function of S (see chapter 3.4). Increasing stepwise the distance between the current electrodes while keeping the distance between the potential electrodes fixed, information on resistivity at greater depths is obtained. As S increases, the potential difference ΔV becomes lower. At a certain stage it is necessary to enlarge P in order to increase ΔV, and be able to measure ΔV within the particular equipment limitations. Because of this, the resulting curve is composed of segments, one for each different P value. It frequently happens that the segments are shifted relative to each other. The reason for this shift is discussed further in chapter 3.6.

The different half-current electrode spacings, S, are usually taken to be evenly distributed on a logarithmic scale, most frequently with 10 points per decade. There should be at least three overlapping points for successive P segments. When the measurement of the Schlumberger sounding is finished, the apparent resistivity curve is interpreted into the resistivity distribution of the earth. This is either done one-dimensionally, where the resistivity is a function of depth only (layered earth) or two-dimensionally, where the resistivity also varies along one horizontal direction. Both methods are discussed in this report and examples given.

2.3.2 Head-on profiling

Schlumberger soundings cannot detect narrow vertical or subvertical resistivity structures, such as faults, dykes or fractures. Instead the Head-on profiling method is used. The geothermal fluids are often associated with this kind of structures. Therefore this method is quite relevant in geothermal exploration. The Head-on arrangement is similar to the Schlumberger array, but it has an extra current electrode, C, located at an "infinite" distance from A and B. An "infinite" distance means that when current is injected through C and A (or B), then the potential distribution in the vicinity of M (or N) is negligible influenced by C and can be approximated by a monopole field. Keeping this distance AC = BC $\geq 4 \cdot$AB, the error caused by this electrode is around 2.5% (Flóvenz, 1984). The set-up for the Head-on arrangement is shown in figure 1.

A current I is injected into the earth in three different cases, closing the circuits AC, BC and AB, and the resulting potential difference ΔV between M and N is measured each time. Three resistivity values are calculated:

$$\rho_{ac} = \frac{\Delta V_{ac}}{I} \pi \frac{S^2 - P^2}{P} \quad \text{and} \quad \rho_{bc} = \frac{\Delta V_{bc}}{I} \pi \frac{S^2 - P^2}{P}$$

for the circuits AC and BC, and the already known

$$\rho_{ab} = \frac{\Delta V_{ab}}{I} \frac{\pi}{2} \frac{S^2 - P^2}{P}$$

for circuit AB. Then all the 4 electrodes AMNB are moved stepwise a certain distance along the profile and a new measurement is made. The three different resistivities ρ_{AC}, ρ_{BC} and ρ_{AB}, are calculated and plotted as a function of the central position of the array. The profile is placed along a straight line, that preferably crosses more or less perpendicularly the structure which is under observation.

If the array crosses a vertical or near-vertical conductive structure, the current density will be higher at positions where the potential electrodes are located between the source current electrode and the conductive structure (see Flóvenz, 1984). It will be lower everywhere else. Since the current density is proportional to the electric field ($\vec{J} = \sigma\vec{E}$) and the electric field is proportional to the apparent resistivity (ρ_a), the apparent resistivity will be higher at those positions already mentioned. To take advantage of this fact, the common procedure before plotting the field graphs, is to subtract the apparent resistivities measured at AB, from those measured at AC and BC. The values $\rho_{AC} - \rho_{AB} = \rho_{AC\text{-}AB}$ and $\rho_{BC} - \rho_{AB} = \rho_{BC\text{-}AB}$ are calculated and plotted together with the ρ_{AB} curve.

In the case discussed above, in which the potential electrodes are between the current electrode and the conductive structure, the corresponding difference will always be positive, while the difference between ρ_{AB} and the apparent resistivity measured with the other current electrode, will always be negative. As the complete array is moved along the straight line, across the conductive structure, the situation reverses, and the curves $\rho_{AC\text{-}AB}$ and $\rho_{BC\text{-}AB}$ will cross each other. This cross is above the vertical conductive structure. An example is given in figure 2.

2.4 AC-methods

2.4.1 Introduction

The Alternate Current methods (AC-methods) make use of an alternate current

induced in the earth and the associated magnetic field. The alternate current may be artificially induced as in TEM or natural as in MT.

2.4.2 Transient Electromagnetics (TEM)

As stated before, TEM makes use of a magnetic field for inducing currents in the earth. Here, a qualitative description of the central loop Transient Electromagnetic Method is presented. For a complete description of TEM, see e.g. Árnason (1989).

A magnetic field of known strength is built by transmitting a current into a loop of wire at the surface of the earth. The current is abruptly turned off and the decaying magnetic field induces electrical current in the earth. This electrical current induces a secondary magnetic field also decaying with time. The decay rate is measured by measuring the induced voltage in a small loop or coil placed at the center of the main loop.

As the current distribution and the induced voltage depend on the resistivity structure beneath the coil, the decay rate of the induced voltage can be interpreted in terms of the resistivity structure.

The TEM signal is usually presented as a late time apparent resistivity given by the formula:

$$\rho_a\ (r,t) = \frac{\mu_0}{4\pi}\left[\frac{2\mu_0 A_r n_r A_s n_s}{5t^{5/2}V(r,t)}\right]^{2/3}$$

where:

t: Time elapsed, after the current in the transmitter loop is turned off

A_r : Cross sectional area of the coil [m^2]

n_r : Number of windings

μ_0 : Magnetic permeability in vacuum [henry/m]

A_s : Cross sectional area of the loop [m^2]

n_s : Number of windings in the loop

The central loop TEM has several advantages over the conventional DC sounding methods such as.

- The transmitter couples inductively to the earth and no current has to be injected into the earth. Most important where the surface is dry and resistive.

- The measured signal is a decaying magnetic field, not an electrical field at the surface, making the results much less dependent on local resistivity conditions at the receiver site. Distortions due to local resistivity inhomogeneities at the receiver site can be a severe problem in DC soundings, as will be discussed in next chapter. This is also a big problem in MT soundings.

- This method is much less sensitive to lateral resistivity variations than the DC methods. Therefore one-dimensional inversion is better justified in the interpretation of central loop TEM soundings than in DC soundings. Results from Nesjavellir high-temperature area in Iceland show that one-dimensional interpretation of central loop TEM soundings can give basicly the same resolution as the much more time consuming and expensive two-dimensional modelling of DC-data (Árnason and Hersir, 1989).

- In DC soundings the monitored signal is low when the subsurface resistivity is low, like in geothermal areas, whereas in TEM soundings this situation reverses, the lower the resistivity the stronger the signal.

2.4.3 Magnetotellurics (MT)

Magnetotellurics make use of a natural electromagnetic field generated by the interaction of the geomagnetic field and solar winds in the upper atmosphere layers.

The incident magnetic field $\vec{H}$ is measured on the ground with the help of coils for instance, together with the associated electric field, $\vec{E} = \frac{\Delta V}{L}$.

These two fields are related through Faraday's induction law, $\text{curl}\vec{E} = \nabla \times \vec{E} = -\mu \frac{\partial \vec{H}}{\partial t}$, where μ is the magnetic permeability (henry/m). In the frequency domain this can be expressed:

$$\vec{E}(\omega) = Z(\omega)\vec{H}(\omega)$$

Where Z is a filter depending on the resistivity structure in the earth and ω is the frequency (sec^{-1}). $\vec{H}$ is an input in the filter and $\vec{E}$ is an output. The depth of penetration (δ) is a function of the resistivity (ρ) and the period (T) of the incident magnetic field and is given as:

$$\delta = 0.5\sqrt{T\rho}$$

The apparent resistivity is:

$$\rho_a = \frac{1}{\omega\mu}\frac{|E_x|^2}{|H_y|^2} = 0.2T|Z|^2[\Omega m]$$

where:

$$E_x(\omega) = Z(\omega)H_y(\omega)$$

The procedure for Magnetotellurics can be summarized as follows:

- Measurement of the naturally occurring magnetic field, $\vec{H}$ and the induced electric field, $\vec{E}$ both as a function of time.

- Fourier transforming the time series from the time domain to the frequency domain, they become a function of the period, T.

- One-dimensional interpretation, comparison with other results.

- Two-dimensional interpretation.

3. THE THEORY OF ONE-DIMENSIONAL INTERPRETATION OF SCHLUMBERGER SOUNDINGS

In this chapter it will be shown how it is possible, by starting with the Ohm's law $\vec{J}=\sigma\vec{E}$, to arrive at the solution for the potential at the surface $V(r) = \frac{\rho_1 I}{2\pi r} + \frac{\rho_1 I}{\pi}\int_0^\infty \Theta_1(\lambda)\, J_0(\lambda r)d\lambda$. This equation is the key equation in interpreting the field data, obtained through $\rho_a = \frac{\pi}{2}\frac{S^2 - P^2}{P}\frac{\Delta V}{I}$, in terms of the distribution of the subsurface resistivity. Also there is a discussion on how the potential can be worked out by using the linear filter method for both the gradient approach and the finite potential electrode separation. Convergent shifts in the apparent resistivity curve are discussed chapter 3.6. In chapter 3.7 the facts that can adversely affect the adequate one-dimensional interpretation are considered. These are mainly because of lateral resistivity changes and lateral topographic variations. The constant shifts due to a two-dimensional bodies near the surface are discussed too.

3.1 Laplace equation and its solution

In order to get information on the resistivity distribution in the earth, the first step is to use an elementary model, the simplest one. Therefore in this chapter only one-dimensional models (layered earth) will be considered. It is assumed that the resistivity only changes in Z direction but is invariant in both X and Y directions.

In this model there are n-layers, each separated layer has its own parameters i.e. resistivity ρ_i and thickness d_i. The depth to each layer's lower boundary, h_i, is given by $h_i = \sum_{j=1}^{i} d_j$ and i = 1,2,..., n-1. The bottom layer has resistivity ρ_n and infinite thickness. All the layers have infinite lateral extent and they are homogeneous and isotropic. A current source is placed at the surface of a halfspace and a current of intensity I is injected into the earth. The current distribution and the electric field are related through Ohm's law:

$$\vec{J}=\sigma\vec{E} \tag{3.1}$$

where:

σ : Conductivity [1/Ωm]

$\vec{E}$: Electric field [Volt/m]

$\vec{J}$: Current density [A/m^2]

The divergence of the current density in a given volume is equal to the difference in the current flow into and out of the volume. This difference is equal to zero except at a current source and current sink. The divergence is therefore equal to zero throughout the halfspace except on the surface where it is given by:

$$\mathrm{div}\vec{J}=\nabla\cdot\vec{J}=I\delta(\vec{x}) \tag{3.2}$$

and, $\delta(\vec{x})$ is the Dirac delta "function". The coordinate system has been taken to have the origin at the source.

The electric field, $\vec{E}$ is defined as the negative gradient of the potential, V:

$$\vec{E}=-\nabla V \tag{3.3}$$

Since:

$$\begin{aligned}\mathrm{div}\,\vec{J} &= \nabla\cdot\vec{J}\\ &= \nabla\cdot\sigma\vec{E}\\ &= \nabla\cdot\sigma(-\nabla V)\\ &= -\sigma\nabla^2 V\end{aligned}$$

in regions where σ is constant and equation (3.2) becomes:

$$-\sigma\nabla^2 V=I\delta(\vec{x})$$

As $\sigma = 1/\rho$ and in the uppermost layer, $\rho = \rho_1$ then:

$$-\nabla^2 V = \rho_1 I \delta(\vec{x}) \tag{3.4}$$

Equation (3.4) is an inhomogeneous differential equation of second order. A special solution for this equation is given by (see e.g. Hersir and Árnason, 1989):

$$V = \rho_1 I / 2\pi R \tag{3.5}$$

where:

$$R = (x^2 + y^2 + z^2)^{1/2}$$

Changing from Cartesian to cylindrical coordinates, $x = r \cdot \cos\theta$, $y = r \cdot \sin\theta$ and $z = z$ and using the identity $\cos^2\theta + \sin^2\theta = 1$ then:

$$R^2 = r^2(\cos^2\theta + \sin^2\theta) + z^2 = (r^2 + z^2)$$

The special solution given by equation (3.5) can now be written as:

$$V = \frac{\rho_1 I}{2\pi} (r^2 + z^2)^{-1/2} \tag{3.6}$$

It can be shown (see e.g. Hersir and Árnason, 1989) that:

$$\frac{1}{(r^2 + z^2)^{1/2}} = \int_0^\infty e^{-\lambda z} J_0(\lambda r)\, d\lambda$$

where J_0 is the Bessel function of order zero. Consequently:

$$V = \frac{\rho_1 I}{2\pi} \int_0^\infty e^{-\lambda z} J_0(\lambda r)\, d\lambda \tag{3.7}$$

This last equation is only valid for the uppermost layer where, $\text{div}\, J = I\, \delta(\vec{x})$. For all the other layers $\text{div}\, J = 0$. Therefore, for $i > 1$:

$$-\sigma_i \nabla^2 V = 0$$

or:

$$\nabla^2 V = 0 \tag{3.8}$$

Equation (3.8) is the **LAPLACE** equation, which can be written in Cartesian coordinates as:

$$\frac{\partial^2 V}{\partial x^2} + \frac{\partial^2 V}{\partial y^2} + \frac{\partial^2 V}{\partial z^2} = 0 \tag{3.9}$$

In cylindrical coordinates equation (3.9) becomes:

$$\frac{\partial^2 V}{\partial r^2} + \frac{1}{r}\cdot\frac{\partial V}{\partial r} + \frac{\partial^2 V}{\partial z^2} + \frac{1}{r^2}\cdot\frac{\partial^2 V}{\partial \theta^2} = 0$$

Because the layers are both homogeneous and isotropic, the potential is symmetrical around the Z-axis, i.e. independent of θ. Therefore:

$$\frac{\partial^2 V}{\partial r^2} + \frac{1}{r}\cdot\frac{\partial V}{\partial r} + \frac{\partial^2 V}{\partial z^2} = 0 \tag{3.10}$$

Special solutions to this homogeneous differential equation of the second order are found by separating the variables, i.e.:

$$V(r,z) = U(r)\,W(z) \tag{3.11}$$

Substituting (3.11) into (3.10):

$$W(z)\frac{d^2U(r)}{dr^2} + \frac{W(z)}{r}\frac{dU(r)}{dr} + U(r)\frac{d^2W(z)}{dz^2} = 0 \tag{3.12}$$

Dividing by U(r)W(z):

$$\frac{1}{U(r)}\frac{d^2U(r)}{dr^2} + \frac{1}{rU(r)}\frac{dU(r)}{dr} + \frac{1}{W(z)}\frac{d^2W(z)}{dz^2} = 0 \tag{3.13}$$

Since U is only a function of r and W only a function of z, this can only be satisfied if:

$$\frac{1}{U(r)}\frac{d^2U(r)}{dr^2} + \frac{1}{rU(r)}\frac{dU(r)}{dr} = -\lambda^2 \tag{3.14}$$

and:

$$\frac{1}{W(z)}\frac{d^2W(z)}{dz^2} = \lambda^2 \tag{3.15}$$

Where λ is an arbitrary constant. The general solution for equation (3.15) is given by:

$$W(z) = Ae^{\lambda z} + Be^{-\lambda z} \tag{3.16}$$

Where A and B both are arbitrary constants. The solution for equation (3.14), which is finite as $r \rightarrow 0$ is:

$$U(r) = DJ_0(\lambda r) \tag{3.17}$$

where, D is an arbitrary constant.

Since $V(r,z) = U(r) \cdot W(z)$ special solutions for equation (3.13) are given by the product of equations (3.16) and (3.17), i.e.:

$$V = \Phi(\lambda)e^{\lambda z}J_0(\lambda r) + \Psi(\lambda)e^{-\lambda z}J_0(\lambda r) \tag{3.18}$$

Where λ, $\Phi(\lambda)$ and $\Psi(\lambda)$ are constants.

The general solution of the homogeneous equation within each layer is a linear combination of the special solutions as λ varies from 0 to ∞:

$$V_i = \int_0^{\infty}\left[\Phi_i(\lambda)e^{\lambda z} + \Psi_i(\lambda)e^{-\lambda z}\right]J_0(\lambda r)d\lambda \tag{3.19}$$

for $i = 1,2,...,n$. The potential vanishes at infinity ($r \rightarrow \infty$). The Bessel function of order zero, $J_0(\lambda r)$ becomes zero if and only if λr is a real number. Since the integrand in equation (3.19) is symmetrical in λ only positive values of λ need to be considered.

The general solution for the inhomogeneous differential equation of second order in the uppermost layer (equation 3.4)) can be written as a sum of the general solution for

the homogeneous equation (3.19) and the special solution for the inhomogeneous equation (3.7):

$$V = \frac{\rho_1 I}{2\pi}\int_0^\infty \left[e^{-\lambda z} + \Theta_1(\lambda)\, e^{-\lambda z} + X_1(\lambda)\, e^{\lambda z} \right] J_0(\lambda r)\, d\lambda \qquad (3.20)$$

where:

$$\Theta_1(\lambda) = \frac{2\pi}{\rho_1 I}\Psi_1(\lambda) \text{ and } X_1(\lambda) = \frac{2\pi}{\rho_1 I}\Phi_1(\lambda)$$

The solutions for the other layers ($i > 1$) can be written on the same form as equation (3.20) by defining, for $i > 1$:

$$\Theta_i(\lambda) = \frac{2\pi}{\rho_1 I}\Psi_i(\lambda) - 1 \text{ and } X_i(\lambda) = \frac{2\pi}{\rho_1 I}\Phi_i(\lambda)$$

The task is now to determine the functions $\Theta_i(\lambda)$ and $X_i(\lambda)$. That is done by using the boundary conditions for the potential, V, which are the following:

1) The potential is continuous across every boundary between layers, i.e. $V_i(h_i) = V_{i+1}(h_i)$. This means that when z approaches h_i from above and below the boundary, the same potential value will be found.

2) The vertical component of the current density, $J_z = \sigma \frac{\partial V}{\partial z}$ is continuous across every boundary between layers, i.e. $\frac{1}{\rho_i}\frac{\partial V_i}{\partial z} = \frac{1}{\rho_{i+1}}\frac{\partial V_{i+1}}{\partial z}$ at $z = h_i$.

3) At the surface ($z=0$) the vertical component of the current density (J_z) is equal to zero and consequently the electrical field also, except for a small neighbourhood around the current source.

4) The potential vanishes at infinity, i.e. $V \to 0$ when $z \to \infty$ and $r \to \infty$.

In the lowermost layer ($i=n$) condition 4 requires that $X_n(\lambda) = 0$. Hence equation (3.20) for the lowermost layer becomes:

$$V_n = \frac{\rho_1 I}{2\pi} \int_0^\infty \left[1 + \Theta_n(\lambda)\right] e^{-\lambda z} J_0(\lambda r)\, d\lambda \qquad (3.21)$$

Differentiating equation (3.20) with respect to z for the uppermost layer (i=1) gives:

$$\frac{\partial V_1}{\partial z} = \frac{\rho_1 I}{2\pi} \int_0^\infty \left[-\lambda e^{-\lambda z} - \lambda \Theta_1(\lambda) e^{-\lambda z} + \lambda X_1(\lambda) e^{\lambda z}\right] J_0(\lambda r)\, d\lambda$$

and on the surface z = 0 :

$$\left[\frac{\partial V_1}{\partial z}\right]_{z=0} = \frac{\rho_1 I}{2\pi} \int_0^\infty \left[-\lambda - \lambda \Theta_1(\lambda) + \lambda X_1(\lambda)\right] J_0(\lambda r)\, d\lambda$$

For the uppermost layer condition 3 gives, $J_z = \frac{1}{\rho_1}\left[\frac{\partial V}{\partial z}\right]_{z=0} = 0$. Hence:

$$\int_0^\infty \left[-\lambda - \lambda \Theta_1(\lambda) + \lambda X_1(\lambda)\right] J_0(\lambda r)\, d\lambda = 0 \qquad (3.22)$$

Differentiating the special solution to the inhomogeneous equation, given by equations (3.6) and (3.7), with respect to z gives:

$$\frac{\partial V}{\partial z} = \frac{\rho_1 I}{2\pi} \int_0^\infty -\lambda e^{-\lambda z} J_0(\lambda r)\, d\lambda = \frac{\rho_1 I}{2\pi} \frac{-z}{(r^2+z^2)^{3/2}} \qquad (3.23)$$

letting $z \to 0$:

$$\left[\frac{\partial V}{\partial z}\right]_{z=0} = \frac{\rho_1 I}{2\pi} \int_0^\infty -\lambda J_0(\lambda r)\, d\lambda = 0$$

or:

$$\int_0^\infty \lambda J_0(\lambda r)\, d\lambda = 0$$

Applying this result to equation (3.22) means that:

$$\int_0^\infty \left[X_1(\lambda) - \Theta_1(\lambda)\right] \lambda J_0(\lambda r)\, d\lambda = 0$$

Hence for the first layer:

$$X_1(\lambda) = \Theta_1(\lambda) \tag{3.24}$$

and equation (3.20) at the surface (z=0) therefore becomes:

$$V(r) = \frac{\rho_1 I}{2\pi} \int_0^\infty \left[1 + 2\Theta_1(\lambda)\right] J_0(\lambda r)\, d\lambda \tag{3.25}$$

Conditions 1 and 2, at the boundaries between layers ($z=h_i$, for $i=1,2,...n-1$), give:

$$V_{i-1} = V_i \tag{3.26}$$

and

$$\frac{1}{\rho_{i-1}} \frac{\partial V_{i-1}}{\partial z} = \frac{1}{\rho_i} \frac{\partial V_i}{\partial z} \tag{3.27}$$

Equations (3.26) and (3.27) constitute a system of 2(n-1) equations with 2(n-1) unknown functions $\Theta_i(\lambda)$ and $X_i(\lambda)$. Koefoed (1979) has shown how this system of 2(n-1) equations can be solved.

As an example of how this system of equations can be solved, a simple case is taken, the two layered model. By using equation (3.24), equation (3.20) for layer 1 at the boundary (z=h) becomes:

$$V_1 = \frac{\rho_1 I}{2\pi} \int_0^\infty \left[e^{-\lambda h} + \Theta_1(\lambda) e^{-\lambda h} + \Theta_1(\lambda) e^{\lambda h}\right] J_0(\lambda r) d\lambda$$

For layer 2 at the boundary (z=h), remembering n=2 and using equation (3.21), the potential is given by:

$$V_2 = \frac{\rho_1 I}{2\pi} \int_0^\infty \left[e^{-\lambda h} + \Theta_2(\lambda) e^{-\lambda h}\right] J_0 \lambda(r) d\lambda$$

Boundary condition 1 gives:

$$V_1(h) = V_2(h)$$

and therefore:

$$[e^{-\lambda h} + e^{\lambda h}]\Theta_1(\lambda) = e^{-\lambda h}\Theta_2(\lambda) \tag{3.28}$$

Taking the derivatives of the potential with respect to z, at z=h:

$$\left[\frac{\partial V_1}{\partial z}\right]_h = \frac{\rho_1 I}{2\pi}\int_0^\infty \left[-\lambda e^{-\lambda h} - \lambda\Theta_1(\lambda)e^{-\lambda h} + \lambda\Theta_1(\lambda)e^{\lambda h}\right]J_0(\lambda r)d\lambda$$

and:

$$\left[\frac{\partial V_2}{\partial z}\right]_h = \frac{\rho_1 I}{2\pi}\int_0^\infty \left[-\lambda e^{-\lambda h} - \lambda\Theta_2(\lambda)e^{-\lambda h}\right]J_0(\lambda r)d\lambda$$

Then the boundary condition 2 gives:

$$\frac{1}{\rho_1}(e^{-\lambda h} - e^{\lambda h})\Theta_1(\lambda) = \frac{1}{\rho_2}e^{-\lambda h}\Theta_2(\lambda) \tag{3.29}$$

Solving equations (3.28) and (3.29) gives:

$$\Theta_1(\lambda) = \frac{k_1 e^{-2\lambda h}}{1 - k_1 e^{-2\lambda h}}$$

where:

$$k_1 = \frac{(\rho_2 - \rho_1)}{(\rho_2 + \rho_1)}$$

3.2 Stefanescu's integral and the Kernel function.

The potential at the surface is given by equation (3.25). It can be rewritten as:

$$V(r) = \frac{\rho_1 I}{2\pi} \int_0^\infty J_0(\lambda r)\, d\lambda + \frac{\rho_1 I}{\pi} \int_0^\infty \Theta_1(\lambda)\, J_0(\lambda r)\, d\lambda \qquad (3.30)$$

It can be shown that for the Bessel function of order zero, J_0 the following is valid (see e.g. Hersir and Árnason, 1989):

$$\int_0^\infty e^{-z\lambda} J_0(\lambda r)\, d\lambda = \frac{1}{(r^2 + z^2)^{1/2}}$$

and for $z=0$ this becomes:

$$\int_0^\infty J_0(\lambda r)\, d\lambda = \frac{1}{r}$$

Equation (3.30) can therefore be written as:

$$V(r) = \frac{\rho_1 I}{2\pi r} + \frac{\rho_1 I}{\pi} \int_0^\infty \Theta_1(\lambda)\, J_0(\lambda r) d\lambda \qquad (3.31)$$

Equation (3.31) is a key equation, describing the potential V(r) at the surface of a stratified medium, generated by a point current source at the surface. In equation (3.31) the parameters involved are the following:

V : Potential at a point on the surface a distance r from the point source

I : Current intensity at a point source

ρ_1 : Resistivity of the uppermost layer

λ : Integral variable

r : Distance between the current source and potential point

$J_0(\lambda r)$: Bessel function of order zero

$\Theta_1(\lambda)$: Stefanescu's Kernel function dependent on the layers parameters ρ_i and h_i

3.3 The Linear Filter Method

In order to evaluate the integral in equation (3.31), the socalled digital linear filter method is used. The method is based on the theory of sampling, stating that it is possible to reconstruct every function, F(y) completely with a finite number of discretely sampled values taken at even intervals, Δy as long as its Fourier spectrum vanishes for frequencies higher than the Nyquist frequency, $1/2\Delta y$. The function, F(y) is written as a linear combination of the sample values. The coefficients in the linear combination are called filter coefficients and their number the length of the filter. The function F(y), can be written as an infinite sum:

$$F(y) = \sum_{j=-\infty}^{\infty} F(y_0 + j\Delta y) \frac{\sin[\pi(y-y_0-j\Delta y)/\Delta y]}{\pi(y-y_0-j\Delta y)/\Delta y} \tag{3.32}$$

where F(y) is sampled at the points, $y_0 + j\Delta y$, $|j| = 0,1,2,....$

By changing the variables $y = -\ln(\lambda)$, $x = \ln(r)$ and $\eta = x - y$ and representing the Kernel function, $\tilde{\Theta}_1(y) = \Theta_1(\lambda)$ as a linear combination according to equation (3.32), it can be shown that equation (3.31) can be written in the following way (see e.g. Hersir and Árnason, 1989):

$$V(r) = \frac{\rho_1 I}{2\pi r} + \frac{\rho_1 I}{\pi} \sum_{j=-\infty}^{\infty} f_j \tilde{\Theta}_1(y_0 + j\Delta y) \tag{3.33}$$

where the filter coefficients, f_j are given as:

$$f_j = e^{-x} \int_{-\infty}^{\infty} \frac{\sin[\pi(-\eta+x-y_0-j\Delta y)/\Delta y]}{\pi(-\eta+x-y_0-j\Delta y)/\Delta y} J_0(e^{\eta}) e^{\eta} d\eta \tag{3.34}$$

The filter coefficients depend only on $x-y_0-j\Delta y$ i.e. the geometry of the array, but they are independent of the layer parameters. They can therefore be calculated once and for all and stored as numbers. V(r) is now found at points evenly distributed on a logarithmic scale i.e. ($x = x_0 + k\Delta x$) where Δx is the interval between measured points in a Schlumberger sounding. Choosing $\Delta x = \Delta y$ and using equation (3.33):

$$V(x_0 + k\Delta y) = \frac{\rho_1 I}{2\pi} e^{-(x_0 + k\Delta y)}[1 \tag{3.35}$$

$$+ 2 \sum_{j=-\infty}^{\infty} \tilde{\Theta}_1(y_0 + j\Delta y) \int_{-\infty}^{\infty} \frac{\sin[\pi(-\eta + x_0 - y_0 - (j-k)\Delta y)/\Delta y]}{\pi(-\eta + x_0 - y_0 - (j-k)\Delta y)/\Delta y} J_0(e^{\eta}) e^{\eta} d\eta]$$

Knowing the layer parameters, ρ_i, d_i, the Kernel function, Θ_1, can always be calculated at the sample points by solving the system of 2(n-1) equations given in (3.26) and (3.27). Using the result together with the filter coefficients, stored as numbers, the potential described in equation (3.31) is easily calculated. The potential difference is thereafter calculated by using:

$$\Delta V = 2[V(S-P) - V(S+P)] \tag{3.36}$$

where:

ΔV : Potential difference

S : Semidistance between current electrodes

P : Semidistance between potential electrodes

3.4 The Apparent Resistivity

The potential due to a point current source at the surface of an electrically homogeneous and isotropic earth is governed by the relation:

$$V_P = \frac{\rho I}{2\pi r} \tag{3.37}$$

Where:

V_P : Potential at point P [Volt]

ρ : Resistivity of the halfspace [Ωm]

I : Injected current [A]

r : Distance from the point source to the point P where the potential is considered [m]

Applying equation (3.37), it is easy to calculated the potential difference between the potential electrodes at the surface for any combination of the current sources. In this case, i.e. the tetra-electrode Schlumberger configuration, the potential difference, can be evaluated for ρ, giving:

$$\rho = \frac{\pi}{2} \frac{S^2 - P^2}{P} \frac{\Delta V}{I} \tag{3.38}$$

In the reality the earth is not homogeneous and equation (3.38) no longer expresses the true resistivity of the earth but a quantity called the **APPARENT RESISTIVITY**, defined as.

$$\rho_a = \frac{\pi}{2} \frac{S^2 - P^2}{P} \frac{\Delta V}{I} \tag{3.39}$$

Equation (3.39) is a basic one, because it is the link between surface measurements and subsurface resistivity distribution.

3.5 The Gradient Approach

When Schlumberger soundings are interpreted, it is often assumed that the distance between the potential electrodes is infinitesimal compared to the distance between the current electrodes. In this approach, often called the gradient approach, it is furthermore assumed that the potential changes linearly between the potential electrodes. The potential difference is found by differentiating V:

$$\frac{\Delta V}{2P} = -2\left(\frac{\partial V}{\partial r}\right)_{r=S}$$

This gives after some calculations (see e.g. Hersir and Árnason, 1989):

$$\rho_a = \rho_1 + 2\rho_1 S^2 \int_0^\infty \Theta_1(\lambda) J_1(\lambda S) \lambda d\lambda \tag{3.40}$$

The integral is evaluated by using the filter method. The filter coefficients are though different from those given in equation (3.34). In the gradient approach only one integral has to be evaluated in order to calculate the apparent resistivity instead of two for the finite electrode separation method, previously describes using equations (3.31), (3.36) and (3.39).

In fact this is the most common method for interpretation of Schlumberger soundings. The method has the disadvantage that it does not simulate the real position of the current and potential electrodes. This is rather cumbersome since, as will be seen in next chapter, it brings the interpretation to an approximate solution. This is because when ρ_a is calculated using this approach, it always results in a continuous curve, since P is kept fixed (infinitesimal). The different segments of the ρ_a curve will always tie in each other, a case that hardly occurs in nature.

3.6 The Effect of Finite Electrode Separation

The depth of penetration of Schlumberger soundings, is not only a function of the distance between the current electrodes, 2S. It is actually a function of the shortest distance between the current electrode and the potential electrode, S-P (Árnason, 1984). For the same S and different P, different values of ρ_a reflect different resistivity at different depths. For instance, if the difference (S-P) in a two layer case, is of the same order of magnitude as the depth to the layer boundary, the measured ρ_a value will be dominated by the resistivity of the first layer, ρ_1, independent of the distance between the current electrodes.

The usual procedure in carrying out a Schlumberger sounding, is to keep P as small as possible. As S increases, ΔV decreases and it becomes necessary to enlarge P. The changes of S and P are reflected in the ρ_a curve which is composed of shifted segments. These shifts are convergent, because the larger (S-P) becomes, the more the apparent resistivity values, measured with the same S, approach that of the gradient approximation (Árnason, 1984).

An example of a convergent shift can be seen in many of the interpreted soundings from Planillas Geothermal Field, Mexico (see Reyes, 1989).

3.7 Sources of errors in Schlumberger soundings

In Schlumberger soundings, a current of a certain strength is injected into the earth through a current circuit and the associated potential field is measured. It is necessary to know the exact amount of both the current and the induced potential.

Besides the associated potential field, there are always present spurious potential sources such as induced polarization, spontaneous polarization, telluric currents, induction and all kinds of conductors acting as shortcut (e.g. the sea if the sounding is close enough to the coast). It is possible to correct for the influence of the sea on the measured ρ_a curve (Hersir, 1988). These spurious potentials or "noise" can be handled through statistical means. By taking many measurement values of ΔV and I, and calculate their mean values and statistical deviations or under more difficult conditions it is possible to obtain a weighted mean-value from all the mean values were the weighting is determined by the standard deviation in each case. Doing this the random error will be to at least some extent averaged out.

There is another kind of effect that affects the shape of the apparent resistivity curve and keeps it different from a "well behaved one", which can easily be interpreted by one dimensional interpretation. Two-dimensional resistivity distribution at the site or close to the potential electrodes can provoke a constant shift in the apparent resistivity curve. It can easily lead the interpretation astray (Árnason, 1984). The way to handle these shifts, is to fix the segment of the curve measured with the largest P, used in the sounding, and correct the others by a factor that forces the segments to tie in. This is done by assuming that the segment of the apparent resistivity curve which is measured with the largest P, has the least local influence. This effect caused by resistivity inhomogeneities can also be compensated for in two dimensional interpretation.

Errors arise, when both topographic and two-dimensional effects, are erroneously treated as being caused by a one-dimensional resistivity distribution.

Besides this, there still remains an uncertainty inherent in the method, called equivalence. There are two types of equivalences. In both cases there is a layer whose thickness and resistivity is undetermined. For both cases the depth to this layer's interface, must be the same or less than the thickness of this undetermined layer, (see e.g. Koefoed, 1979). The first one, is a bell type curve, i.e. a resistive layer which is embedded between two conductive layers. In this case, the only known parameter for the intermediate layer, is the transversal resistance, given by the product, $\rho_i \, d_i = T$. The second one, is a bowl type curve, i.e. a conductive layer which is embedded between two resistive layers. In this case, the only known parameter for the intermediate layer, is the longitudinal conductance, given by the quotient $\frac{d_i}{\rho_i} = S_L$.

In the presence of equivalence layers in one-dimensional interpretation, it is advisable to add some independent information from other investigations. If they are not available, correlations can be made utilizing other soundings in the neighborhood.

4. COMPUTER PROGRAMS FOR INTERPRETATION OF SCHLUMBERGER SOUNDINGS

This chapter describes the programs applied for one- and two-dimensional interpretation. In chapter 4.1.1 a description is given of how the gradient approach, discussed in chapter 3.5, is applied in the PC-program SLINV. The program is a one-dimensional automatic iterative program which evaluates the integral given in equation (3.40) using the filter method. In chapter 4.1.2 the second program, named ELLIPSE is described. At Orkustofnun (NEA) it runs on either a VAX- or HP-mainframe. ELLIPSE is also an automatic iterative program. It applies both convergent and constant shifting, using the finite electrode separation described in chapter 3.3 (see equations (3.31), (3.36) and (3.38)). Finally, in chapter 4.2 the third program, FELIX is introduced. FELIX is a two-dimensional finite element program which takes the topography into account.

4.1 One-dimensional interpretation

The theory presented in chapter 3 is applied in one-dimensional interpretation. As mentioned before, there are two methods for evaluating equation (3.31), the gradient approach and the more exact one, the finite electrode separation method. The former is less time consuming and was therefore implemented on a personal computer.

4.1.1 The gradient approach, the SLINV program

The SLINV program (SchLumberger INVersion) was written by Knútur Árnason for the UNU Geothermal Training Programme. For a detailed description of the program see Árnason and Hersir (1988). SLINV is a non-linear least-squares inversion program using a Levenberg-Marquardt inversion algorithm together with a fast forward routine based on the linear filter method. It automatically adjusts the layer parameters in order to fit a calculated curve to the measured apparent resistivity curve. In this chapter a qualitative description will be presented, to illustrate the practical use of the program.

In the field the potential difference, ΔV and the injected current, I are measured for different current electrode spacing, 2S and different potential electrode spacing, 2P. These quantities are used to construct an apparent resistivity curve. If the curve present shifts, as commonly happens, it must be "corrected". As already shown in chapters 3.6 and 3.7, there are two kinds of shifts, the convergent and the constant shift. The constant shift can be handled by fixing the segment of the curve measured with the largest P, used in the sounding, and correct the others by a factor that forces the segments to tie in (see chapter 3.7). This is accomplished by a manual procedure prior to the automatic process, but there is no way to get extra information from the convergent shifts in this kind of interpretation. After this step, the corrected curve is fed into the program. By inspection, an initial guess is made by the interpreter in order to choose the initial layer parameters ρ_i and d_i together with the number of layers. It is important to notice that the SLINV program although it changes the layer parameters, does not vary the number of layers.

Using these layer parameters, the kernel function $\Theta_1(\lambda)$ is calculated and the corresponding apparent resistivity values are determined by evaluating equation (3.40) with the help of the linear filter method. The calculated curve is compared with the measured one, and the computer changes the layer parameters until a good fit is achieved. By inspection, the interpreter checks if the fit is good enough, if not, the number of layers can be changed and the process reinitiated.

4.1.2 The finite electrode separation, the ELLIPSE program

ELLIPSE is a powerful mathematical program available only at Orkustofnun (NEA). For a description of the program, see Hersir and Árnason (1989). It simulates the actual position of the electrodes when evaluating ΔV in equation (3.36) by means of equation (3.31). In this way the computer program is able to extract the information contained in convergent type shifts, which are due to a finite potential electrode separation and strong resistivity contrasts between layers. The constant shifts are automatically corrected by fixing the segment of the curve measured with the largest P and applying correction factors to the other segments so that they all tie together. ELLIPSE requires an initial guess model and by means of an iterative process the

layer parameters are changed until a fit is achieved. The interpreter then decides if the fit is good enough by displaying the calculated curve on the screen. The ELLIPSE program was written by Ragnar Sigurdsson at Orkustofnun (NEA). The FORTRAN 77 algorithm is implemented on a mainframe HP 9000/840, running under UNIX and makes use of some routines from the International Mathematical Subroutines Library (IMSL). This program was used for one-dimensional interpretation of most of the Schlumberger soundings carried out in Planillas Geothermal Field, Mexico as is described in chapter 5.

4.2 Two-dimensional interpretation, the FELIX program

The FELIX program is a most powerful tool for two-dimensional interpretation. It was written by Ragnar Sigurdsson at Orkustofnun (NEA). The program makes use of the finite element method to evaluate the potential distribution in a two-dimensional resistivity distribution composed of triangular and rectangular resistivity blocks with infinite extension in the third dimension. The surface can be made irregular in order to model the topography.

FELIX requires as an input, the two-dimensional resistivity distribution, the topography and the locations of soundings along the measured profile. The program calculates the potential distribution over all nodes in the net and the apparent resistivity curves for up to ten Schlumberger soundings over the irregular landscape along the profile. It takes into account the potential distortions caused by the topography, and simulates the actual electrode positions utilized in the field.

The calculated and measured curves are compared and the interpreter decides how to change the block distribution, the resistivities, dimensions or even add and eliminate different blocks. Then the program is run again and the process repeated until a good fit is obtained.

In Iceland FELIX is used for modelling resistivity data from head-on profiling and for two-dimensional interpretation of DC-coaxial dipole soundings.

5. INTERPRETATION OF SCHLUMBERGER SOUNDINGS FROM PLANILLAS GEOTHERMAL FIELD, MEXICO

5.1 Introduction

A resistivity survey was carried out at Planillas rhyolitic dome and the associated area, applying Schlumberger soundings. The purpose of this survey was to study the subsurface resistivity distribution, with the aim of correlating resistivity with geological parameters, and thus get a better understanding of the rock water system connected with the geothermal manifestations and the structural conditions in the area.

As already mentioned, resistivity is directly related to effective porosity (i.e. amount of interconnected pores), temperature and water content. These parameters are of interest in exploring geothermal reservoirs. There are other variables that can obscure this relation, as for instance clay content, interface conduction and highly concentrated brines.

This chapter presents a description of the results of the interpretation of the Schlumberger soundings made during the author's training course. The facilities at Orkustofnun (NEA) were utilized.

5.2 Geological setting

Planillas Geothermal Field is located 7 km south of Primavera Geothermal Area. A regional geological survey of the Tertiary system has been executed to make clear the structure and rock facies of the system surrounding the Primavera Caldera (see JICA, 1989, page 13-17). The results of this survey will be taken into account, in order to understand the stress field causing the shallow and deep fractures and the fault system in Planillas.

The rock formation beneath Primavera, and hence most likely in Planillas, is composed of, in ascending order, basement granitic rocks, the Cordilleran volcanics, the Tala tuff, rhyolitic domes and air fall pumice (see JICA, 1989).

The geothermal fluids associated with Primavera Geothermal Area are mainly stored in extensional fractures developed within the lower Cordilleran volcanics (see figure 3). The system of extensional fractures and strike slip faulting has a NW-SE trend. The Tertiary formation, i.e. Cordilleran volcanics, must lie beneath the Tala tuff formation and have the same fracture trend below Planillas Geothermal Field as Primavera Geothermal Area.

Moreover, Planillas together with Primavera is located in a point that can be considered as "the hub of a wheel" (see JICA, 1989) with the NW-SE and E-W trending portions of the Mexican Volcanic Belt, and the N-S trending Cordilleran-Colima graben. The Colima graben seems to be a failed rift, and the Mexican Volcanic Belt a failed transform fault. In this geological circumstance, the NW-SE or the N-S trending fracture would be open (see figure 3).

5.3 Schlumberger soundings

5.3.1 Introduction

The Mexican Comision Federal de Electricidad, CFE, conducted a geophysical survey, with the author's participation, in which more than 200 Schlumberger soundings were carried out. The location of the Schlumberger soundings from Planillas is shown in figure 4. They were interpreted as an integral part of the author's training and the results are discussed in this chapter.

The Schlumberger soundings were performed using a Scintrex transmitter IPC-15, delivering a power of 15 KW nominal, 12 KW actual into the current circuit. An analog high impedance null voltmeter Hewlett Packard was connected to the potential circuit, with non-polarizable potential electrodes using a $CuSO_4$ solution. The spontaneous polarization was eliminated with an attached battery circuit and each measurement was repeated five or six times. Thereafter the mean value was calculated.

The calculated apparent resistivity curves present shifting, having an overlap of five points. These shifts were corrected manually by fixing the segment measured with the largest P and multiplying the other segments with a multiplication factor, in order to accomplish the input curve required for the SLINV program.

With the purpose of comparing the results from the interpretation of the SLINV program, the soundings were also interpreted using the ELLIPSE program, feeding the computer with the actual apparent resistivity curves as obtained from the field record. In chapter 5.3.2 the comparison is presented together with the interpretation from the whole area, using ELLIPSE. The two dimensional interpretation is presented in chapter 5.3.3.

The measured apparent resistivity curves of all the Schlumberger soundings that were interpreted from Planillas are published in a separate report, which is divided into three parts (Reyes, 1989). The first two parts show the results of one-dimensional interpretation (models, mean deviations and fits between measured and modeled data) using the SLINV program and the ELLIPSE program, respectively. The third part shows how well the calculated apparent resistivity curves from the two-dimensional model fit with the measured curves.

5.3.2 One-dimensional interpretation

The Schlumberger soundings from Planillas (for location see figure 4), were interpreted one-dimensionally using the SLINV program and the ELLIPSE program. The mean deviations from the interpretation using ELLIPSE ranged from 3.7 for sounding 007 and up to 19.7 for sounding 167. The average mean deviation was 10.3 (Reyes, 1989).

Two perpendicular resistivity cross sections, A-A' and B-B', oriented NE-SW and NW-SE, respectively, were made using both SLINV and ELLIPSE for comparing of the results. The soundings interpreted with SLINV gave results close to that of ELLIPSE, a difference within 10% or less was noted between thickness and resistivity values.

As explained earlier in the report the difference between the models, originating from SLINV and ELLIPSE, is mostly due to high resistivity contrasts between layers. The difference between these one-dimensional inversion techniques is demonstrated in the next example. By looking at sounding 135 (see Reyes, 1989) it is possible to ponder, that even though the inversion gives the same number of layers, the resulting layer parameters are different (see table 1):

SOUNDING 135			
RESISTIVITY [Ωm]		THICKNESS [m]	
SLINV	ELLIPSE	SLINV	ELLIPSE
1204	1847	2.8	5.7
5556	4759	183.9	183.0
281	113	1835.2	221.0
11661	356		

Table 1 Inversion models for sounding 135, SLINV and ELLIPSE inversion

Inspecting the shallow part of the curve, a shift is noticed between the segment of the curve measured with P = 2.5 m and with P = 10.0 m. The latter segment has higher ρ_a values than the former segment, as expected, because of the ratio between layer resistivities, ρ_2/ρ_1 = 2.5. The program SLINV can not handle the shift because it is not fed into the program. The "corrected" continuous curve fed to SLINV, depends on the interpreter criteria.

Prior to interpretation of sounding 135 by SLINV, it was manually "corrected", by lifting all the segment measured with P = 2.5 m, until it tied in with the segment measured with P = 10.0 m.

In this case, the model from SLINV has higher resistivity values for the second layer than ELLIPSE. Sounding 135 is particularly troublesome in the deeper part. The measured ρ_a values spread a lot. Both programs take the best fitted curve, in the least-squares sense, but ELLIPSE is able to model the shifts.

Table 2 shows the comparison for sounding 185, a curve almost without shifting (see Reyes, 1989):

SOUNDING 185			
RESISTIVITY [Ωm]		THICKNESS [m]	
SLINV	ELLIPSE	SLINV	ELLIPSE
823	997	1.6	1.9
238766	19332	2.6	2.8
3175	3666	121	102
263	356	332	291
15	14.5	705	587
110	71		

Table 2 Inversion models for sounding 185, SLINV and ELLIPSE inversion

From table 2 it can be deduced, that the two resulting models are practically the same, as could be expected, since sounding 185 presents almost no shifting.

Although there is a marked difference between the models originating from the inversion using SLINV and ELLIPSE, respectively, it is interesting to note that they give very similar resistivity distribution. This tells, that even in extreme cases (high resistivity contrasts between layers, like sounding 135) SLINV gives sufficient results if the data are treated "correctly" prior to the inversion.

Two resistivity cross sections were made. Their location is shown in figure 4. Cross section A-A' runs NE-SW along Cerros Las Planillas rhyolitic dome, from Agua Caliente to La Cebada. Section B-B' crosses A-A' almost perpendicularly close to the steam vents, which are found at a relatively high elevation (2200 m a.s.l.). Two iso-resistivity maps were made, showing resistivity distribution at two different levels, 1.500 and 1.000 m a.s.l. Here, resistivity cross sections and iso-resistivity maps will be described.

Both cross sections were made using SLINV (see figure 5 and figure 7) and ELLIPSE (see figure 6 and 8), respectively. Each pair looks quite similar. Therefore for practical purposes only the ELLIPSE inversion will be discussed. The iso-resistivity maps were drawn according to the results from the ELLIPSE inversion.

Resistivity cross section A-A' (figure 6) crosses Cerros Las Planillas rhyolitic dome from SW to NE. It includes 13 soundings with half the current electrode spacing (S) ranging from 40 up to 3.000 m. The surface layers have a thickness around 150 m and a resistivity of about 1.500 Ωm or higher. This must correspond to the rhyolites and the dry part of the Tala Tuff.

Beneath the surface layers there is a layer with resistivity of 100-1.500 Ωm which must correspond to partially saturated rocks, with high resistivity water or low porosity layers mainly belonging to the upper Cordilleran volcanics (lithic tuff). Below these layers there is a resistivity low, stretching to the east and to the west as far as the cross section has been drawn.

At both the western and the eastern branch of the profile there is a resistivity high beneath the resistivity low. Between soundings 004 and 152, higher resistivity beneath the resistivity low is not found. Below sounding 162 there is a structure characterized by resistivity values of 100-1.500 Ωm. It might reflect an impermeable barrier.

Resistivity cross section B-B' (figure 8) runs from NW to SE. It includes 9 soundings and presents the same high resistivity surface layers as cross section A-A'. They must correspond to the surface rhyolites and the dry Tala tuff formations. The second series of layers, of 100-1.500 Ωm resistivity values, must correspond mainly to the lithic tuff (upper Cordilleran). The extension of the low resistivity is well defined by relatively resistive structures at both sides, NW and SE.

The general picture of the resistivity structure at Planillas Geothermal Field, Mexico is shown on two iso-resistivity maps. Figure 9 shows the resistivity at 1.500 m a.s.l. and figure 10 shows the resistivity at 1.000 m a.s.l. The figures show the location of the hot springs and the steam vents as well.

Figure 9 shows a low resistivity, described by the 40 Ωm contour line. It presents a NW-SE trend. The 30 and 20 Ωm contour lines have the same trend. Outside this anomaly the resistivity increases. They are not well defined though. In figure 10, the 20 Ωm contour line presents the same trend, NW-SE. But it also has a mixed trend, running N-S. Outside this anomaly the resistivity increases.

Figure 11 shows a division of Planillas Geothermal Field into resistivity zones, depending on three different categories of soundings. These categories are: The resistive or ascending type (resistivity higher than 40 Ωm at depth), the conductive or descending type (resistivity less than 40 Ωm at depth) and the higher resistivity below the low resistivity or bowl type.

The division shows the general resistivity distribution but more importantly it suggests a probable flow mechanism of the geothermal fluids in the area.

The conductive zone is flanked to the east and to the west by resistive zones and at some parts there is a bowl type zone, at the intersection between the resistive and conductive zones. This could be explained as being due to flow of geothermal fluids ascending within the limits of the conductive zone and laterally leaking into the bowl type zone. The resistive zone could be caused by low porosity or lower temperatures.

5.3.3 Two-dimensional interpretation

Profile A-A' (for location see figure 4) was interpreted two-dimensionally, taking the topography into account. In two-dimensional interpretation the resistivity is assumed to change both with depth and in the direction of the profile but not perpendicular to it. Two-dimensional interpretation is described in chapter 4.2.

The profile consists of 10 soundings, all of them laying parallel to the profile. The resistivity cross section resulting from the one dimensional interpretation (see figure 6) was used as a starting model for the two-dimensional interpretation. After the model had been changed several times, an acceptable model was found. It is is shown in figure 12. The location of the soundings, the hot springs and the steam vents are

shown as well. The curves for the calculated and measured apparent resistivity are published in a separate report (Reyes, 1989). They show how well the model data fits with the measured date for each sounding.

The general distribution of resistivity is different from the one-dimensional case in many ways. For instance, the influence on neighbouring soundings is taken into account in the two-dimensional program. The apparent resistivity curve of some soundings shows a low resistivity mainly caused by their vicinity to low resistivity rather than the resistivity structure beneath them. The resistivity values resulting from one-dimensional interpretation seem in some cases to be overestimated and a narrower low resistivity distribution better defined between soundings 158 and 161 is revealed by the two-dimensional modelling.

The two-dimensional model is characterized by a resistivity low of resistivity less than 15 Ωm and 3.5 km wide in the southwestern slopes of Cerros Las Planillas. This main anomaly is narrower and better defined than in the one-dimensional model. It is bordered by a resistivity high on both sides. To the east and to the west of this anomaly there is a low resistivity, having higher resistivity beneath the low resistivity. Inside the main low resistivity anomaly there is a narrower anomaly, 1.2 km wide and having a resistivity of 7 Ωm.

At the eastern border of the main anomaly, there are steam vents at a relatively high elevation suggesting that the ascending path of this steam is stretched by the border between high and low resistivity values. At the western border of the main anomaly, there are hot springs at a relatively low elevation suggesting a near vertical convection cell.

Application of the FELIX program for two-dimensional interpretation of profile A-A' results in a more clear picture of the resistivity distribution with both depth and horizontal direction.

5.4 Results

One-dimensional interpretation of Schlumberger soundings from Planillas Geothermal Field indicates a low subsurface resistivity anomaly (resistivity less than 40 Ωm). At 1.500 m a.s.l. the anomaly presents a NW-SE trend. It continues at greater depths (1.000 m a.s.l.) with the same NW-SW trend together with an additional mixed N-S trend having lower resistivity values (less than 20 Ωm).

The geothermal fluids associated with Primavera Geothermal Area are stored in extensional strike slip faults with NW-SE orientation, within the lower Cordilleran volcanics (andesites), reactivated and opened by a vertical stress field. Primavera Geothermal Area is located 7 km north of Planillas Geothermal Field. The same geological formations, i.e. lower Cordilleran volcanics are located beneath Planillas Geothermal Field. Two-dimensional interpretation of a profile perpendicular to the low resistivity anomaly suggests an over estimation of the resistivity values in the one-dimensional interpretation, due to lateral and topographic effects. The two-dimensional interpretation is characterized by a less than 15 Ωm anomaly, 3.5 km wide in the southwestern slopes of Las Planillas flanked by two relatively resistive structures, reaching towards the surface. At the NE flank there are steam vents and near the SW flank hot springs are found, at a relatively low elevation. Inside this main anomaly there is a narrower anomaly, 1.2 km wide having a resistivity of 7 Ωm. This suggests a possible vertical flow of geothermal fluids in the middle of the low resistivity anomaly probably convecting along an open fault oriented NW-SE within the lower Cordilleran volcanics and leaking laterally SW and NE into the upper Cordilleran volcanics (lithic tuffs).

The interpretation of Schlumberger soundings from Planillas Geothermal Field has proved to be of great importance in the understanding of the geothermal field. It has also showed that one-dimensional interpretation is not adequate. Two-dimensional interpretation is necessary where the rugged terrain of the area is taken into account. For that purpose more Schlumberger soundings are needed. They ought to be densely spaced (of no more than 500 m between soundings) and oriented along profiles, both parallel and perpendicular to the resistivity anomaly. It is quite possible that the much less time consuming and less expensive Transient Electromagnetic Method (TEM) could give the information needed on the resistivity distribution.

6. CONCLUSION

The depth of penetration of Schlumberger soundings is controlled by the shortest distance between the current electrode and the potential electrode (S-P). This together with the actual use of the finite potential electrodes separation over a resistivity distribution with high contrasts between layers and lateral resistivity variations near the surface at the sounding site, causes converging and constant shifts of the different segments of the apparent resistivity curve. These shifts, if not correctly treated will lead the interpretation astray. The theory of one-dimensional interpretation of Schlumberger soundings is presented in this report in some detail to understand the reasons for these shifts and to make an appropriate use of two computer programs for one-dimensional interpretation. A two-dimensional interpretation program, which takes the topography into account, is also discussed.

One-dimensional interpretation of Schlumberger soundings from Planillas Geothermal Field indicates a low subsurface resistivity anomaly. Two-dimensional interpretation of a profile perpendicular to the low resistivity anomaly is characterized by a less than 15 Ωm anomaly, 3.5 km wide in the southwestern slopes of Las Planillas flanked by two relatively resistive structures, reaching towards the surface. At the NE flank there are steam vents and near the SW flank hot springs are found, at a relatively low elevation. Inside this main anomaly there is a narrower anomaly, 1.2 km wide having a resistivity of 7 Ωm. This suggests a possible vertical flow of geothermal fluids in the middle of the low resistivity anomaly probably convecting along an open fault oriented NW-SE within the lower Cordilleran volcanics and leaking laterally SW and NE into the upper Cordilleran volcanics (lithic tuffs).

The interpretation of Schlumberger soundings from Planillas Geothermal Field has proved to be of great importance in the understanding of the geothermal field. A more detailed resistivity survey of the area is suggested. This could either be densely spaced Schlumberger soundings, oriented along profiles and interpreted two-dimensionally taking the rugged terrain into account. Or possibly the much less time consuming and less expensive Transient Electromagnetic Method (TEM).

ACKNOWLEDGEMENT

The author wants to express his profound gratitude to his advisor Gylfi Páll Hersir for his unselfish and unwearied support during the whole training programme. Many thanks go also to Knútur Árnason both for reviewing this manuscript and for writing the SLINV program and for his donation to UNU fellows. Dr. Ingvar Birgir Fridleifsson is thanked for organizing the programme. The author is indebted to Ing. Miguel Ramirez G. and Ing. Antonio Razo M. for their intervention to allow him to participate in this important training.

REFERENCES

Archie, G.E., 1942: The Electrical Resistivity Log as an Aid in Determining some Reservoir Characteristics. Tran. AIME, 146, pp 54-67.

Árnason, K., 1984: The Effect of Finite Potential Electrode Separation of Schlumberger Soundings. 54th Annual International SEG Meeting, Atlanta, Extended abstracts, pp 129-132.

Árnason, K., 1989: Central Loop Transient Electromagnetic Soundings Over a Horizontally Layered Earth. National Energy Authority of Iceland. OS-89032/JHD-06, 129 p.

Árnason, K. and Hersir, G.P., 1988: One Dimensional Inversion of Schlumberger Resistivity Soundings. Computer Program Description and User's Guide. UNU Geothermal Training Programme, Report 8, 59 p.

Árnason, K. and Hersir, G.P., 1989: Geophysical survey at Nesjavellir high-temperature area. SW-Iceland. Manuscript.

Caldwell, G., Pearson, C. and Zayadi, H., 1986: Resistivity of Rocks in Geothermal Systems: A Laboratory Study. Proc. 8th Geothermal Workshop, pp 227-231.

Dakhnov, V.N., 1962: Geophysical Well Logging, Q. Colo. Sch. Mines, 57 (2), 445 p.

Flóvenz, Ó.G., 1984: Application of the Head-on Resistivity Profiling Method in Geothermal Exploration. Geothermal Resources Council, Transactions. Vol. 8, pp 493-498.

Flóvenz, Ó.G., Georgsson, L.S. and Árnason, K., 1985: Resistivity Structure of the Upper Crust in Iceland. Journal of geophysical research. Vol.90, no.B12, pp. 10,136-10,150.

Hersir, G.P., 1988: Correcting for the Coastal Effect on the Apparent Resistivity of Schlumberger Soundings. Orkustofnun OS-880 19/JHD-10 B, 13 p.

Hersir, G.P., 1989: Geophysical Methods in Geothermal Exploration. UNU Geothermal Training Programme.

Hersir, G.P. and Árnason K., 1989: Schlumberger Soundings Over a Horizontally Stratified Earth. Theory, instrumentation and user's guide to the computer program ELLIPSE. UNU Geothermal Training Programme.

JICA, 1988: La Primavera Geothermal Development Project in Mexican United States, final report. Japan international cooperation agency.

Koefoed, O., 1979: Geosounding Principles 1, Resistivity sounding measurements. Elsevier Scientific Publishing Company.

Reyes, V.P., 1988: Resistivity, Induced Polarization, Gravimetry and Magnetometry applied on Los Negritos, Mich. Geotermia, revista mexicana de geoenergia. Vol 4 no. 3, 211 p. In Spanish.

Reyes, V.P., 1989: Appendices to the report: Resistivity methods with application to Planillas Geothermal Field, Mexico. UNU Geothermal Training Programme.

Stefansson, V., G. Axelsson and O. Sigurdsson, 1982: Resistivity Logging of Fractured Basalts. In: Proceedings of Eight Workshop Geothermal Reservoir Engineering, Stanford University, Stanford Calif., pp 189-195.

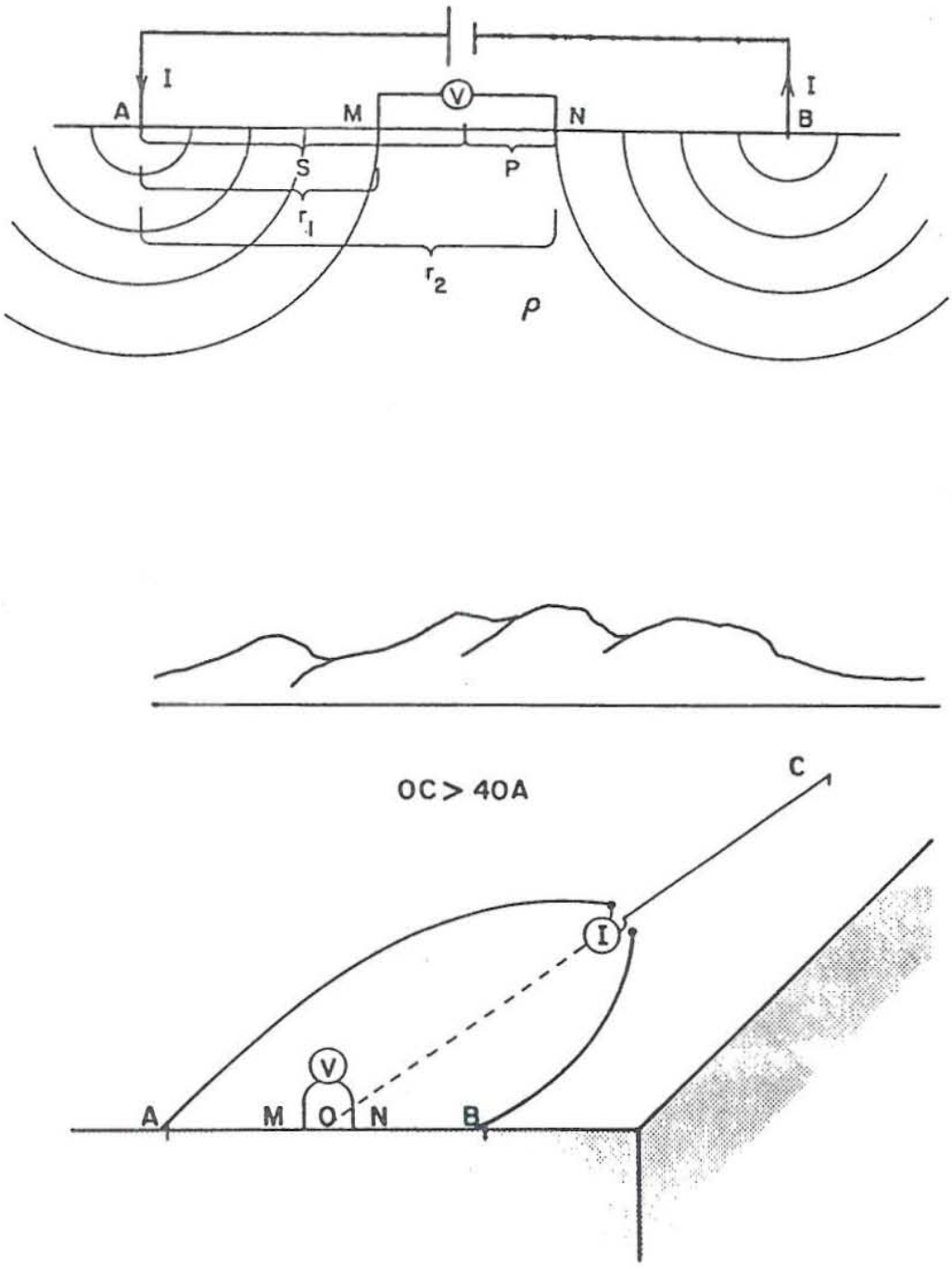

Figure 1 Schlumberger arrangement and Head-on configurations

The uppermost figure shows the Schlumberger configuration while the lowermost one shows the Head-on configuration

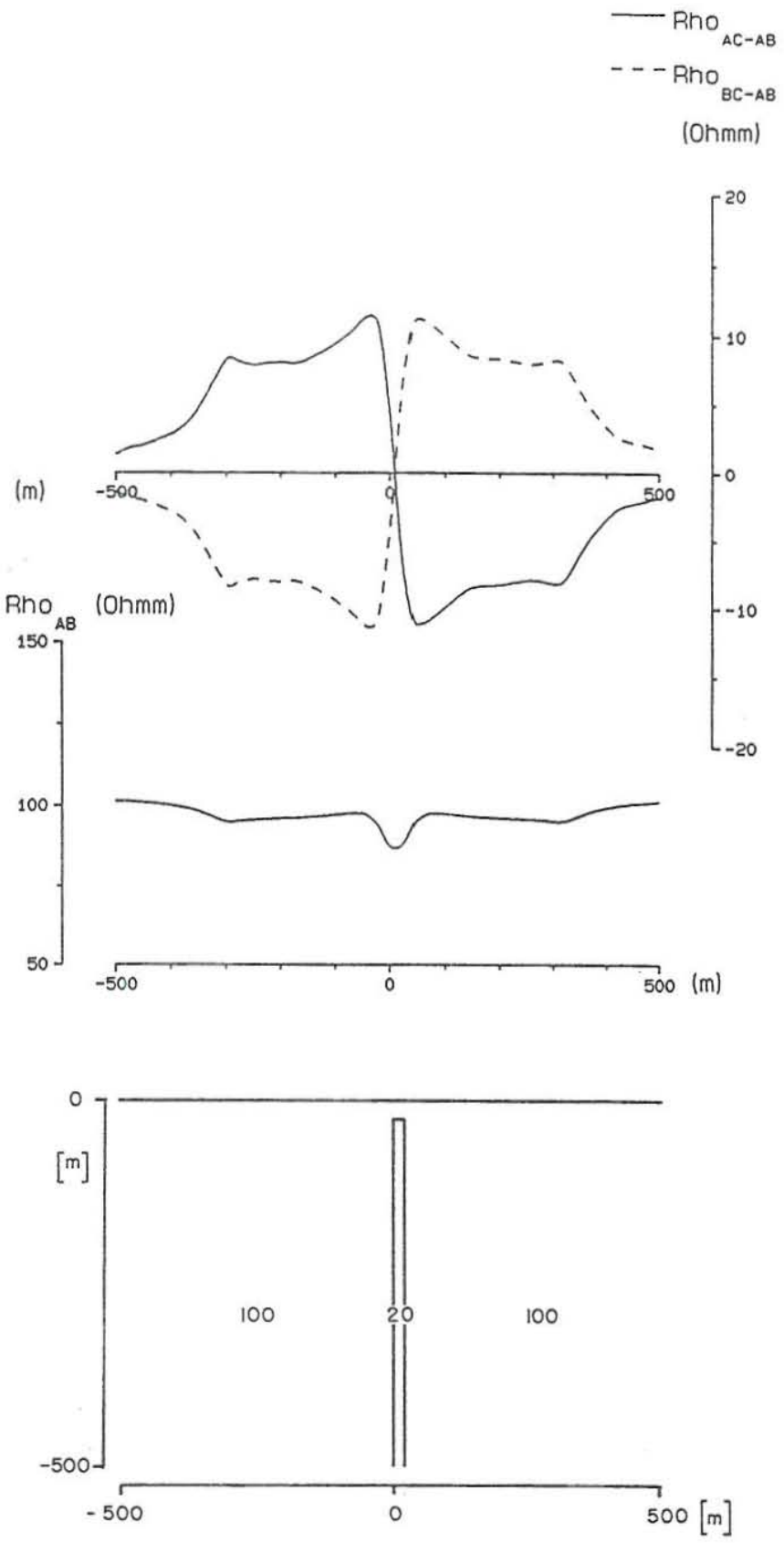

Figure 2 Head-on profiling over conductive vertical structure

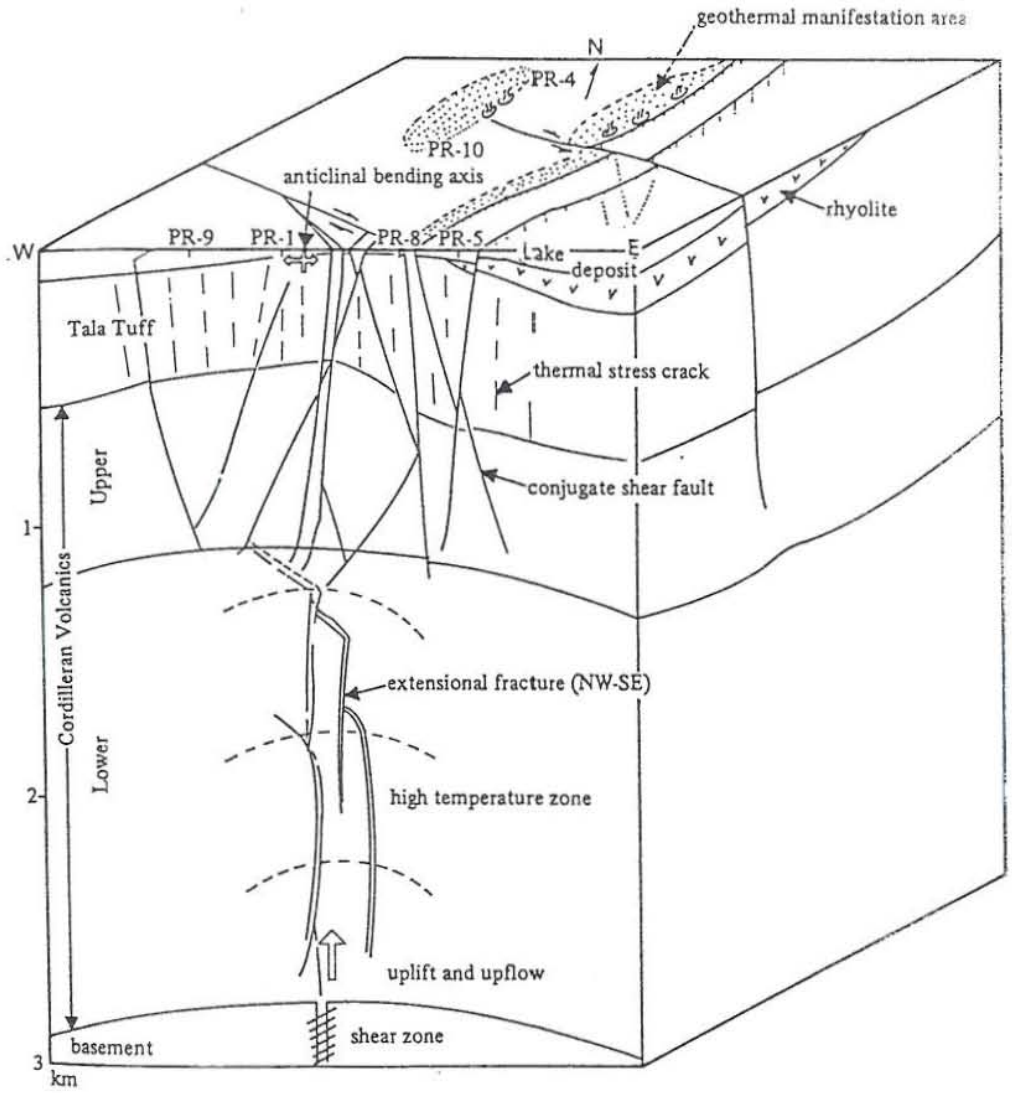

Figure 3 Primavera Geothermal Area, Mexico. Conceptual model showing the different geological units present in the area together with the associated structural system (after JICA, 1989)

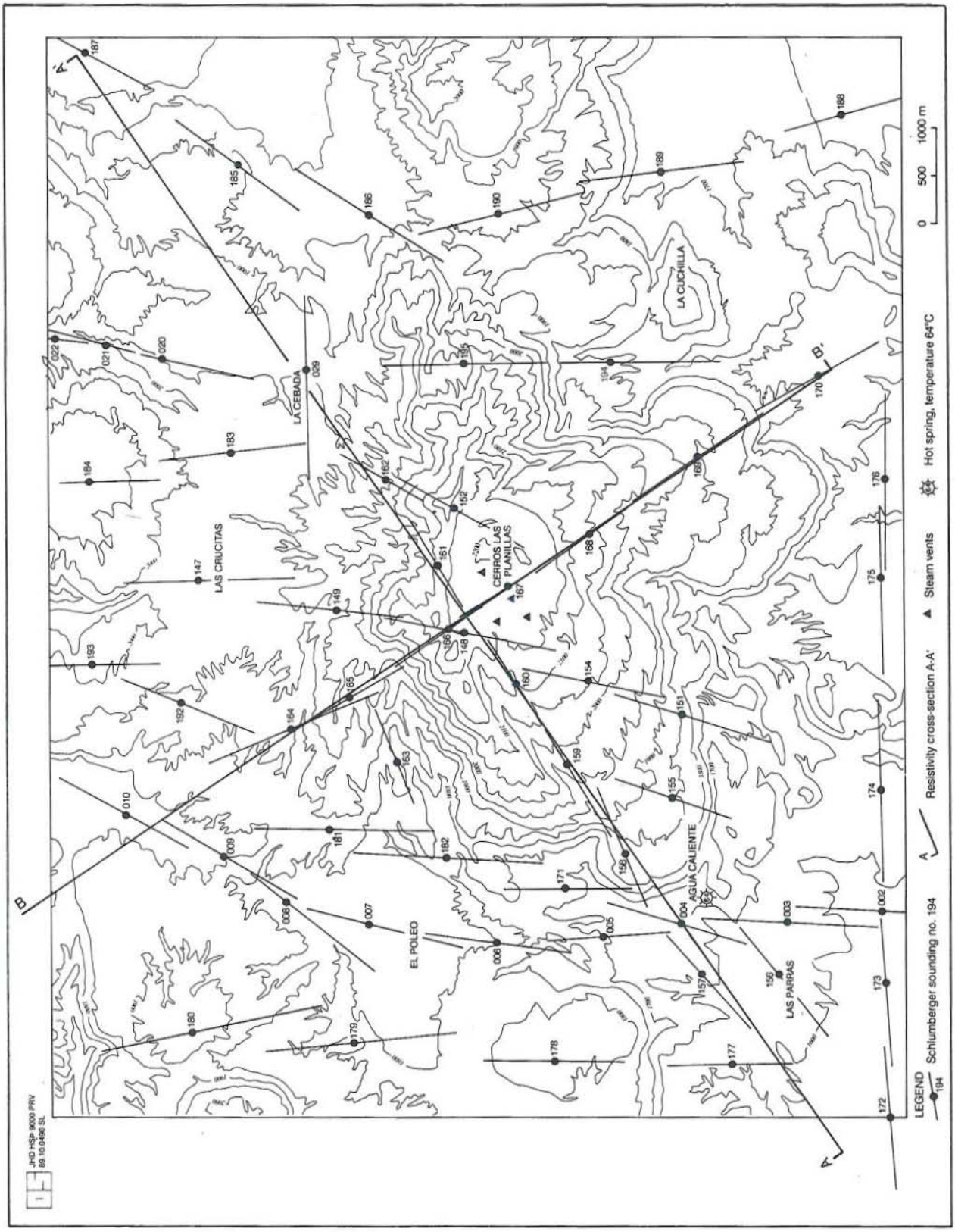

Figure 4 Location map of Schlumberger soundings at Planillas Geothermal Field, Mexico

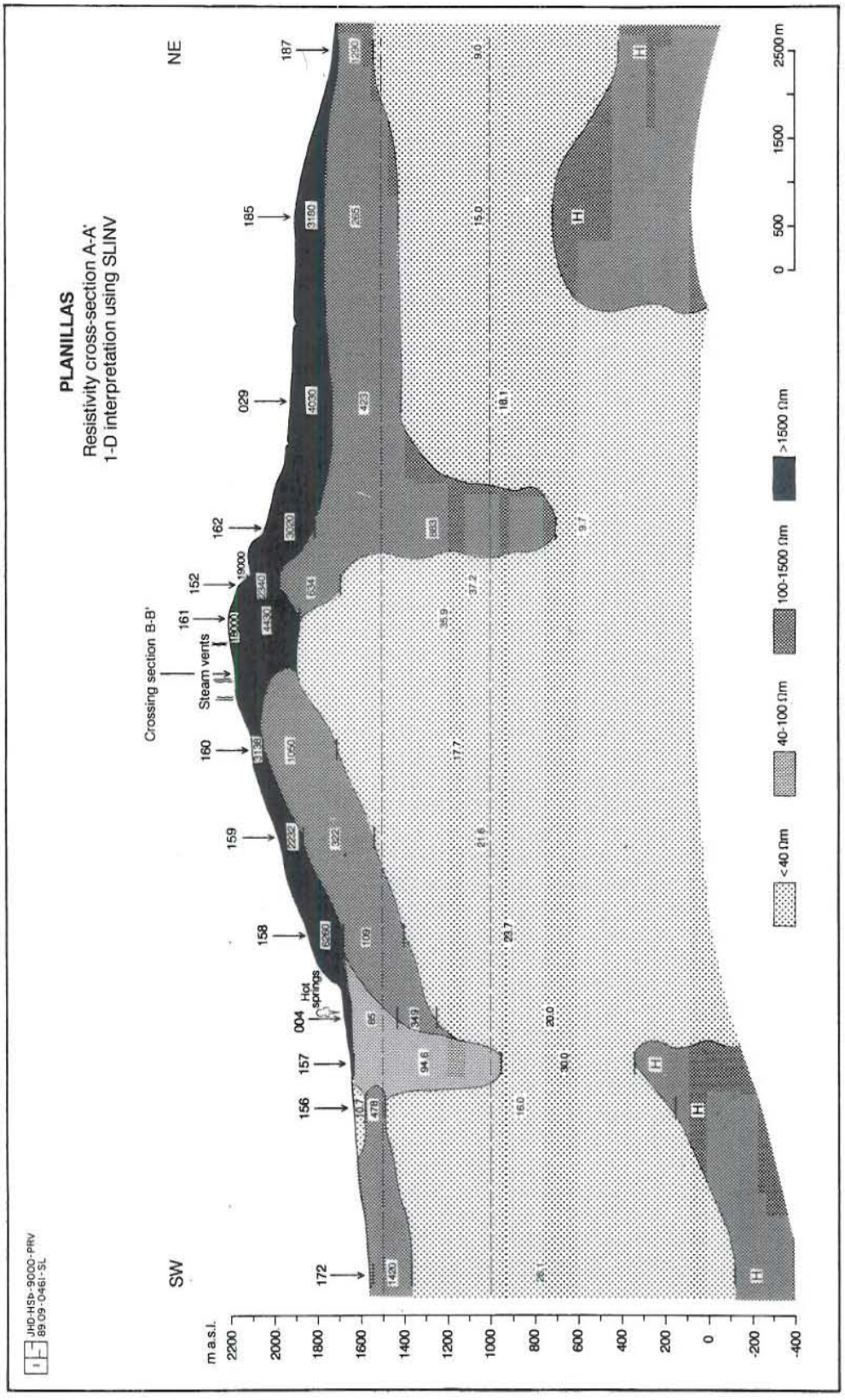

Figure 5 Resistivity cross section A-A', 1-D SLINV-inversion

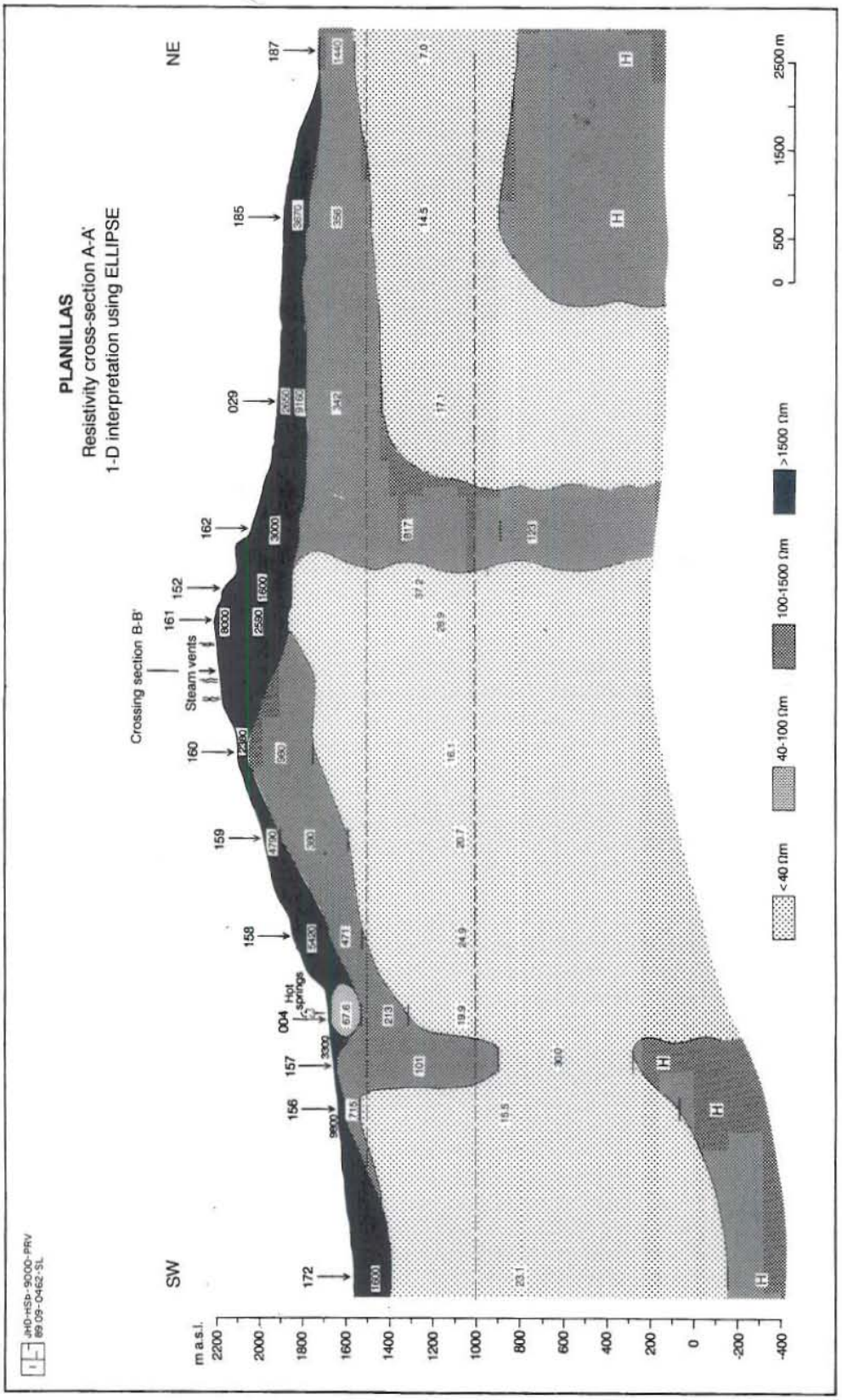

Figure 6 Resistivity cross section A-A', 1-D ELLIPSE-inversion

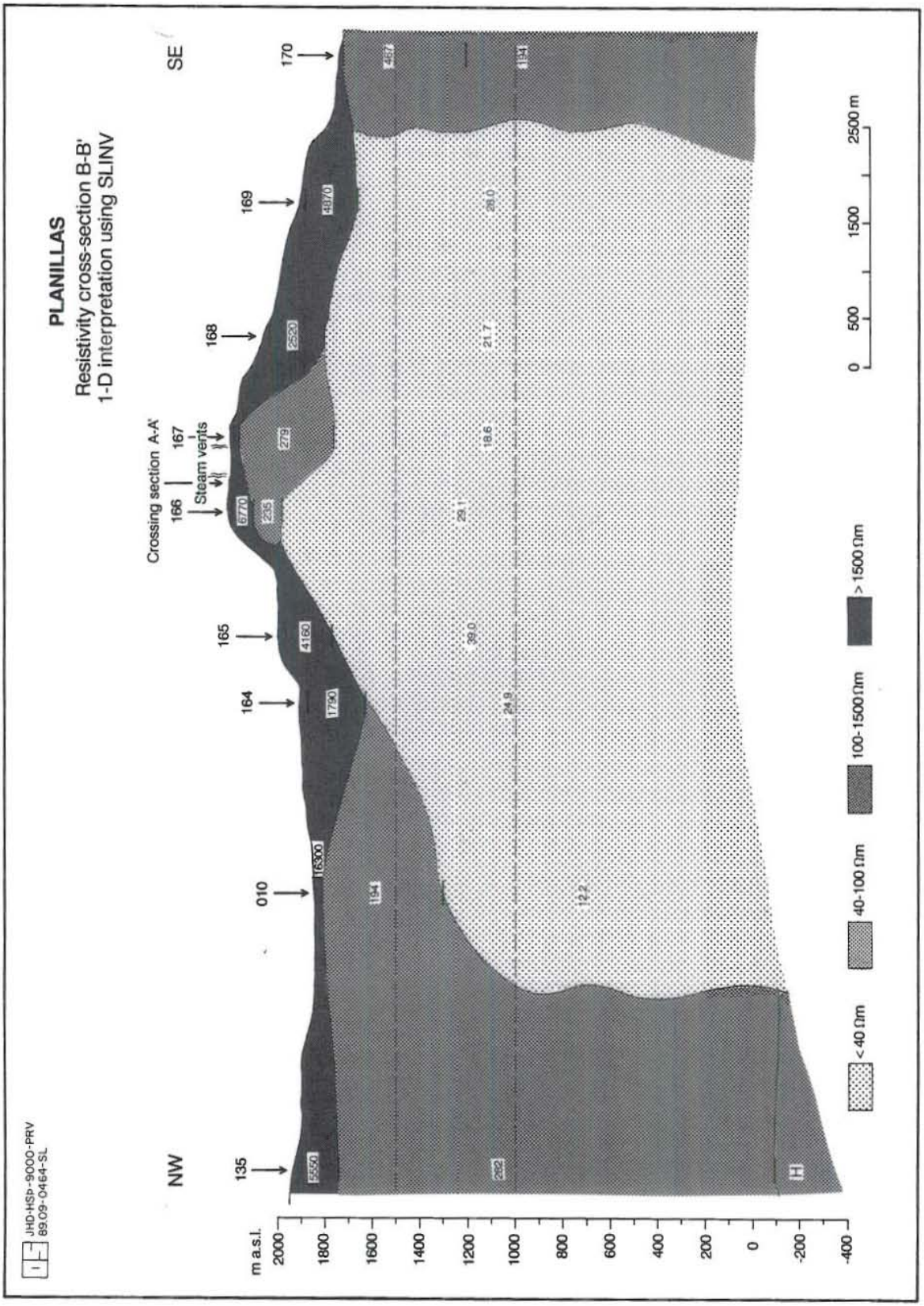

Figure 7 Resistivity cross section B-B', 1-D SLINV-inversion

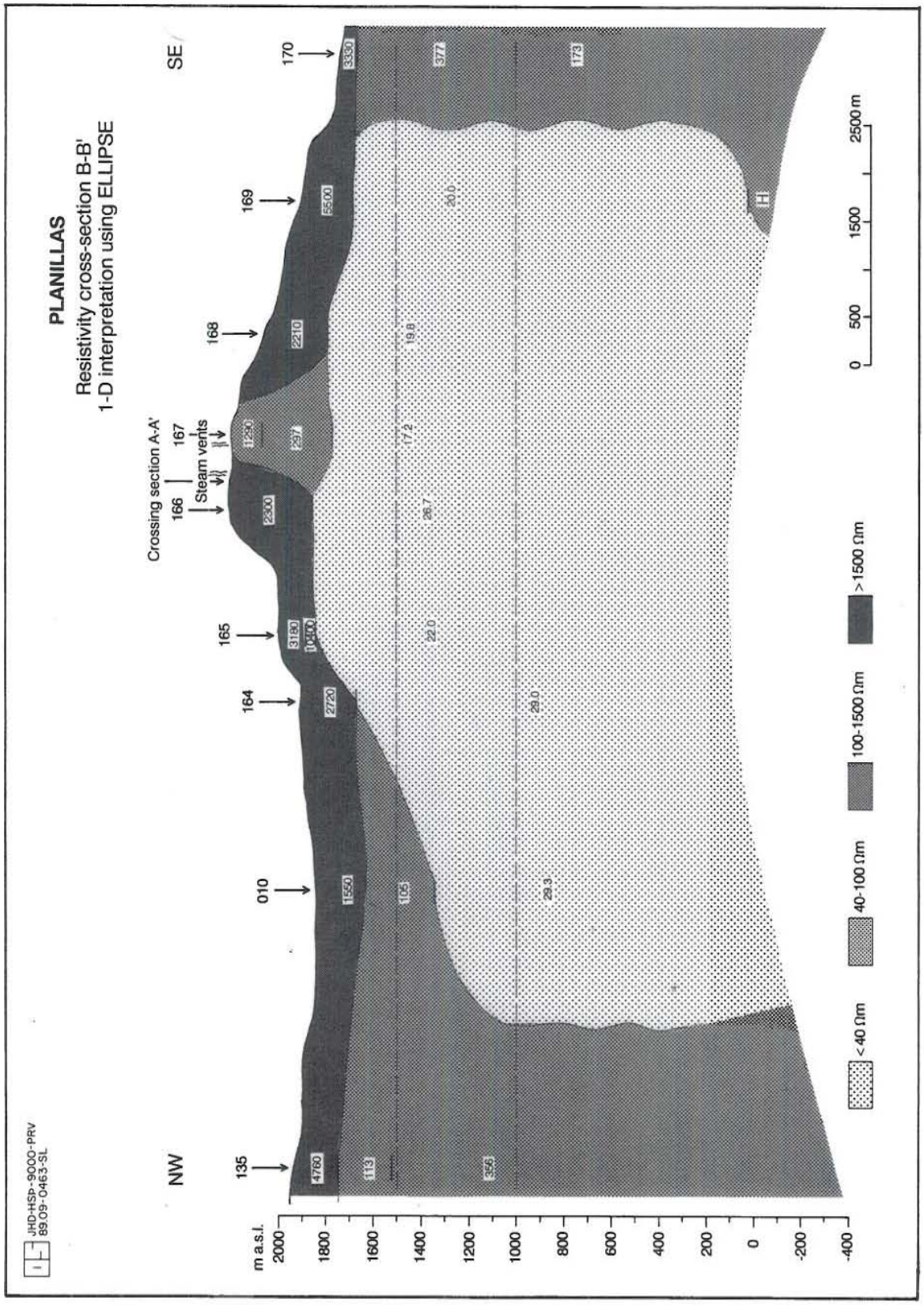

Figure 8 Resistivity cross section B-B', 1-D ELLIPSE-inversion

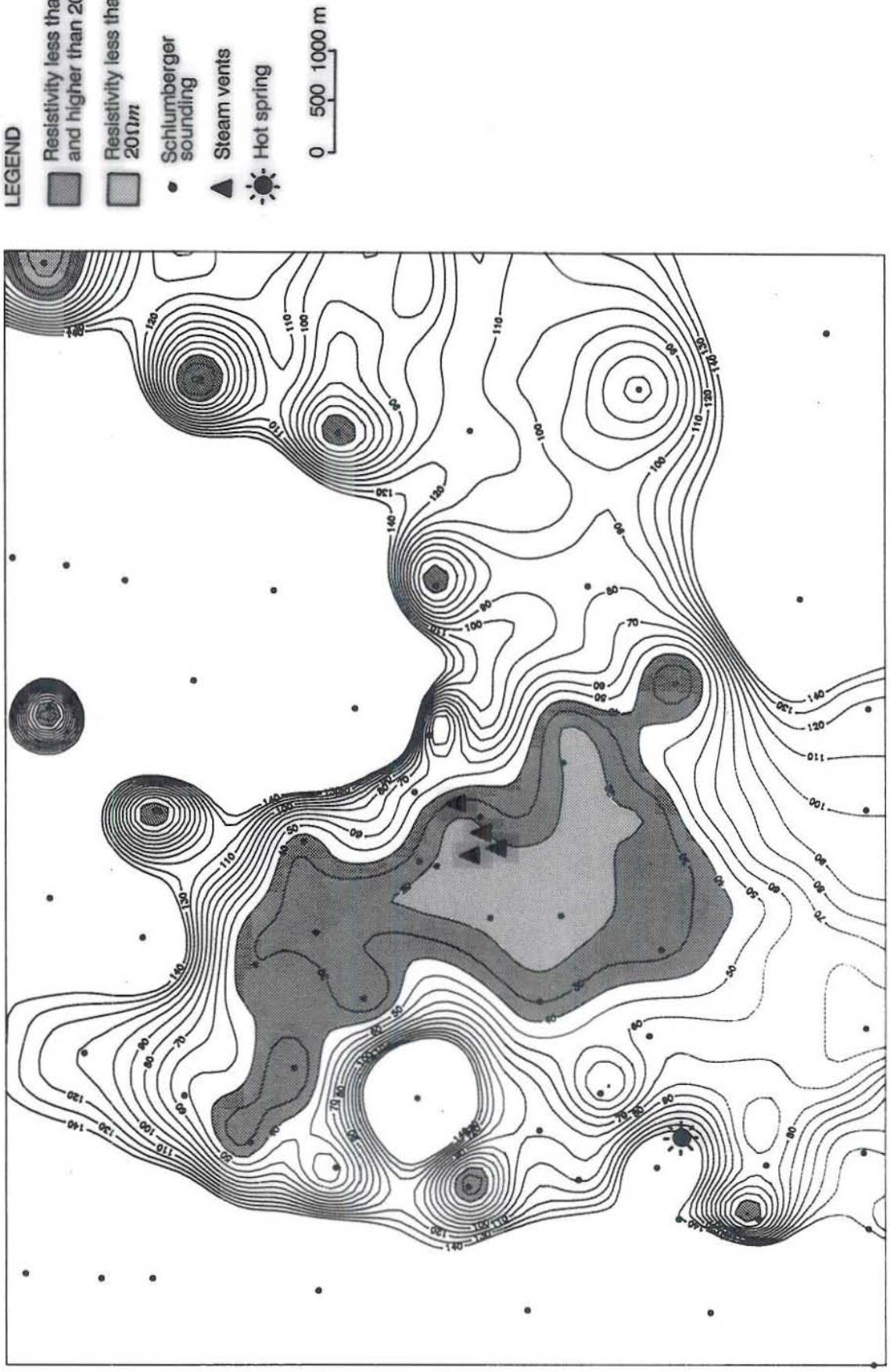

Figure 9 Iso-resistivity map at 1.500 m a.s.l.

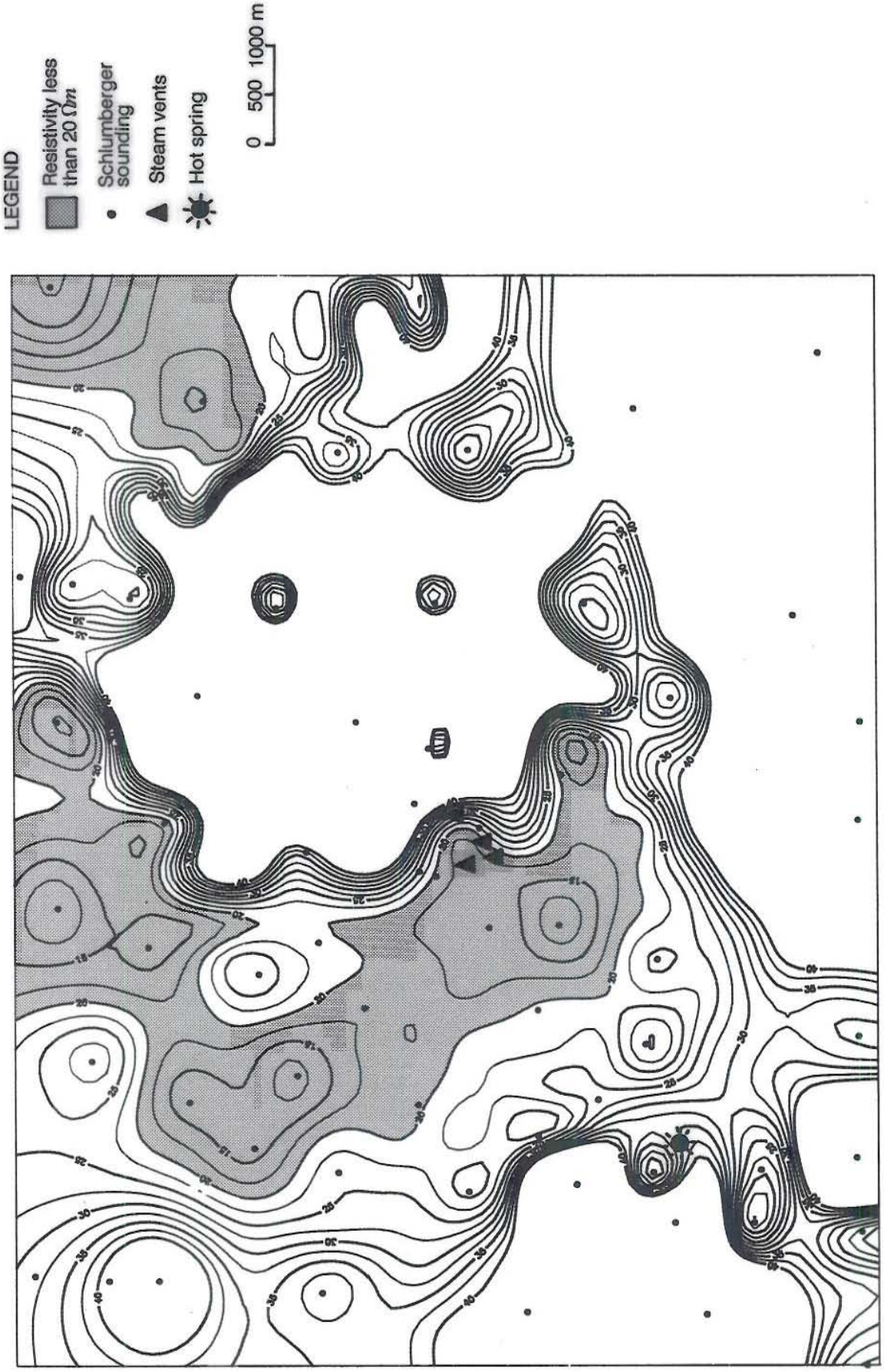

Figure 10 Iso-resistivity map at 1.000 m a.s.l.

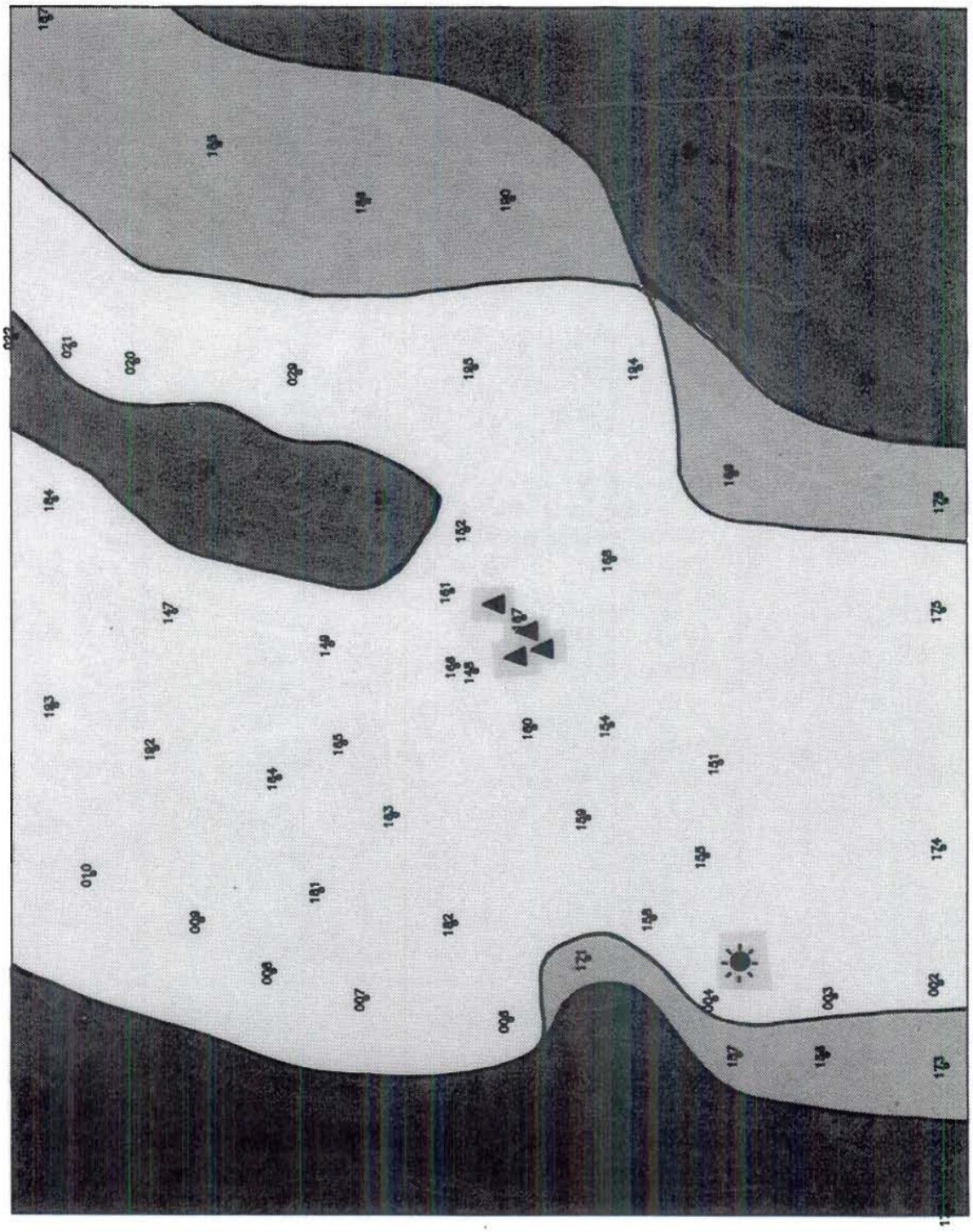

Figure 11 Areas of different resistivity categories

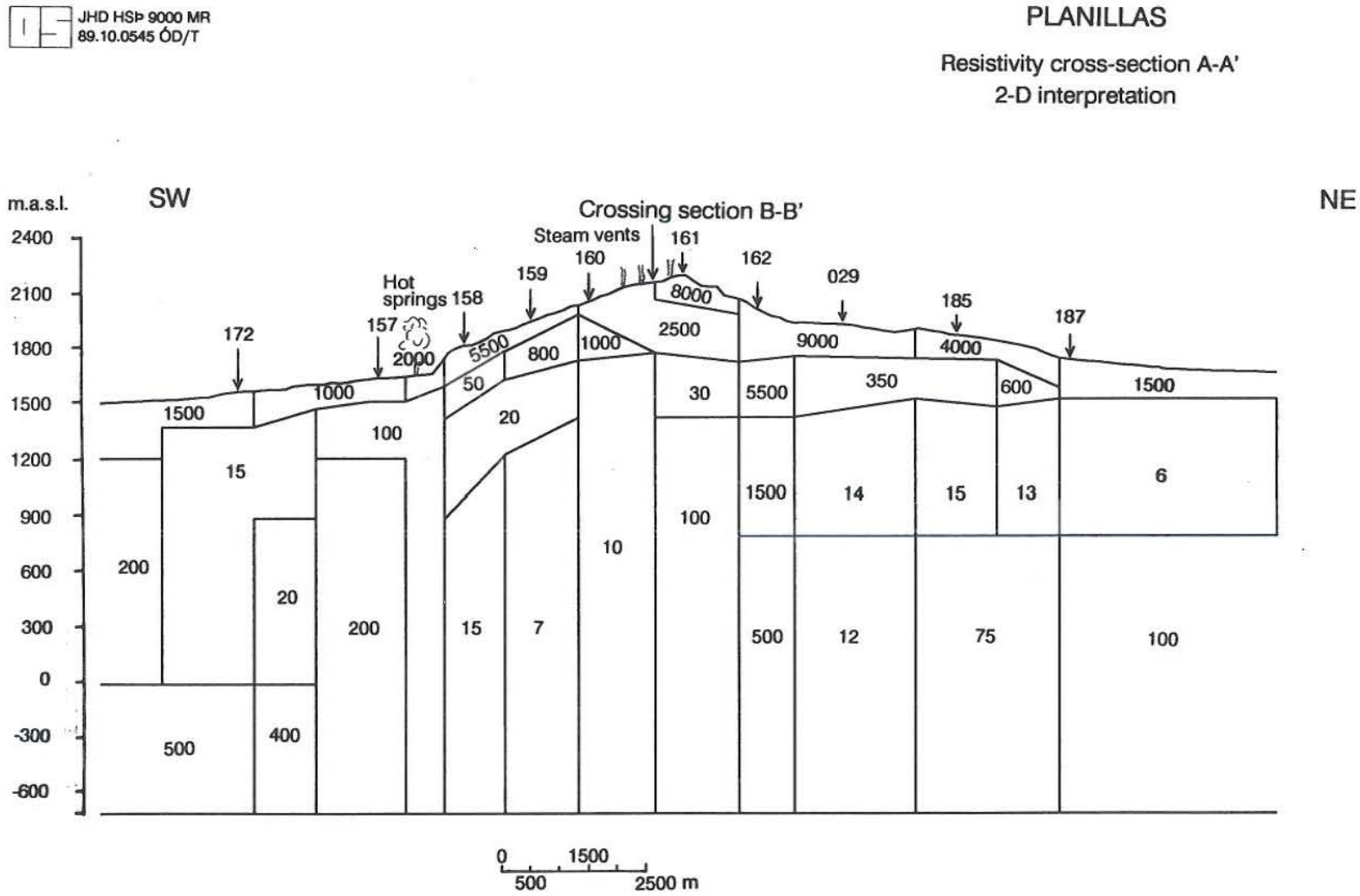

Figure 12 Two-dimensional resistivity model for profile A-A

1989

APPENDICES TO THE REPORT: RESISTIVITY METHODS WITH APPLICATION TO PLANILLAS GEOTHERMAL FIELD, MEXICO

Pablo Reyes Vermot
UNU Geothermal Training Programme
National Energy Authority
Grensásvegur 9
108 Reykkjavík
ICELAND

Permanent Adress:
Comision Federal de Electricidad
Superintendencia General La Primavera
Km. 21+460 Periferico Norte Cd. Granja
Zapopan, Jalisco
MEXICO

These are the appendices to the report: Resistivity methods with application to Planillas Geothermal Field, Mexico: It was written by Pablo Reyes Vermot at the UNU Geothermal Training Programme in 1989. It is divided into three parts. The first two parts show the results of one dimensional interpretation (models, mean deviations and fits between measured and modelled data) using the SLINV program and the ELLIPSE program, respectively. The third part shows how well the calculated apparent resistivity curves from the two dimensional model (see figure 12 in the main report) fit with the measured curves.

APPENDIX I

One dimensional interpretation of Schlumberger soundings. SLINV-program:

Models, corresponding calculated apparent resistivity curves (shown as continuous curves) and measured apparent resistivity curves (shown as points).

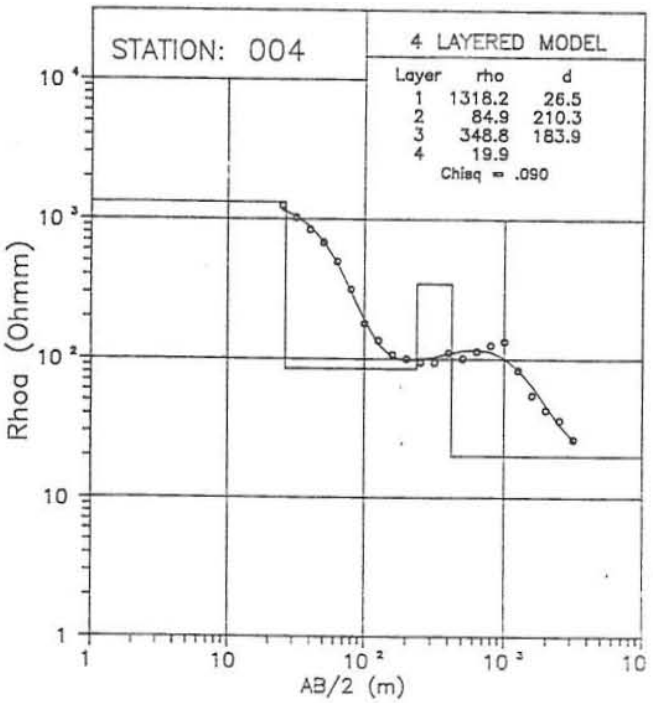
STATION: 004
4 LAYERED MODEL
Layer rho d
1 1318.2 26.5
2 84.9 210.3
3 348.8 183.9
4 19.9
Chisq = .090
Rhoa (Ohmm)
AB/2 (m)

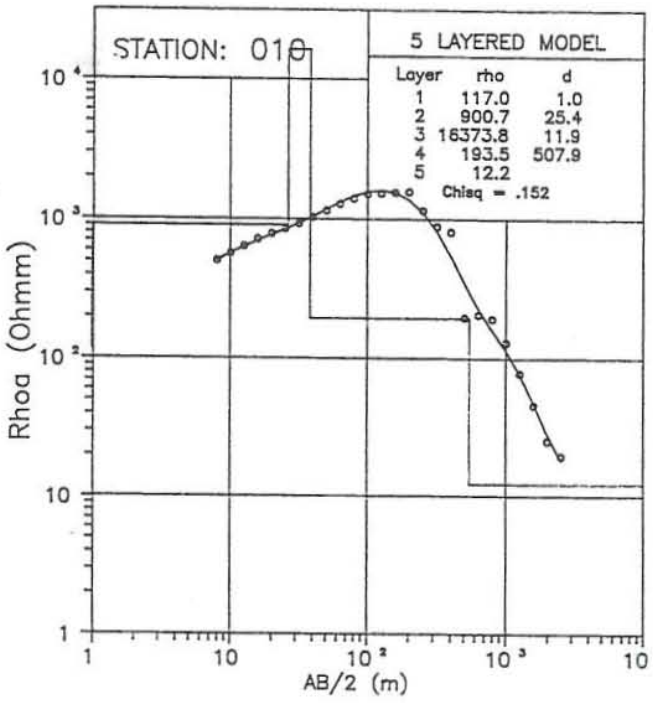
STATION: 010
5 LAYERED MODEL
Layer rho d
1 117.0 1.0
2 900.7 25.4
3 16373.8 11.9
4 193.5 507.9
5 12.2
Chisq = .152
Rhoa (Ohmm)
AB/2 (m)

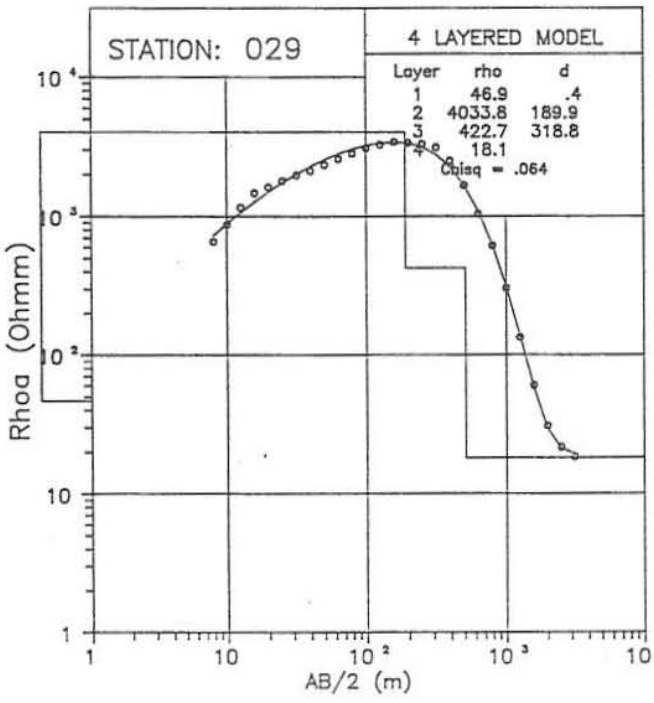
STATION: 029
4 LAYERED MODEL
Layer rho d
1 46.9 .4
2 4033.8 189.9
3 422.7 318.8
4 18.1
Chisq = .064
Rhoa (Ohmm)
AB/2 (m)

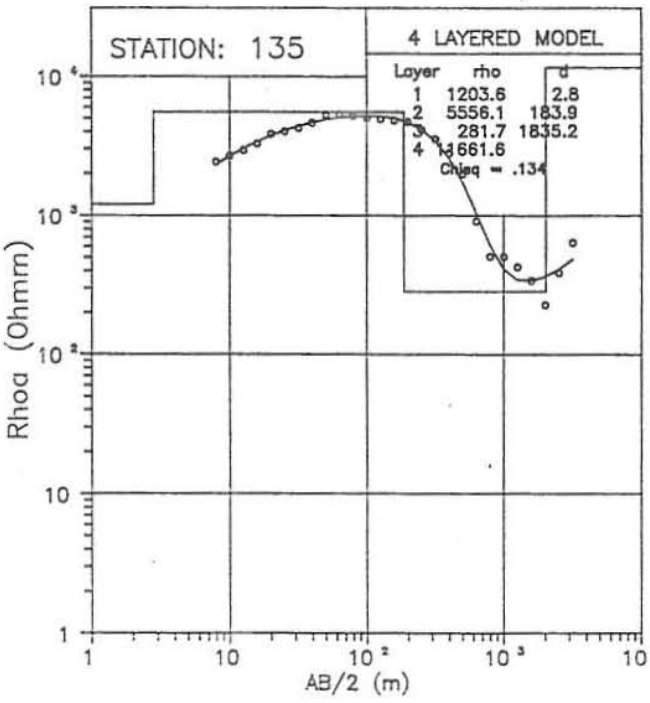
STATION: 135
4 LAYERED MODEL
Layer rho d
1 1203.6 2.8
2 5556.1 183.9
3 281.7 1835.2
4 13661.6
Chisq = .134
Rhoa (Ohmm)
AB/2 (m)

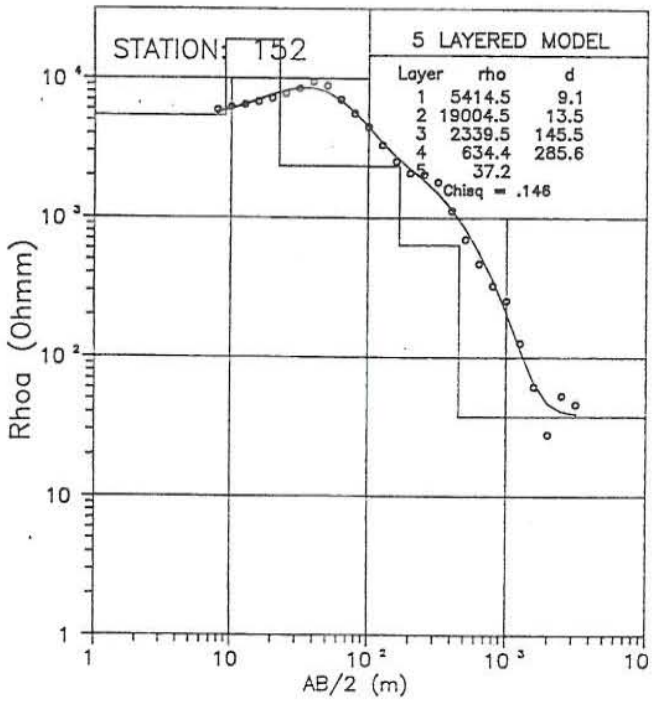
STATION: 152
5 LAYERED MODEL
Layer rho d
1 5414.5 9.1
2 19004.5 13.5
3 2339.5 145.5
4 634.4 285.6
5 37.2
Chisq = .146
Rhoa (Ohmm)
AB/2 (m)

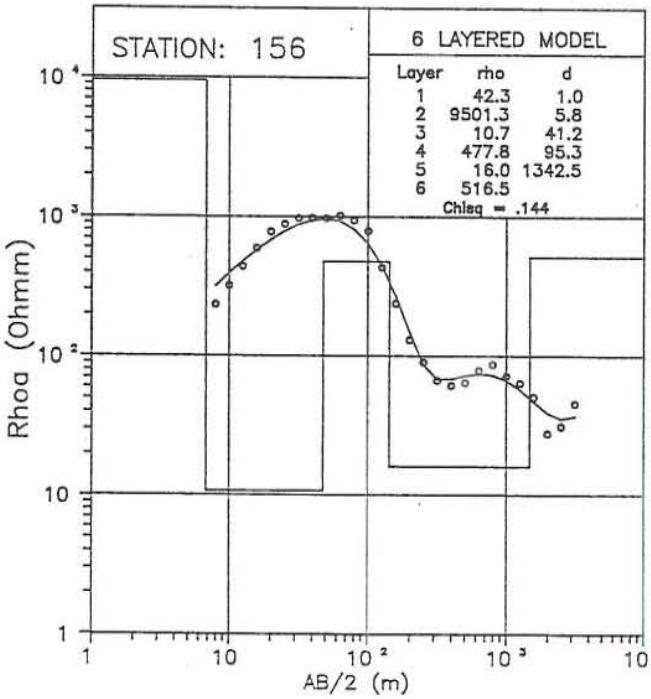
STATION: 156
6 LAYERED MODEL
Layer rho d
1 42.3 1.0
2 9501.3 5.8
3 10.7 41.2
4 477.8 95.3
5 16.0 1342.5
6 516.5
Chisq = .144
Rhoa (Ohmm)
AB/2 (m)

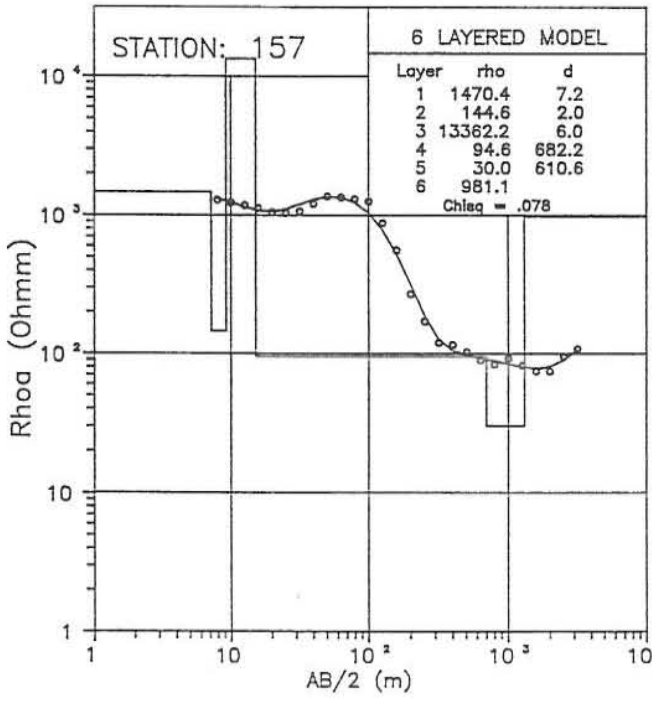
STATION: 157
6 LAYERED MODEL
Layer rho d
1 1470.4 7.2
2 144.6 2.0
3 13362.2 6.0
4 94.6 682.2
5 30.0 610.6
6 981.1
Chisq = .078
Rhoa (Ohmm)
AB/2 (m)

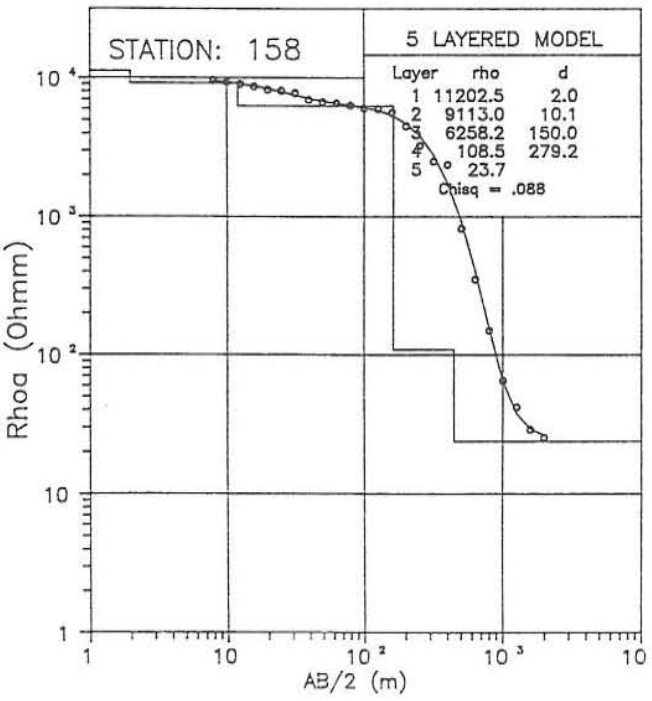
STATION: 158
5 LAYERED MODEL
Layer rho d
1 11202.5 2.0
2 9113.0 10.1
3 6258.2 150.0
4 108.5 279.2
5 23.7
Chisq = .088
Rhoa (Ohmm)
AB/2 (m)

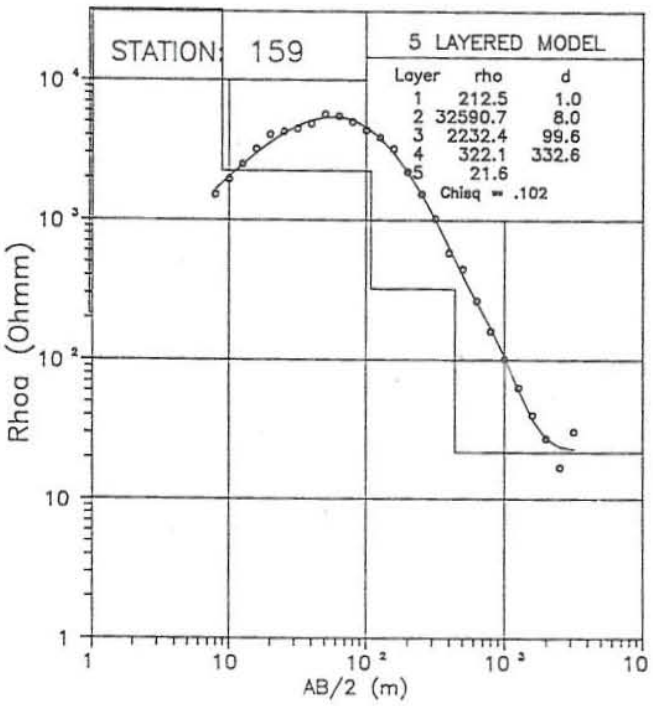
STATION: 159
5 LAYERED MODEL
Layer rho d
1 212.5 1.0
2 32590.7 8.0
3 2232.4 99.6
4 322.1 332.6
5 21.6
Chisq = .102
Rhoa (Ohmm)
AB/2 (m)

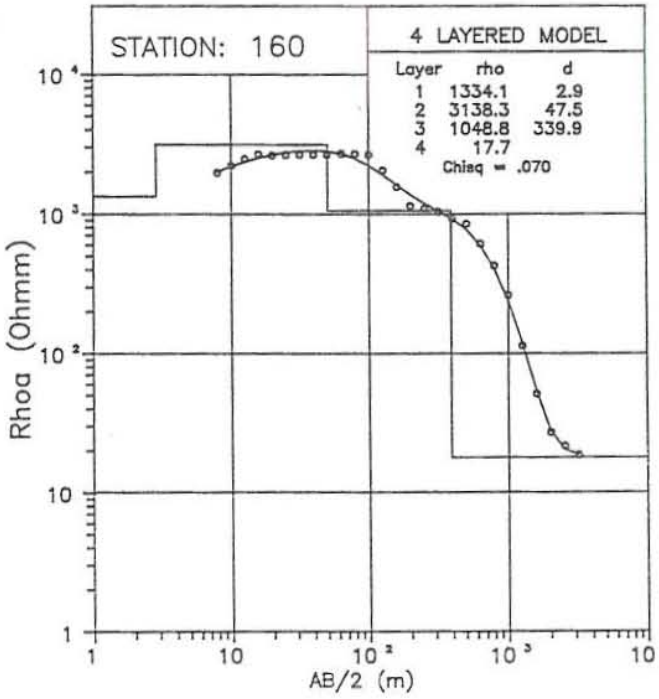
STATION: 160
4 LAYERED MODEL
Layer rho d
1 1334.1 2.9
2 3138.3 47.5
3 1048.8 339.9
4 17.7
Chisq = .070
Rhoa (Ohmm)
AB/2 (m)

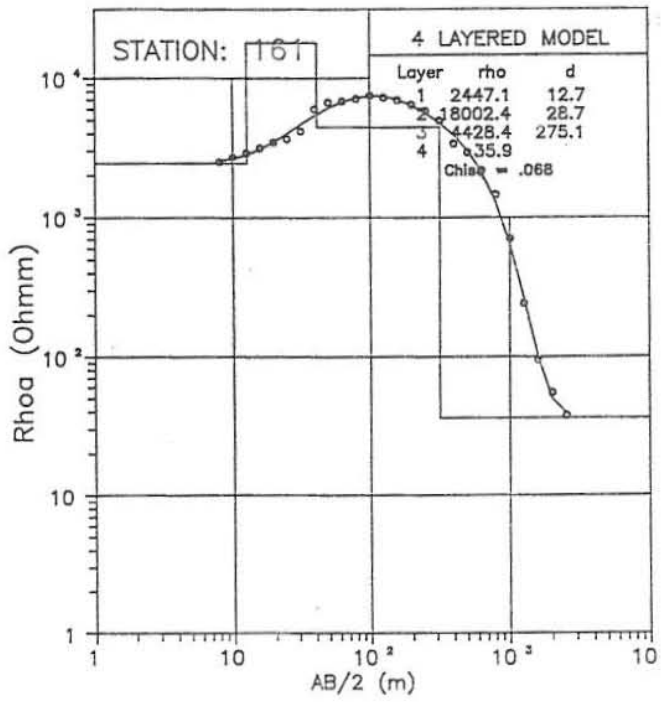
STATION: 161
4 LAYERED MODEL
Layer rho d
1 2447.1 12.7
2 18002.4 28.7
3 4428.4 275.1
4 35.9
Chisq = .068
Rhoa (Ohmm)
AB/2 (m)

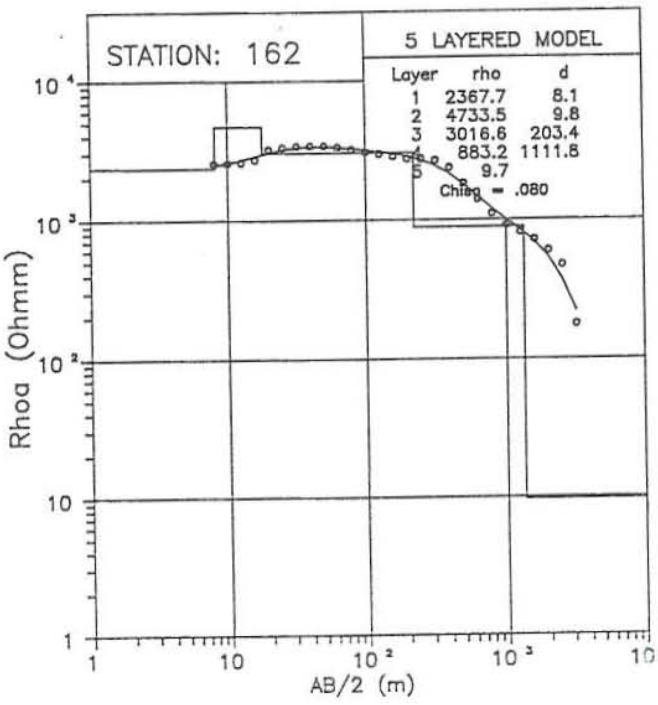
STATION: 162
5 LAYERED MODEL
Layer rho d
1 2367.7 8.1
2 4733.5 9.8
3 3016.6 203.4
4 883.2 1111.8
5 9.7
Chisq = .080
Rhoa (Ohmm)
AB/2 (m)

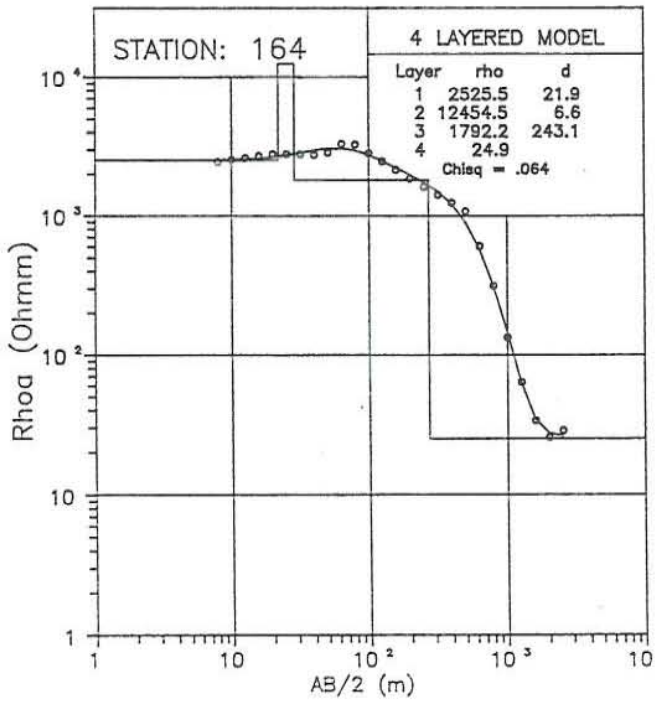
STATION: 164
4 LAYERED MODEL
Layer rho d
1 2525.5 21.9
2 12454.5 6.6
3 1792.2 243.1
4 24.9
Chisq = .064
Rhoa (Ohmm)
AB/2 (m)

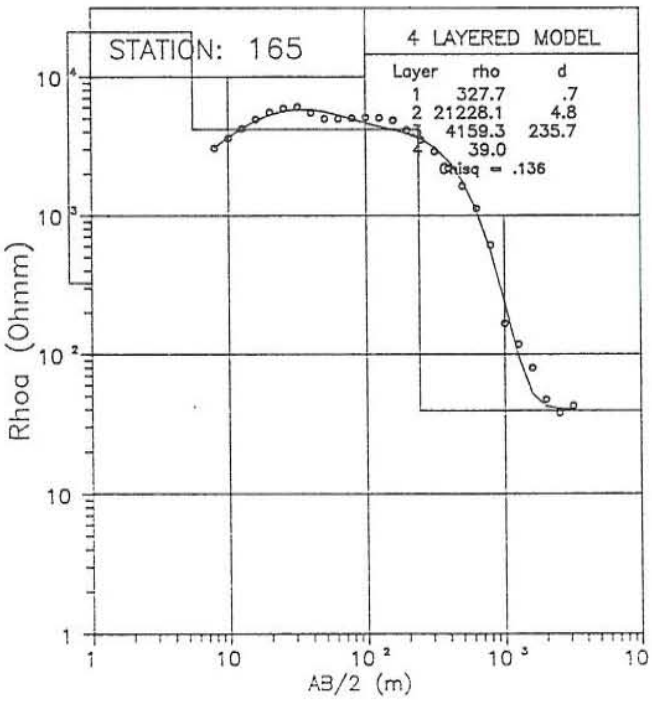
STATION: 165
4 LAYERED MODEL
Layer rho d
1 327.7 .7
2 21228.1 4.8
3 4159.3 235.7
4 39.0
Chisq = .136
Rhoa (Ohmm)
AB/2 (m)

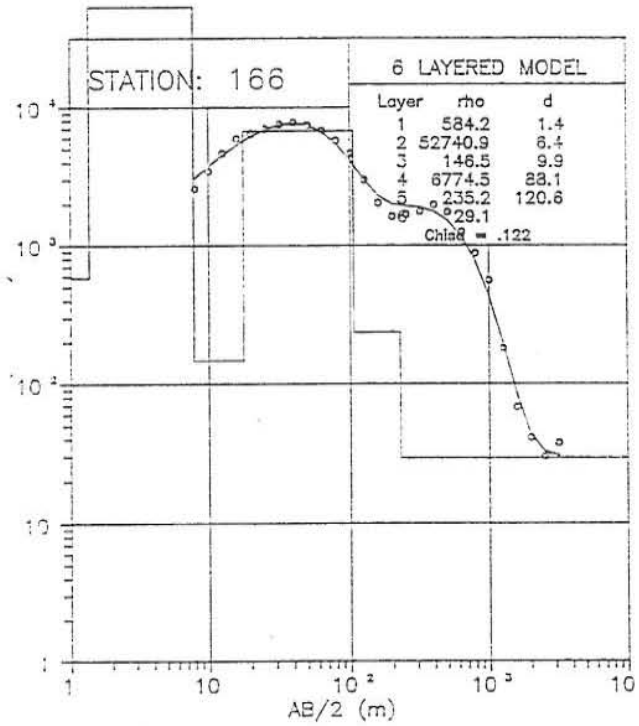
STATION: 166
6 LAYERED MODEL
Layer rho d
1 584.2 1.4
2 52740.9 6.4
3 146.5 9.9
4 6774.5 88.1
5 235.2 120.6
6 29.1
Chisq = .122
AB/2 (m)

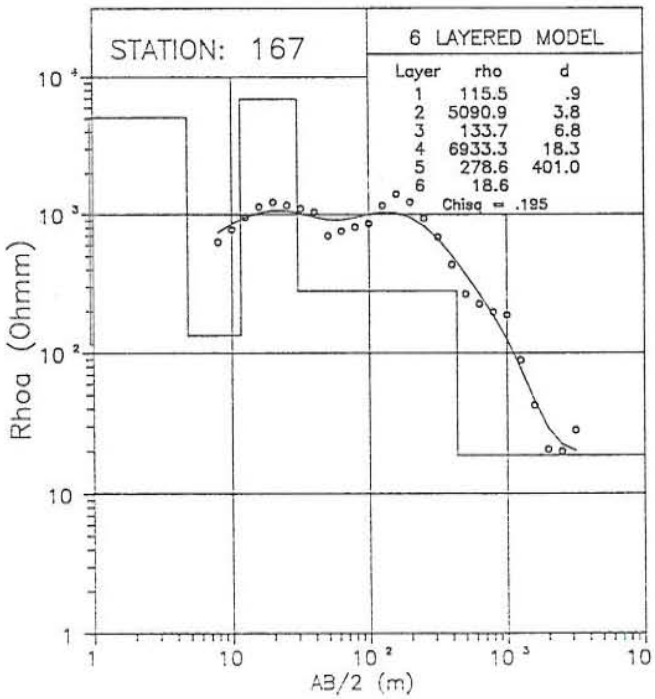
STATION: 167
6 LAYERED MODEL
Layer rho d
1 115.5 .9
2 5090.9 3.8
3 133.7 6.8
4 6933.3 18.3
5 278.6 401.0
6 18.6
Chisq = .195
Rhoa (Ohmm)
AB/2 (m)

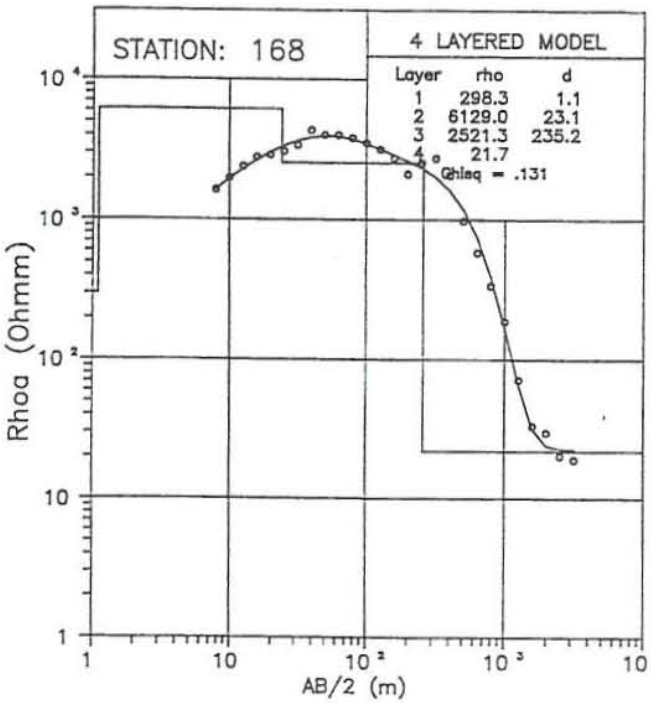
STATION: 168
4 LAYERED MODEL
Layer rho d
1 298.3 1.1
2 6129.0 23.1
3 2521.3 235.2
4 21.7
Chisq = .131
Rhoa (Ohmm)
AB/2 (m)

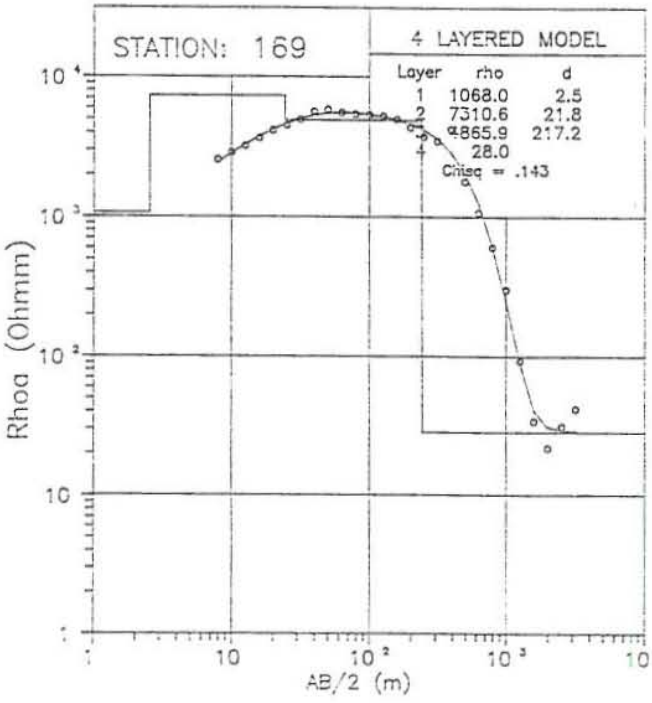
STATION: 169
4 LAYERED MODEL
Layer rho d
1 1068.0 2.5
2 7310.6 21.8
3 865.9 217.2
4 28.0
Chisq = .143
Rhoa (Ohmm)
AB/2 (m)

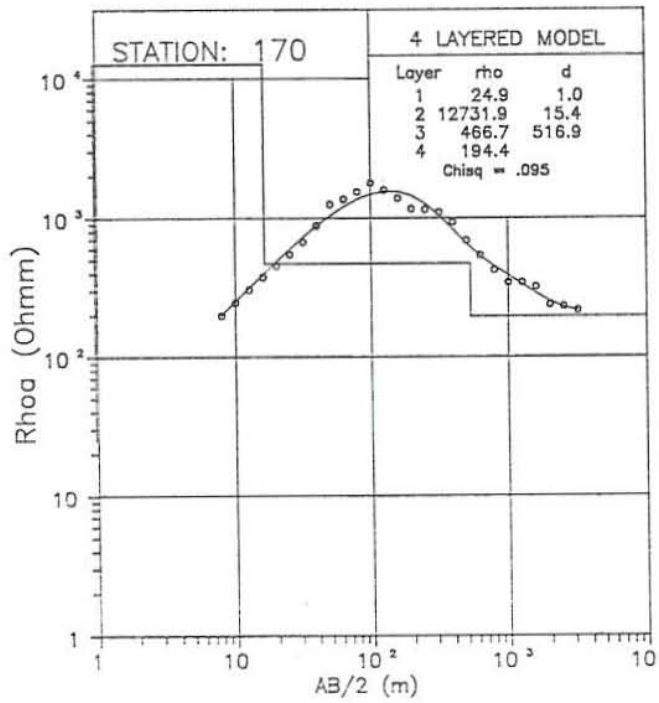
STATION: 170
4 LAYERED MODEL
Layer rho d
1 24.9 1.0
2 12731.9 15.4
3 466.7 516.9
4 194.4
Chisq = .095
Rhoa (Ohmm)
AB/2 (m)

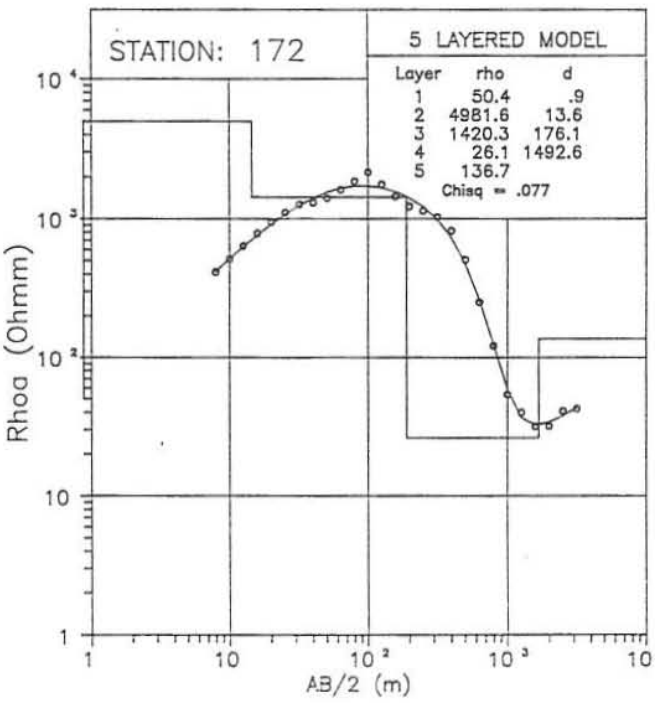
STATION: 172
5 LAYERED MODEL
Layer rho d
1 50.4 .9
2 4981.6 13.6
3 1420.3 176.1
4 26.1 1492.6
5 136.7
Chisq = .077
Rhoa (Ohmm)
AB/2 (m)

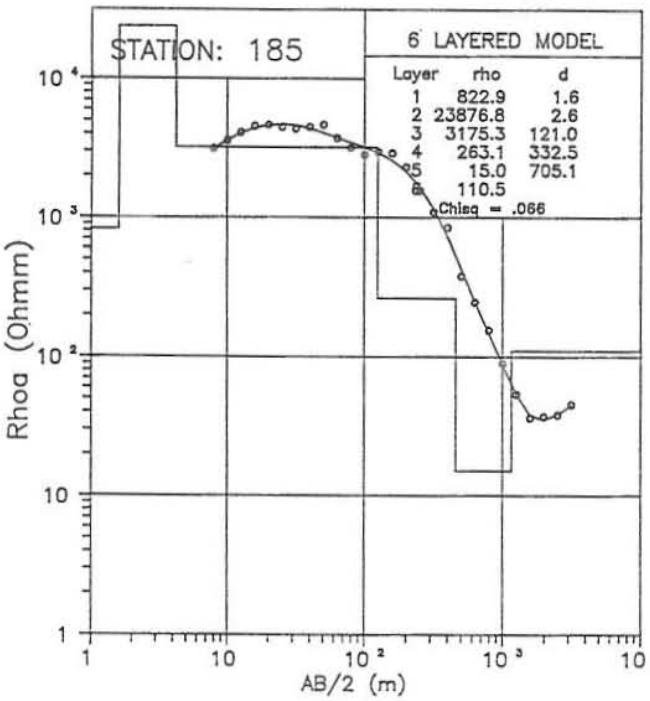
STATION: 185
6 LAYERED MODEL
Layer rho d
1 822.9 1.6
2 23876.8 2.6
3 3175.3 121.0
4 263.1 332.5
5 15.0 705.1
6 110.5
Chisq = .066
Rhoa (Ohmm)
AB/2 (m)

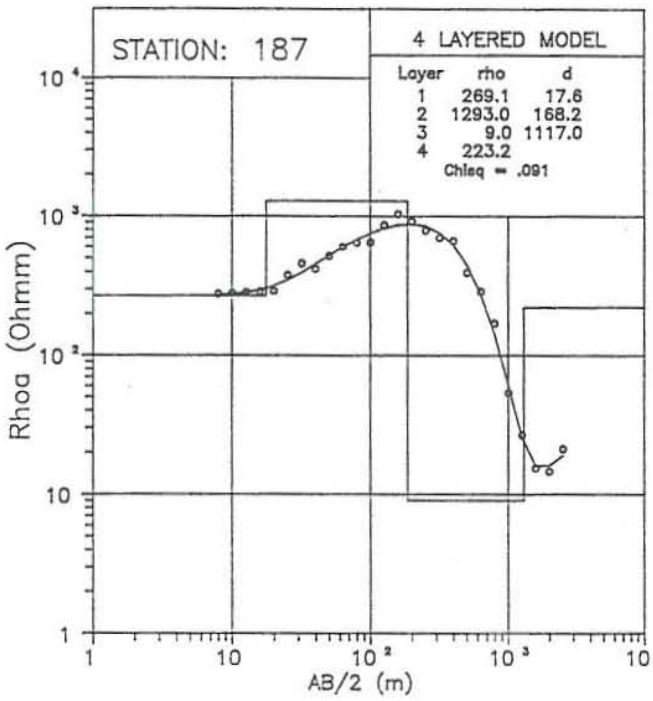
STATION: 187
4 LAYERED MODEL
Layer rho d
1 269.1 17.6
2 1293.0 168.2
3 9.0 1117.0
4 223.2
Chisq = .091
Rhoa (Ohmm)
AB/2 (m)

APPENDIX II

One dimensional interpretation of Schlumberger soundings. ELLIPSE-program:

Models, corresponding calculated apparent resistivity curves (shown as continuous curves) and measured apparent resistivity curves (shown as points).

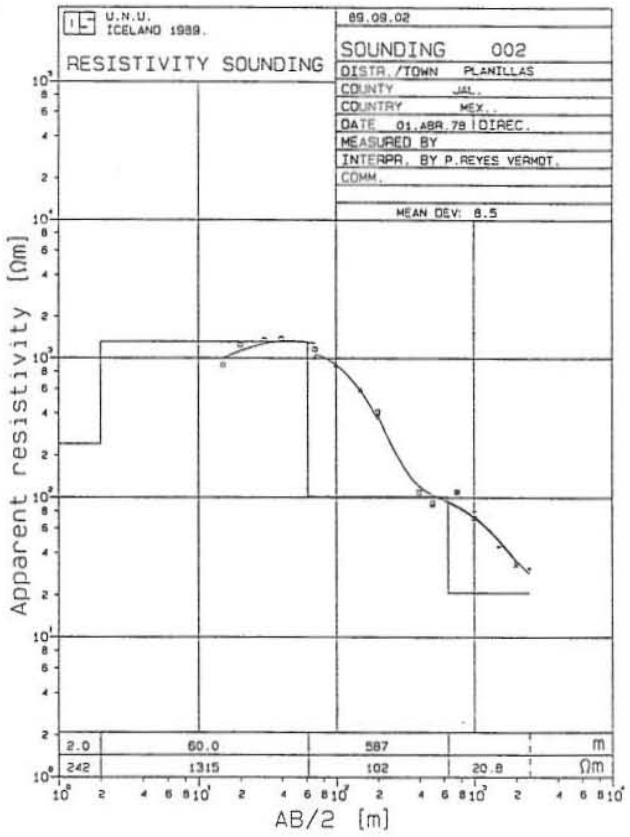
U.N.U.
ICELAND 1989.
RESISTIVITY SOUNDING
89.09.02
SOUNDING 002
DISTR./TOWN PLANILLAS
COUNTY JAL.
COUNTRY MEX.
DATE 01.ABR.78 | DIREC.
MEASURED BY
INTERPR. BY P.REYES VERMOT.
COMM.
MEAN DEV: 8.5
Apparent resistivity [Ωm]
AB/2 [m]
2.0 | 60.0 | 587 | m
242 | 1315 | 102 | 20.8 | Ωm

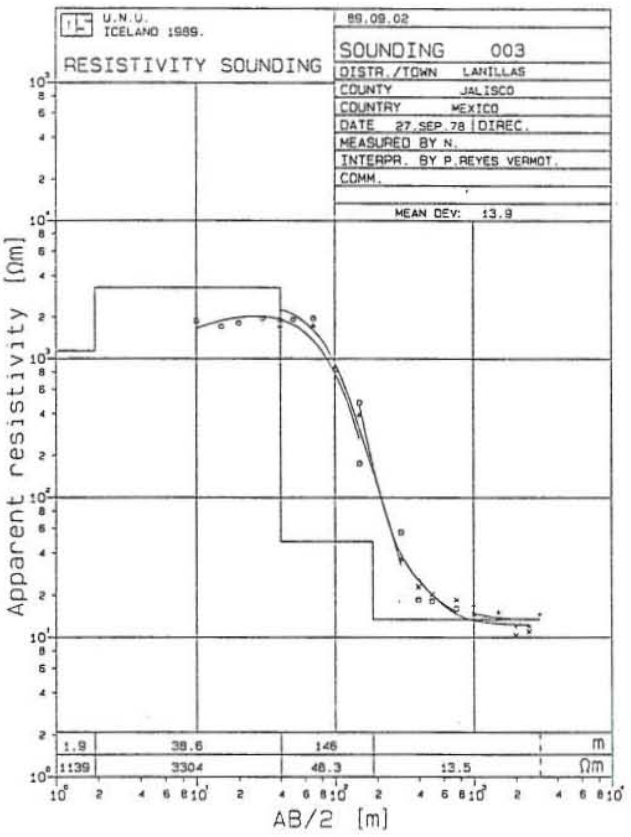
U.N.U.
ICELAND 1989.
RESISTIVITY SOUNDING
89.09.02
SOUNDING 003
DISTR./TOWN LANILLAS
COUNTY JALISCO
COUNTRY MEXICO
DATE 27.SEP.78 | DIREC.
MEASURED BY N.
INTERPR. BY P.REYES VERMOT.
COMM.
MEAN DEV: 13.9
Apparent resistivity [Ωm]
AB/2 [m]
1.9 | 38.6 | 146 | m
1139 | 3304 | 46.3 | 13.5 | Ωm

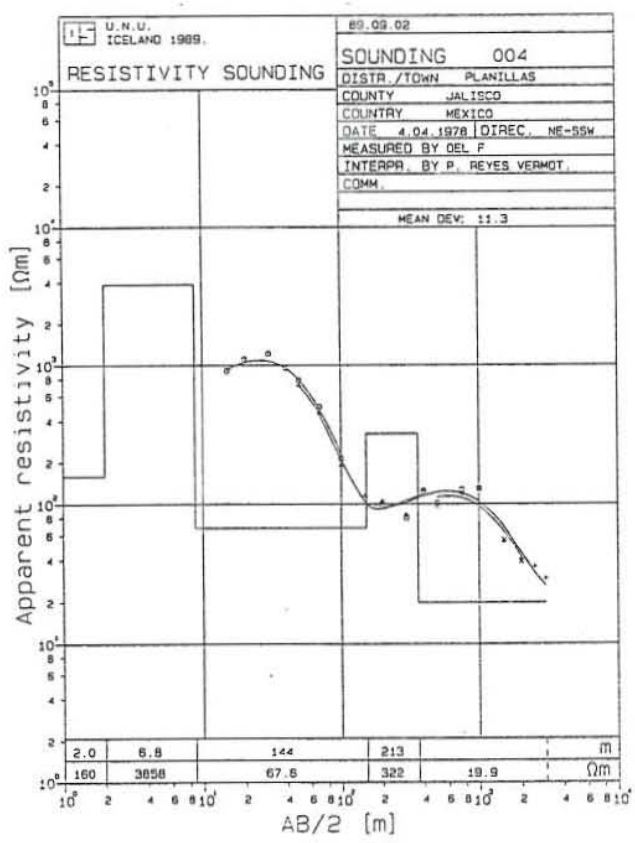
U.N.U.
ICELAND 1989.
RESISTIVITY SOUNDING
89.09.02
SOUNDING 004
DISTR./TOWN PLANILLAS
COUNTY JALISCO
COUNTRY MEXICO
DATE 4.04.1978 | DIREC. NE-SW
MEASURED BY OEL F
INTERPR. BY P. REYES VERMOT.
COMM.
MEAN DEV: 11.3
Apparent resistivity [Ωm]
AB/2 [m]
2.0 | 6.8 | 144 | 213 | m
160 | 3858 | 67.6 | 322 | 19.9 | Ωm

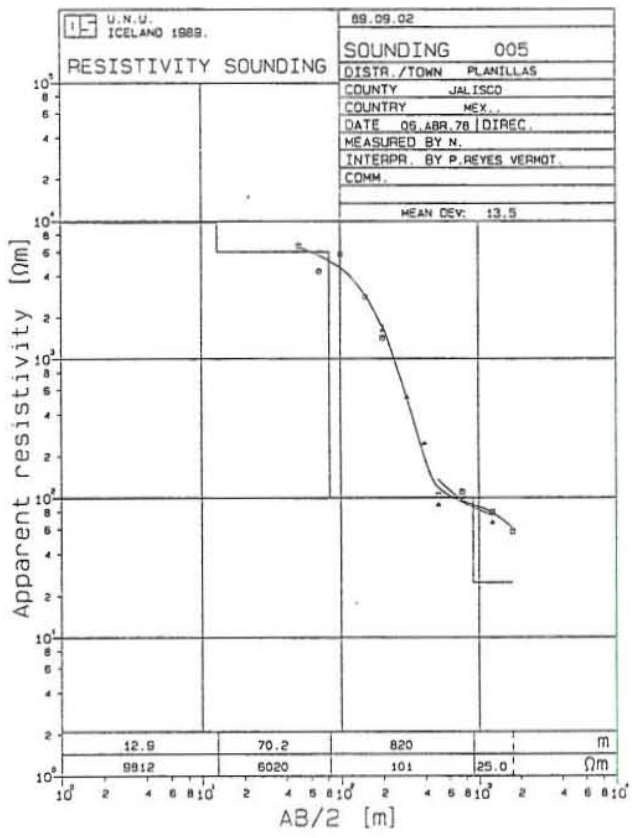
U.N.U.
ICELAND 1989.
RESISTIVITY SOUNDING
89.09.02
SOUNDING 005
DISTR./TOWN PLANILLAS
COUNTY JALISCO
COUNTRY MEX.
DATE 06.ABR.78 | DIREC.
MEASURED BY N.
INTERPR. BY P.REYES VERMOT.
COMM.
MEAN DEV: 13.5
Apparent resistivity [Ωm]
AB/2 [m]
12.9 | 70.2 | 820 | m
9812 | 6020 | 101 | 25.0 | Ωm

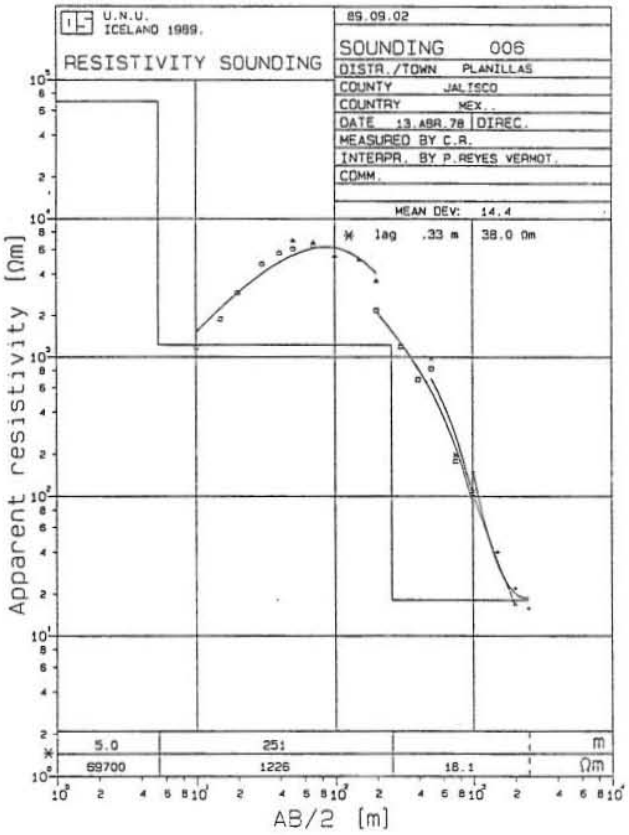
U.N.U.
ICELAND 1989.
RESISTIVITY SOUNDING
89.09.02
SOUNDING 006
DISTR./TOWN PLANILLAS
COUNTY JALISCO
COUNTRY MEX.
DATE 13.ABR.78 DIREC.
MEASURED BY C.R.
INTERPR. BY P.REYES VERMOT.
COMM.
MEAN DEV: 14.4
lag .33 m 38.0 Ωm
5.0 251 m
69700 1226 18.1 Ωm
Apparent resistivity [Ωm]
AB/2 [m]

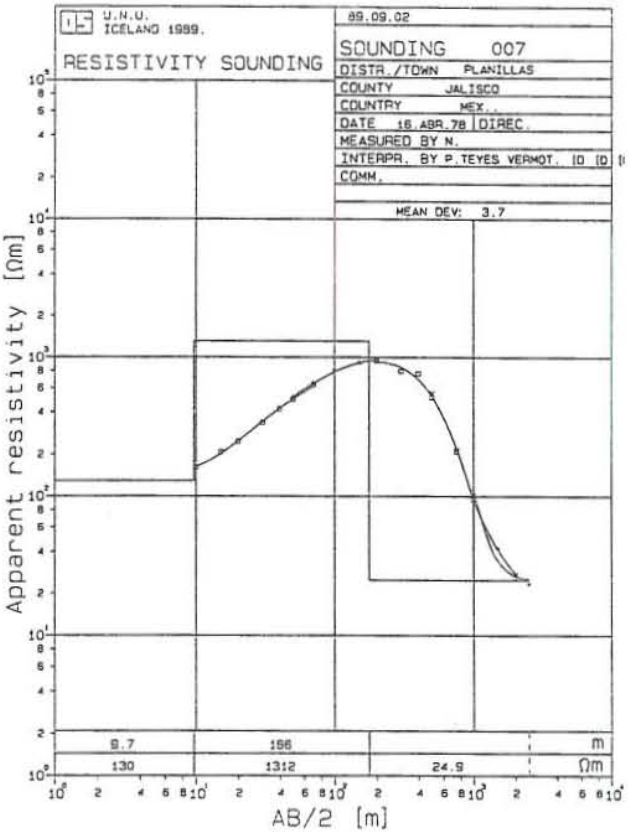
U.N.U.
ICELAND 1989.
RESISTIVITY SOUNDING
89.09.02
SOUNDING 007
DISTR./TOWN PLANILLAS
COUNTY JALISCO
COUNTRY MEX.
DATE 16.ABR.78 DIREC.
MEASURED BY N.
INTERPR. BY P.TEYES VERMOT.
COMM.
MEAN DEV: 3.7
9.7 196 m
130 1312 24.9 Ωm
Apparent resistivity [Ωm]
AB/2 [m]

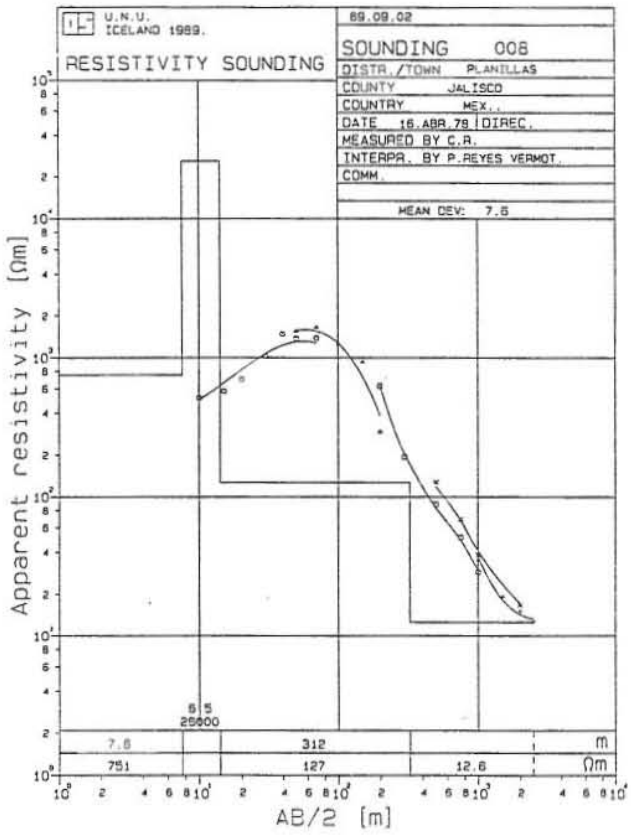
U.N.U.
ICELAND 1989.
RESISTIVITY SOUNDING
89.09.02
SOUNDING 008
DISTR./TOWN PLANILLAS
COUNTY JALISCO
COUNTRY MEX.
DATE 16.ABR.78 DIREC.
MEASURED BY C.R.
INTERPR. BY P.REYES VERMOT.
COMM.
MEAN DEV: 7.6
6 5
25600
7.8 312 m
751 127 12.6 Ωm
Apparent resistivity [Ωm]
AB/2 [m]

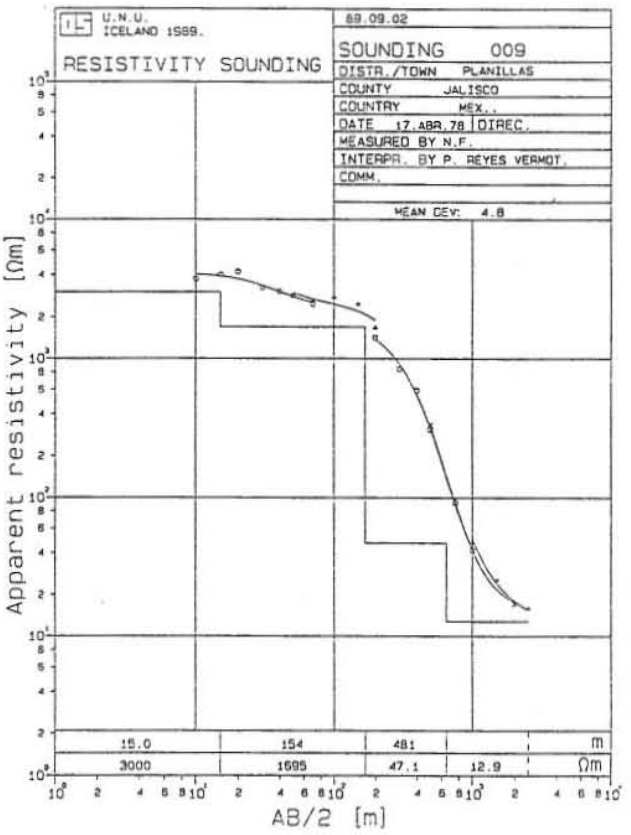
U.N.U.
ICELAND 1989.
RESISTIVITY SOUNDING
89.09.02
SOUNDING 009
DISTR./TOWN PLANILLAS
COUNTY JALISCO
COUNTRY MEX.
DATE 17.ABR.78 DIREC.
MEASURED BY N.F.
INTERPR. BY P. REYES VERMOT.
COMM.
MEAN DEV: 4.8
15.0 154 481 m
3000 1695 47.1 12.9 Ωm
Apparent resistivity [Ωm]
AB/2 [m]

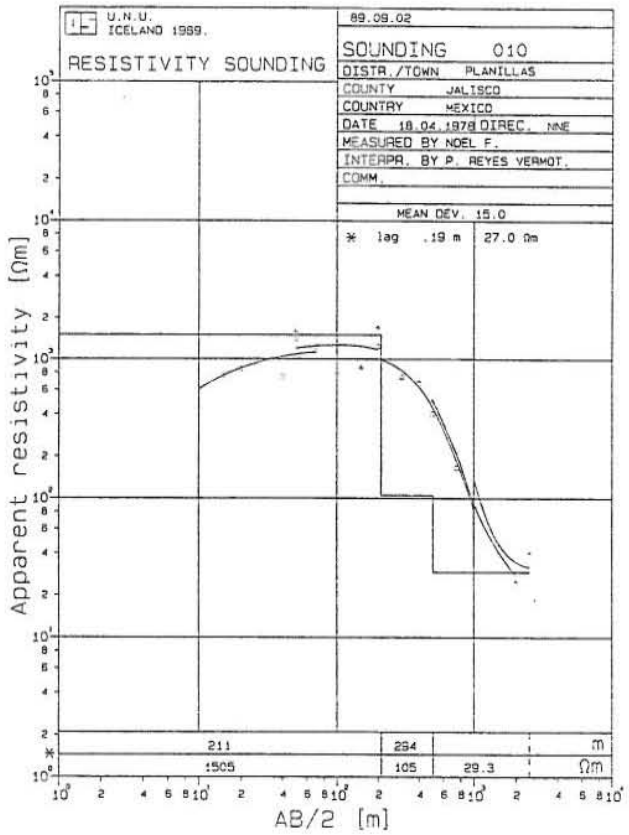
U.N.U.
ICELAND 1989.
RESISTIVITY SOUNDING
89.09.02
SOUNDING 010
DISTR./TOWN PLANILLAS
COUNTY JALISCO
COUNTRY MEXICO
DATE 18.04.1978 DIREC. NNE
MEASURED BY NOEL F.
INTERPR. BY P. REYES VERMOT.
COMM.
MEAN DEV. 15.0
* lag .19 m 27.0 Ωm
211 284 m
1505 105 29.3 Ωm
Apparent resistivity [Ωm]
AB/2 [m]

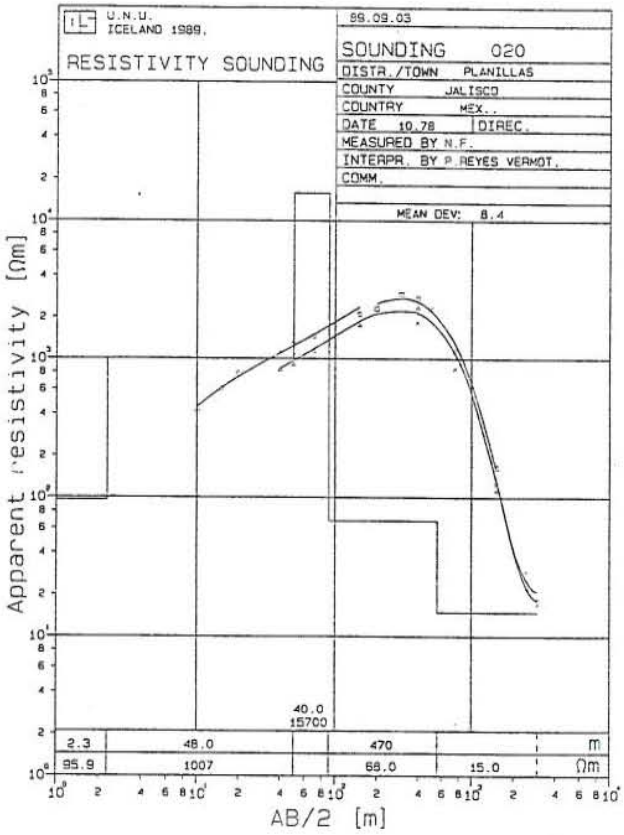
U.N.U.
ICELAND 1989.
RESISTIVITY SOUNDING
89.09.03
SOUNDING 020
DISTR./TOWN PLANILLAS
COUNTY JALISCO
COUNTRY MEX.
DATE 10.78 DIREC.
MEASURED BY N.F.
INTERPR. BY P.REYES VERMOT.
COMM.
MEAN DEV: 8.4
40.0
15700
2.3 48.0 470 m
95.9 1007 66.0 15.0 Ωm
Apparent resistivity [Ωm]
AB/2 [m]

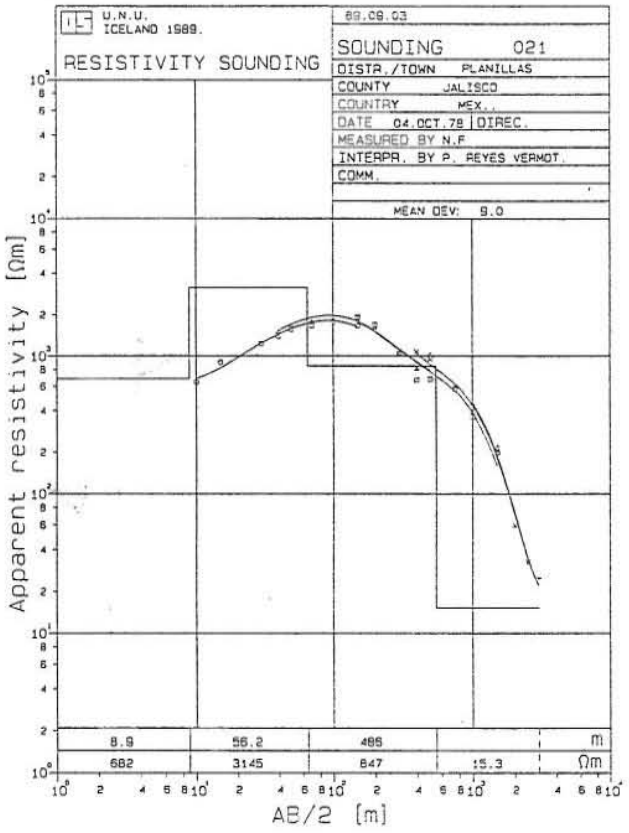
U.N.U.
ICELAND 1989.
RESISTIVITY SOUNDING
89.09.03
SOUNDING 021
DISTR./TOWN PLANILLAS
COUNTY JALISCO
COUNTRY MEX.
DATE 04.OCT.78 DIREC.
MEASURED BY N.F.
INTERPR. BY P. REYES VERMOT.
COMM.
MEAN DEV: 9.0
8.9 56.2 486 m
682 3145 847 15.3 Ωm
Apparent resistivity [Ωm]
AB/2 [m]

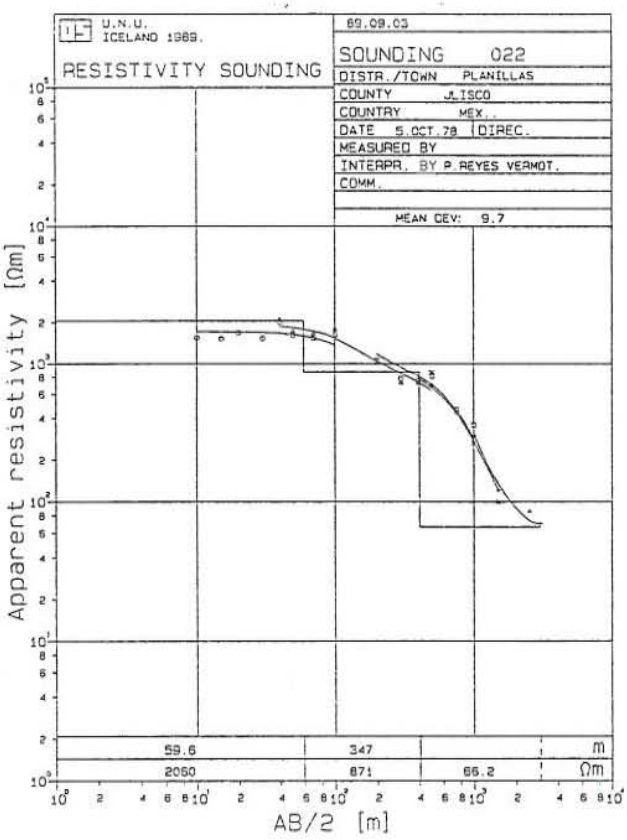
U.N.U.
ICELAND 1989.
RESISTIVITY SOUNDING
89.09.03
SOUNDING 022
DISTR./TOWN PLANILLAS
COUNTY JALISCO
COUNTRY MEX.
DATE 5.OCT.78 DIREC.
MEASURED BY
INTERPR. BY P.REYES VERMOT.
COMM.
MEAN DEV: 9.7
59.6 347 m
2050 671 66.2 Ωm
Apparent resistivity [Ωm]
AB/2 [m]

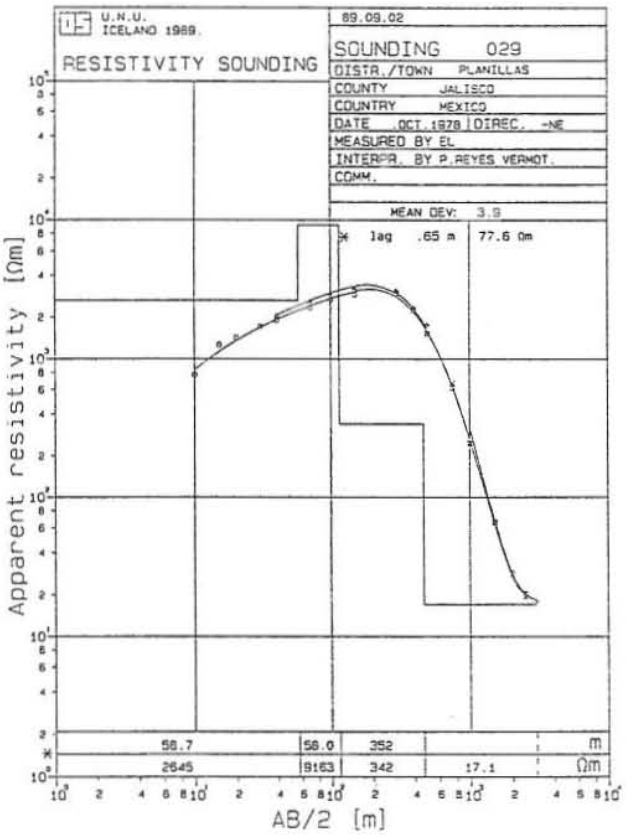
U.N.U.
ICELAND 1989.
RESISTIVITY SOUNDING
89.09.02
SOUNDING 029
DISTR./TOWN PLANILLAS
COUNTY JALISCO
COUNTRY MEXICO
DATE OCT.1978 DIREC. -NE
MEASURED BY EL
INTERPR. BY P.REYES VERMOT.
COMM.
MEAN DEV: 3.9
lag .65 m 77.6 Ωm
Apparent resistivity [Ωm]
AB/2 [m]
56.7 56.0 352 m
2645 9163 342 17.1 Ωm

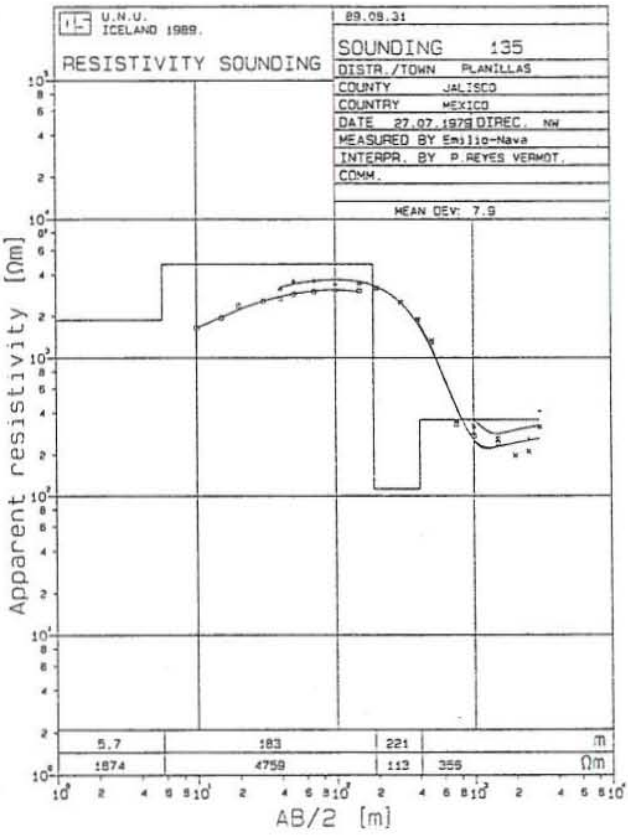
U.N.U.
ICELAND 1989.
RESISTIVITY SOUNDING
89.08.31
SOUNDING 135
DISTR./TOWN PLANILLAS
COUNTY JALISCO
COUNTRY MEXICO
DATE 27.07.1979 DIREC. NW
MEASURED BY Emilio-Nava
INTERPR. BY P.REYES VERMOT.
COMM.
MEAN DEV: 7.9
Apparent resistivity [Ωm]
AB/2 [m]
5.7 183 221 m
1874 4759 113 356 Ωm

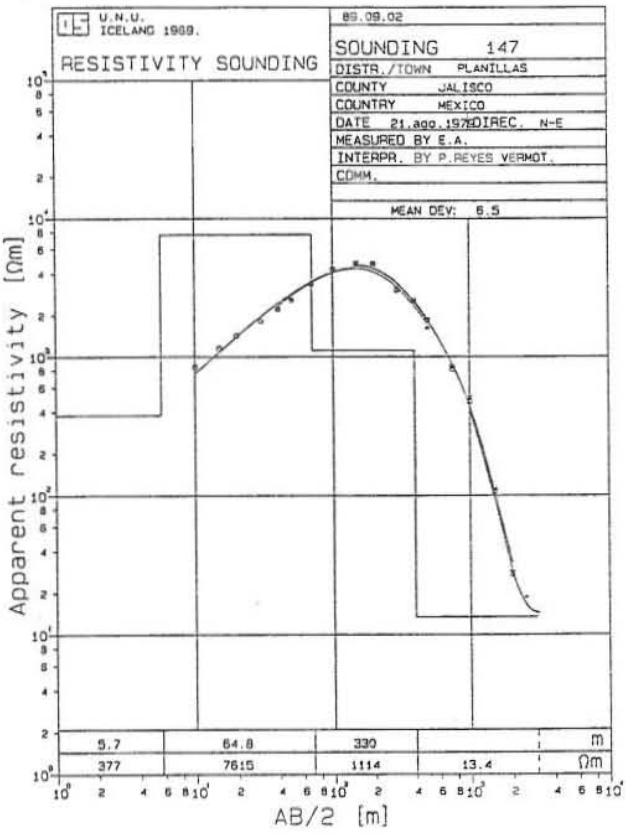
U.N.U.
ICELAND 1989.
RESISTIVITY SOUNDING
89.09.02
SOUNDING 147
DISTR./TOWN PLANILLAS
COUNTY JALISCO
COUNTRY MEXICO
DATE 21.ago.1979 DIREC. N-E
MEASURED BY E.A.
INTERPR. BY P.REYES VERMOT.
COMM.
MEAN DEV: 6.5
Apparent resistivity [Ωm]
AB/2 [m]
5.7 64.8 330 m
377 7615 1114 13.4 Ωm

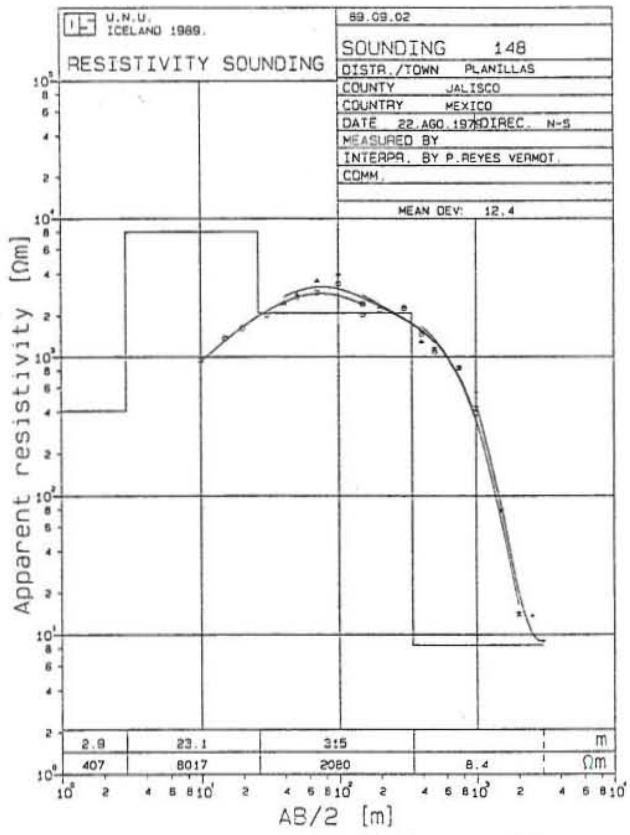
U.N.U.
ICELAND 1989.
RESISTIVITY SOUNDING
89.09.02
SOUNDING 148
DISTR./TOWN PLANILLAS
COUNTY JALISCO
COUNTRY MEXICO
DATE 22.AGO.1979 DIREC. N-S
MEASURED BY
INTERPR. BY P.REYES VERMOT.
COMM.
MEAN DEV: 12.4
Apparent resistivity [Ωm]
AB/2 [m]
2.9 23.1 315 m
407 8017 2080 8.4 Ωm

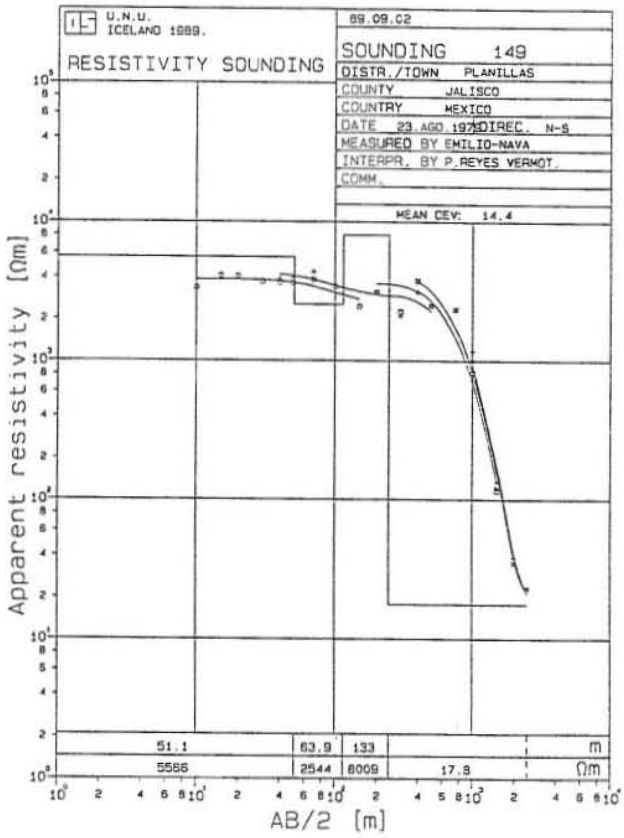
U.N.U.
ICELAND 1989.
RESISTIVITY SOUNDING
89.09.02
SOUNDING 149
DISTR./TOWN PLANILLAS
COUNTY JALISCO
COUNTRY MEXICO
DATE 23.AGO.197 DIREC. N-S
MEASURED BY EMILIO-NAVA
INTERPR. BY P.REYES VERMOT.
COMM.
MEAN DEV: 14.4
Apparent resistivity [Ωm]
AB/2 [m]
51.1 63.9 133 m
5566 2544 8009 17.8 Ωm

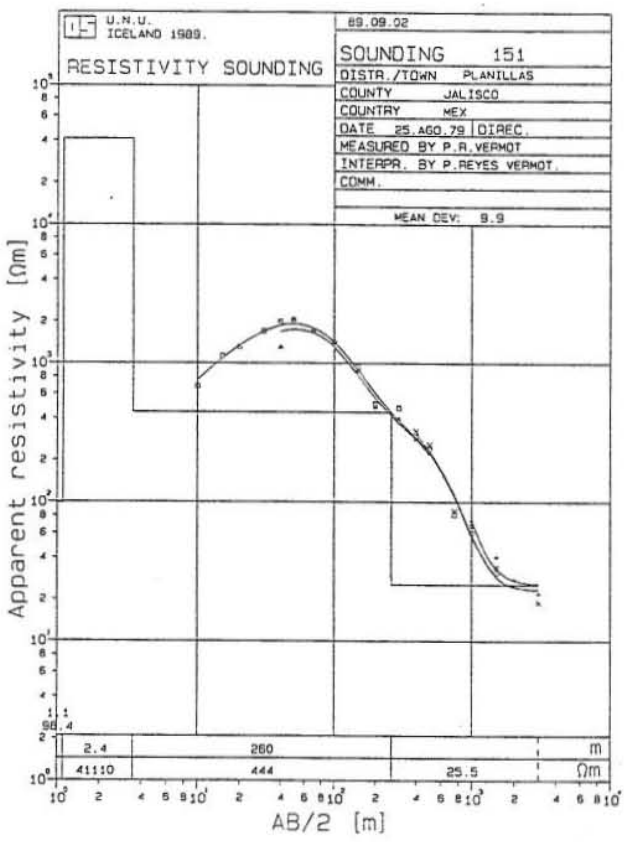
U.N.U.
ICELAND 1989.
RESISTIVITY SOUNDING
89.09.02
SOUNDING 151
DISTR./TOWN PLANILLAS
COUNTY JALISCO
COUNTRY MEX
DATE 25.AGO.79 DIREC.
MEASURED BY P.R.VERMOT
INTERPR. BY P.REYES VERMOT.
COMM.
MEAN DEV: 9.9
Apparent resistivity [Ωm]
AB/2 [m]
2.4 260 m
41110 444 25.5 Ωm

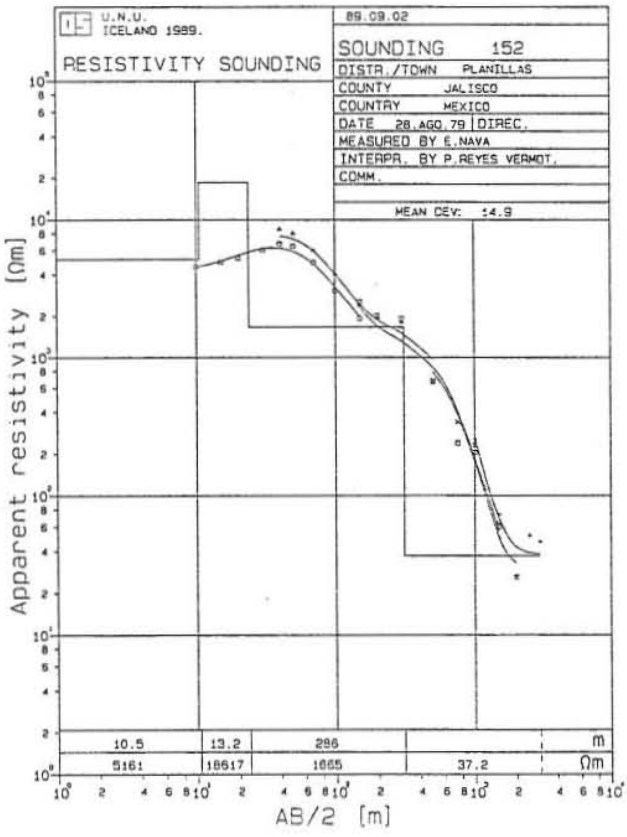
U.N.U.
ICELAND 1989.
RESISTIVITY SOUNDING
89.09.02
SOUNDING 152
DISTR./TOWN PLANILLAS
COUNTY JALISCO
COUNTRY MEXICO
DATE 28.AGO.79 DIREC.
MEASURED BY E.NAVA
INTERPR. BY P.REYES VERMOT.
COMM.
MEAN DEV: 14.9
Apparent resistivity [Ωm]
AB/2 [m]
10.5 13.2 286 m
5161 18617 1665 37.2 Ωm

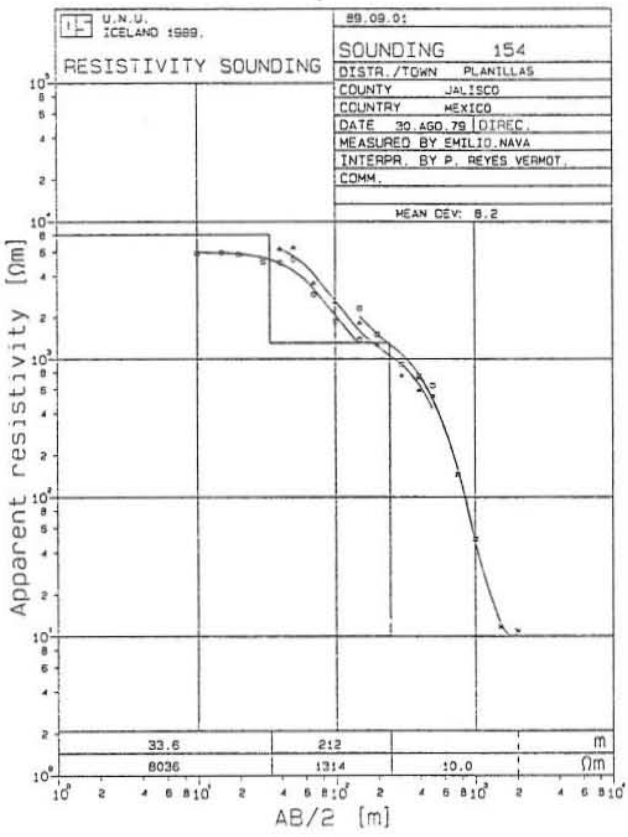
U.N.U.
ICELAND 1989.
RESISTIVITY SOUNDING
89.09.01
SOUNDING 154
DISTR./TOWN PLANILLAS
COUNTY JALISCO
COUNTRY MEXICO
DATE 30.AGO.79 DIREC.
MEASURED BY EMILIO.NAVA
INTERPR. BY P. REYES VERMOT.
COMM.
MEAN DEV: 8.2
Apparent resistivity [Ωm]
AB/2 [m]
33.6 212 m
8036 1314 10.0 Ωm

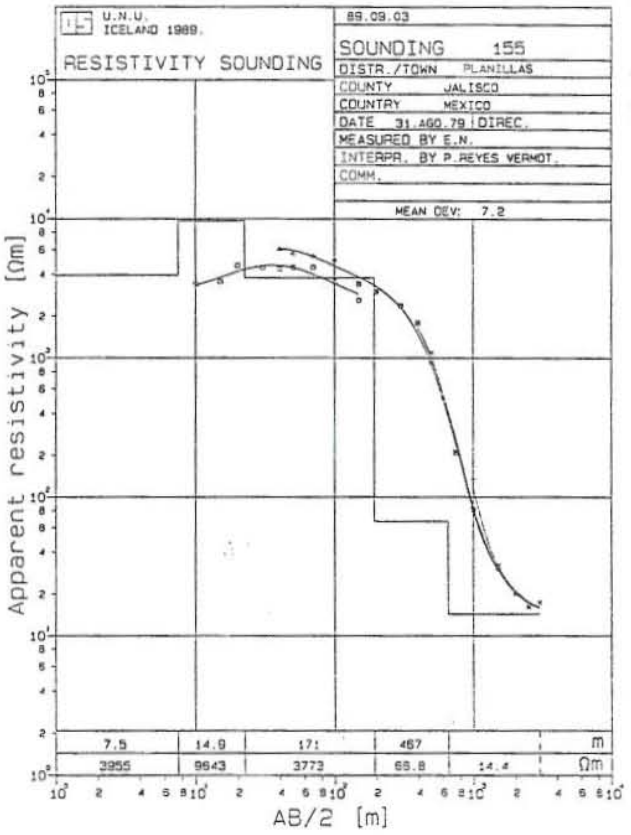
U.N.U.
ICELAND 1989.
RESISTIVITY SOUNDING
89.09.03
SOUNDING 155
DISTR./TOWN PLANILLAS
COUNTY JALISCO
COUNTRY MEXICO
DATE 31.AGO.79 DIREC.
MEASURED BY E.N.
INTERPR. BY P.REYES VERMOT.
COMM.
MEAN DEV: 7.2
Apparent resistivity [Ωm]
AB/2 [m]
7.5 14.9 171 467 m
3955 9643 3773 65.8 14.4 Ωm

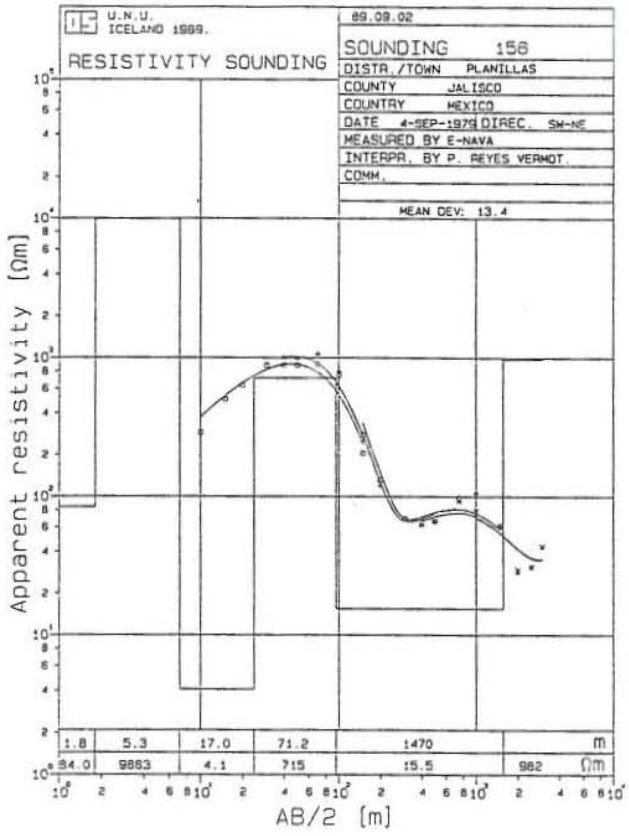
U.N.U.
ICELAND 1989.
RESISTIVITY SOUNDING
89.09.02
SOUNDING 156
DISTR./TOWN PLANILLAS
COUNTY JALISCO
COUNTRY MEXICO
DATE 4-SEP-1979 DIREC. SW-NE
MEASURED BY E-NAVA
INTERPR. BY P. REYES VERMOT.
COMM.
MEAN DEV: 13.4
Apparent resistivity [Ωm]
AB/2 [m]
1.8 5.3 17.0 71.2 1470 m
84.0 9863 4.1 715 15.5 982 Ωm

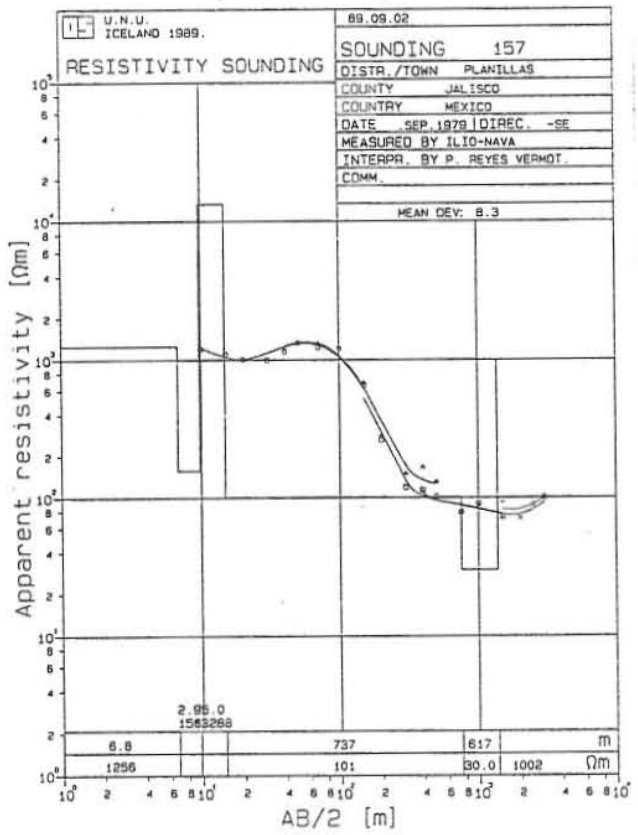
U.N.U.
ICELAND 1989.
RESISTIVITY SOUNDING
89.09.02
SOUNDING 157
DISTR./TOWN PLANILLAS
COUNTY JALISCO
COUNTRY MEXICO
DATE .SEP.1979 DIREC. -SE
MEASURED BY ILIO-NAVA
INTERPR. BY P. REYES VERMOT.
COMM.
MEAN DEV: 8.3
Apparent resistivity [Ωm]
AB/2 [m]
2.95.0
1563268
6.8 737 617 m
1256 101 30.0 1002 Ωm

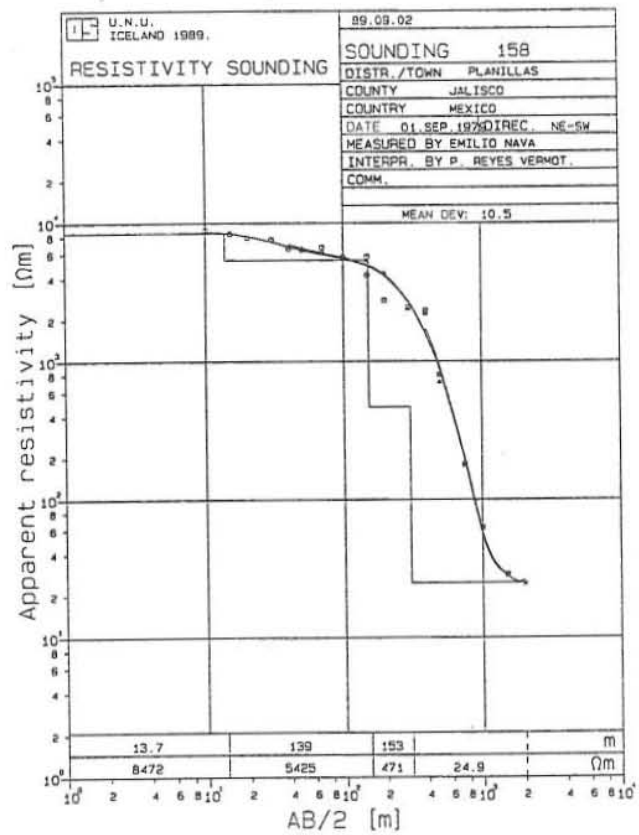
U.N.U.
ICELAND 1989.
RESISTIVITY SOUNDING
89.09.02
SOUNDING 158
DISTR./TOWN PLANILLAS
COUNTY JALISCO
COUNTRY MEXICO
DATE 01.SEP.1979 DIREC. NE-SW
MEASURED BY EMILIO NAVA
INTERPR. BY P. REYES VERMOT.
COMM.
MEAN DEV: 10.5
Apparent resistivity [Ωm]
AB/2 [m]
13.7 139 153 m
8472 5425 471 24.9 Ωm

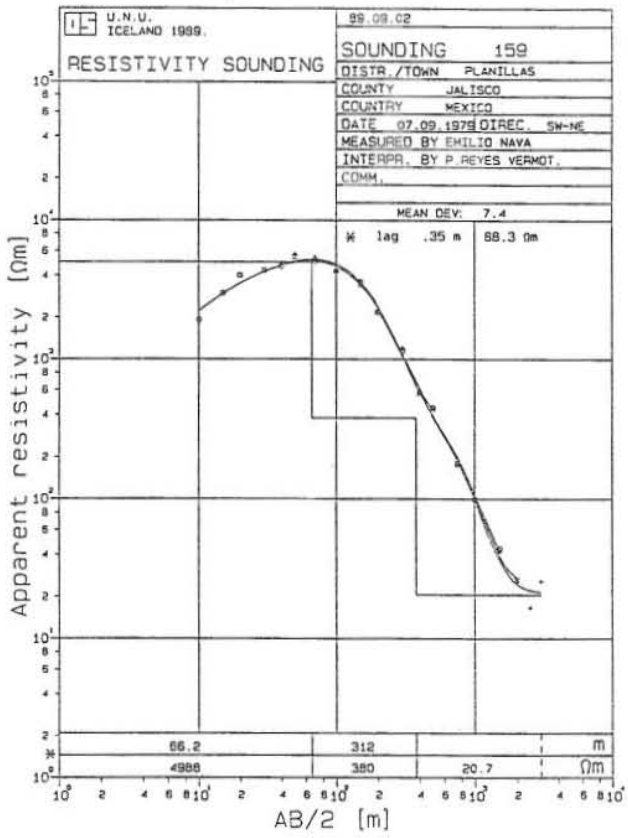
U.N.U.
ICELAND 1989.
RESISTIVITY SOUNDING
89.09.02
SOUNDING 159
DISTR./TOWN PLANILLAS
COUNTY JALISCO
COUNTRY MEXICO
DATE 07.09.1979 DIREC. SW-NE
MEASURED BY EMILIO NAVA
INTERPR. BY P.REYES VERMOT.
COMM.
MEAN DEV: 7.4
lag .35 m 88.3 Ωm
66.2 312 m
4986 380 20.7 Ωm
Apparent resistivity [Ωm]
AB/2 [m]

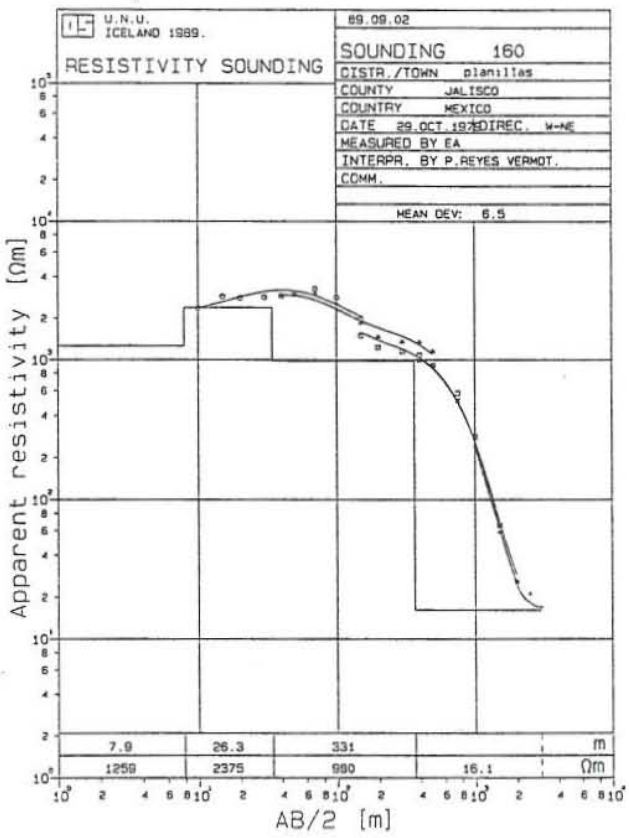
U.N.U.
ICELAND 1989.
RESISTIVITY SOUNDING
89.09.02
SOUNDING 160
DISTR./TOWN planillas
COUNTY JALISCO
COUNTRY MEXICO
DATE 29.OCT.1979 DIREC. W-NE
MEASURED BY EA
INTERPR. BY P.REYES VERMOT.
COMM.
MEAN DEV: 6.5
7.9 26.3 331 m
1259 2375 990 16.1 Ωm
Apparent resistivity [Ωm]
AB/2 [m]

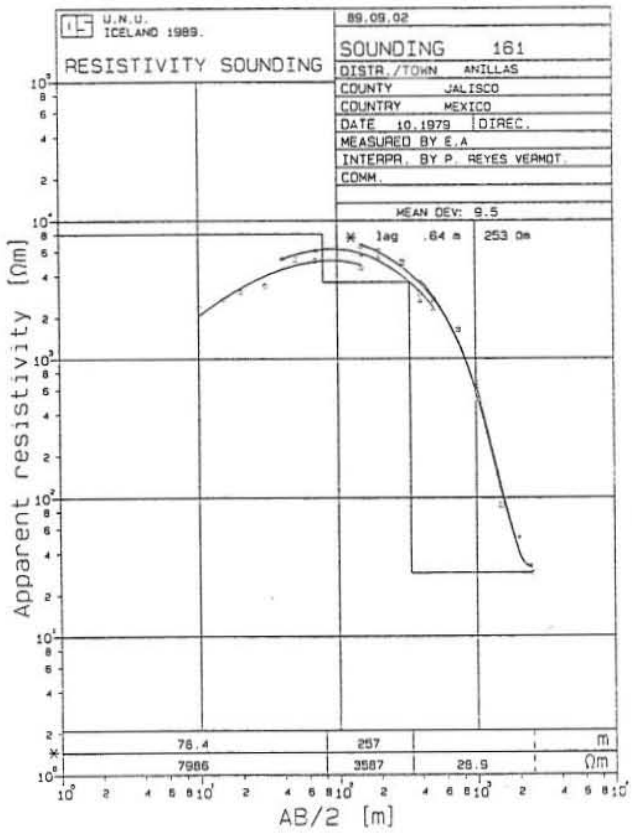
U.N.U.
ICELAND 1989.
RESISTIVITY SOUNDING
89.09.02
SOUNDING 161
DISTR./TOWN ANILLAS
COUNTY JALISCO
COUNTRY MEXICO
DATE 10.1979 DIREC.
MEASURED BY E.A
INTERPR. BY P. REYES VERMOT.
COMM.
MEAN DEV: 9.5
lag .64 m 253 Ωm
78.4 257 m
7986 3587 26.9 Ωm
Apparent resistivity [Ωm]
AB/2 [m]

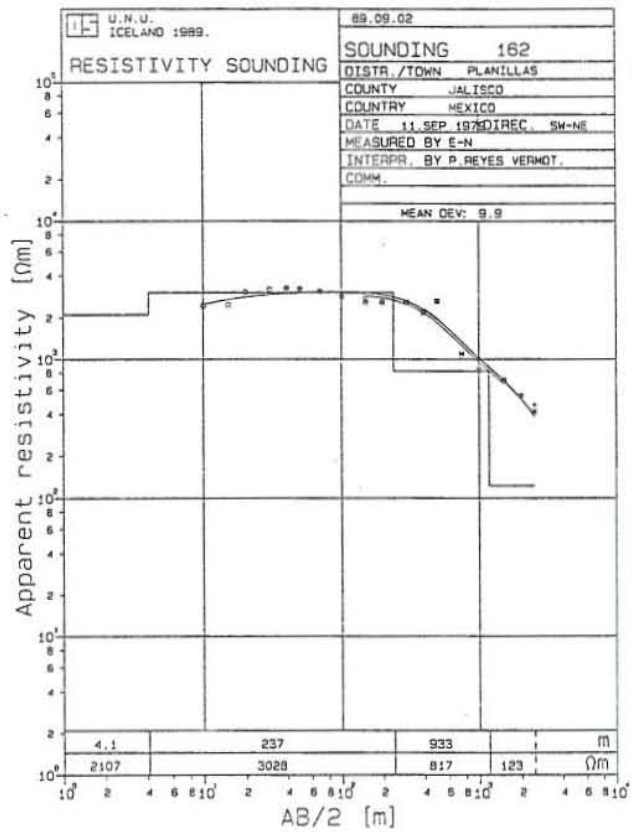
U.N.U.
ICELAND 1989.
RESISTIVITY SOUNDING
89.09.02
SOUNDING 162
DISTR./TOWN PLANILLAS
COUNTY JALISCO
COUNTRY MEXICO
DATE 11.SEP 1979 DIREC. SW-NE
MEASURED BY E-N
INTERPR. BY P.REYES VERMOT.
COMM.
MEAN DEV: 9.9
4.1 237 933 m
2107 3028 817 123 Ωm
Apparent resistivity [Ωm]
AB/2 [m]

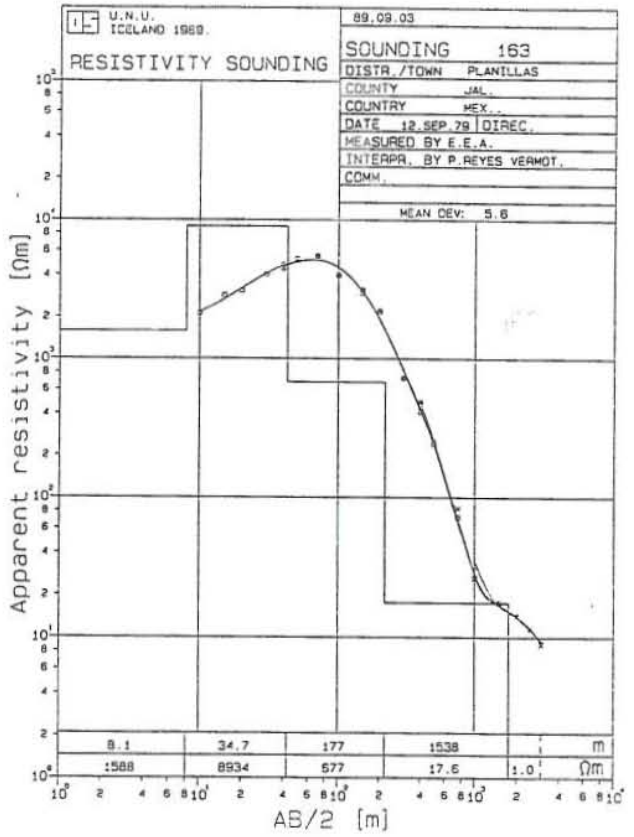
U.N.U.
ICELAND 1989.
RESISTIVITY SOUNDING
89.09.03
SOUNDING 163
DISTR./TOWN PLANILLAS
COUNTY JAL.
COUNTRY MEX.
DATE 12.SEP.79 DIREC.
MEASURED BY E.E.A.
INTERPR. BY P.REYES VERMOT.
COMM.
MEAN DEV: 5.6
8.1 34.7 177 1538 m
1588 8934 577 17.6 1.0 Ωm
Apparent resistivity [Ωm]
AB/2 [m]

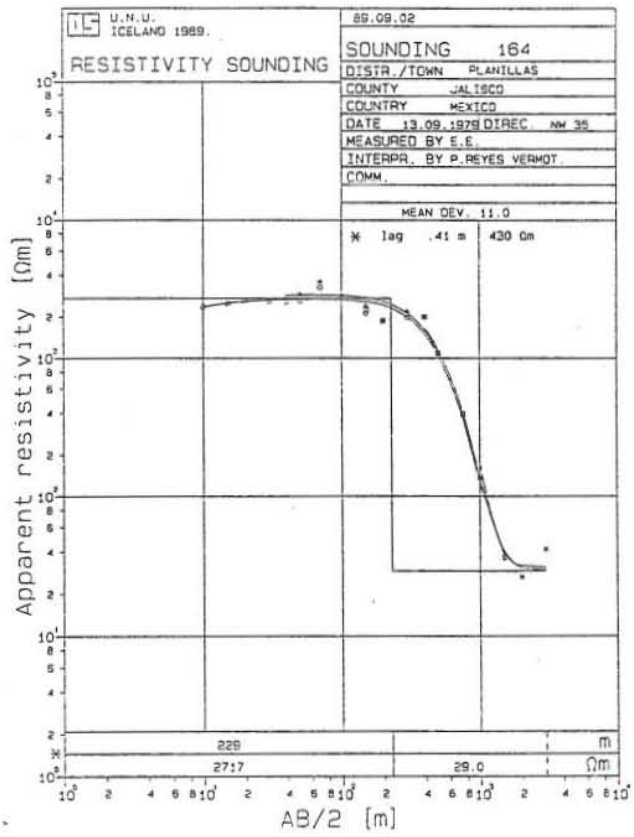
U.N.U.
ICELAND 1989.
RESISTIVITY SOUNDING
89.09.02
SOUNDING 164
DISTR./TOWN PLANILLAS
COUNTY JALISCO
COUNTRY MEXICO
DATE 13.09.1979 DIREC. NW 35
MEASURED BY E.E.
INTERPR. BY P.REYES VERMOT.
COMM.
MEAN DEV. 11.0
* lag .41 m 430 Ωm
228 m
27.7 29.0 Ωm
Apparent resistivity [Ωm]
AB/2 [m]

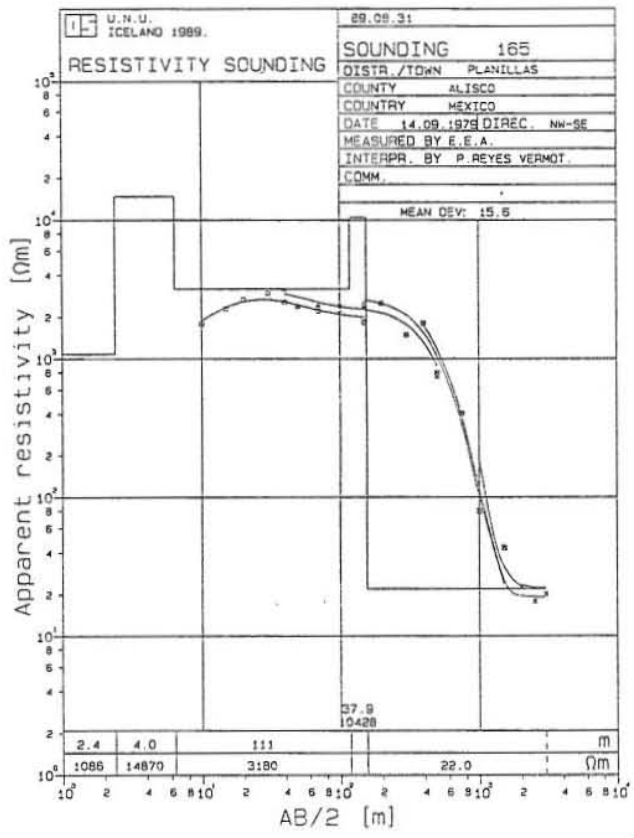
U.N.U.
ICELAND 1989.
RESISTIVITY SOUNDING
89.09.31
SOUNDING 165
DISTR./TOWN PLANILLAS
COUNTY ALISCO
COUNTRY MEXICO
DATE 14.09.1979 DIREC. NW-SE
MEASURED BY E.E.A.
INTERPR. BY P.REYES VERMOT.
COMM.
MEAN DEV: 15.6
37.9
10428
2.4 4.0 111 m
1086 14870 3180 22.0 Ωm
Apparent resistivity [Ωm]
AB/2 [m]

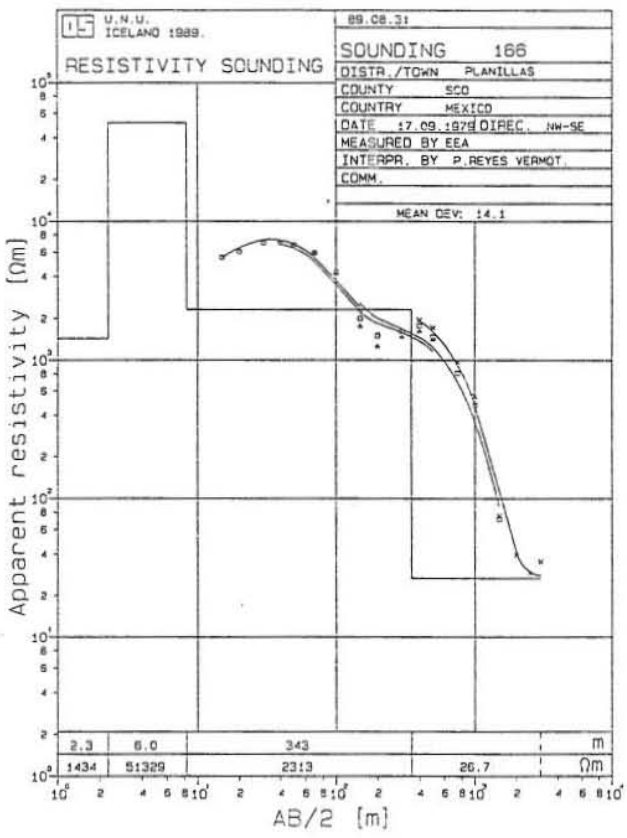
U.N.U.
ICELAND 1989.
RESISTIVITY SOUNDING
89.08.31
SOUNDING 166
DISTR./TOWN PLANILLAS
COUNTY SCO
COUNTRY MEXICO
DATE 17.09.1979 DIREC. NW-SE
MEASURED BY EEA
INTERPR. BY P.REYES VERMOT.
COMM.
MEAN DEV: 14.1
2.3 6.0 343 m
1434 51329 2313 26.7 Ωm
Apparent resistivity [Ωm]
AB/2 [m]

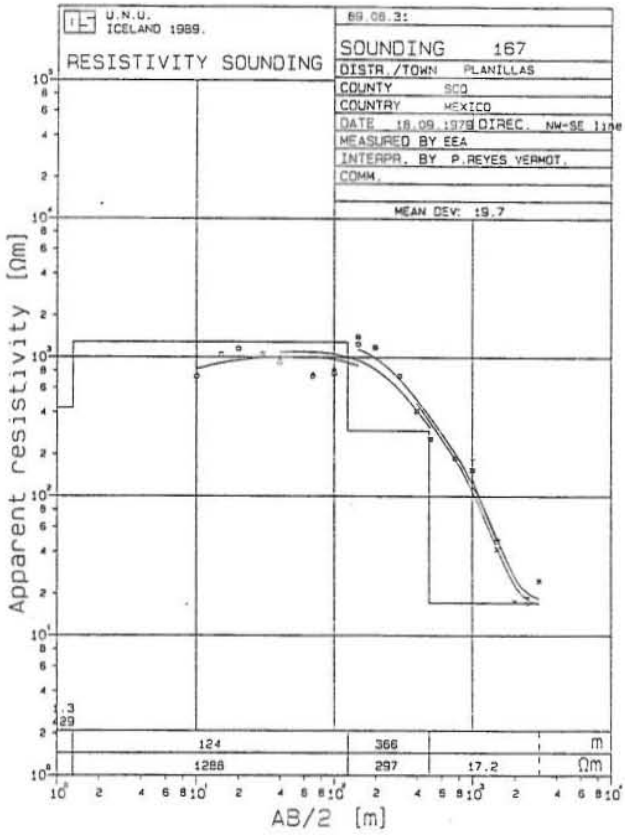
U.N.U.
ICELAND 1989.
RESISTIVITY SOUNDING
89.08.31
SOUNDING 167
DISTR./TOWN PLANILLAS
COUNTY SCO
COUNTRY MEXICO
DATE 18.09.1978 DIREC. NW-SE line
MEASURED BY EEA
INTERPR. BY P.REYES VERMOT.
COMM.
MEAN DEV: 19.7
Apparent resistivity [Ωm]
AB/2 [m]
1.3
29
124 366 m
1288 297 17.2 Ωm

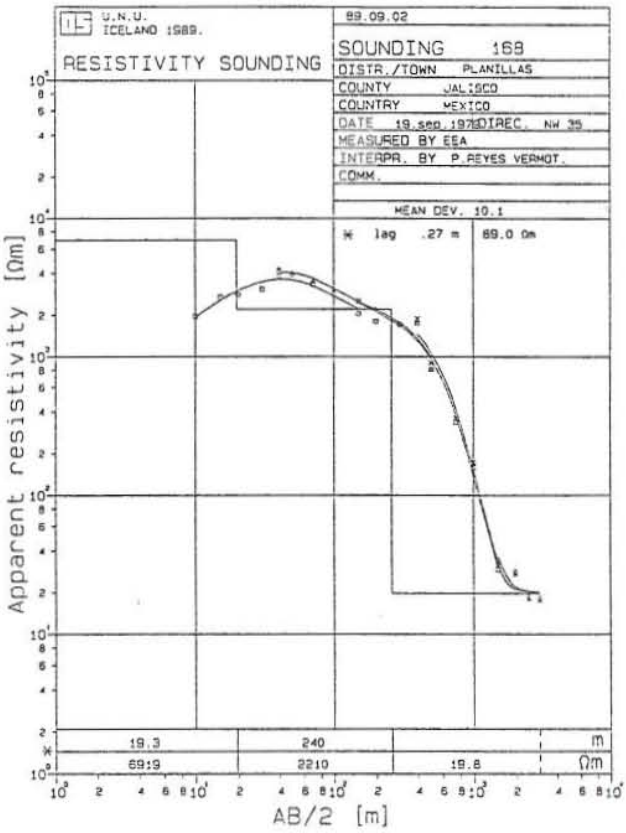
U.N.U.
ICELAND 1989.
RESISTIVITY SOUNDING
89.09.02
SOUNDING 168
DISTR./TOWN PLANILLAS
COUNTY JALISCO
COUNTRY MEXICO
DATE 19.sep.1978 DIREC. NW 35
MEASURED BY EEA
INTERPR. BY P.REYES VERMOT.
COMM.
MEAN DEV. 10.1
* lag .27 m 89.0 Ωm
Apparent resistivity [Ωm]
AB/2 [m]
19.3 240 m
* 69:9 2210 19.8 Ωm

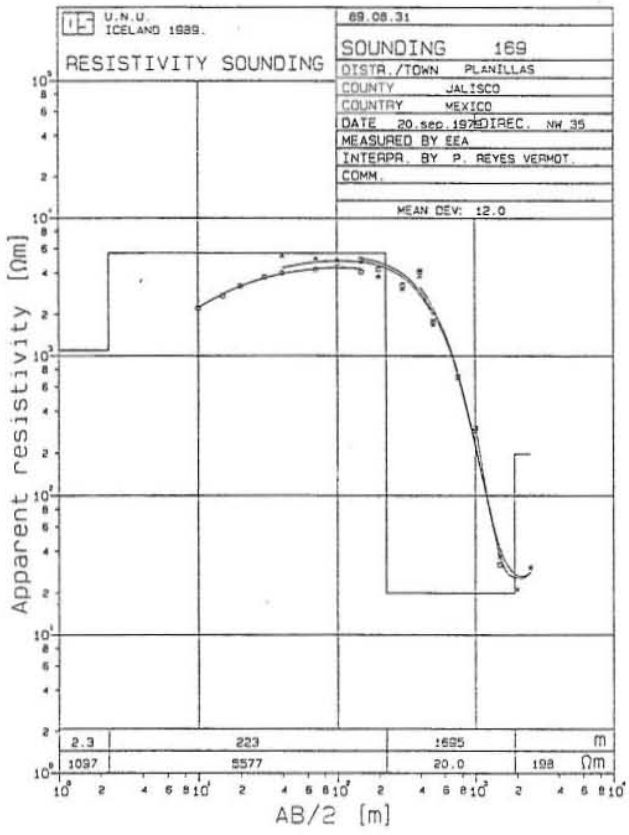
U.N.U.
ICELAND 1989.
RESISTIVITY SOUNDING
89.08.31
SOUNDING 169
DISTR./TOWN PLANILLAS
COUNTY JALISCO
COUNTRY MEXICO
DATE 20.sep.1978 DIREC. NW 35
MEASURED BY EEA
INTERPR. BY P. REYES VERMOT.
COMM.
MEAN DEV: 12.0
Apparent resistivity [Ωm]
AB/2 [m]
2.3 223 1695 m
1097 5577 20.0 198 Ωm

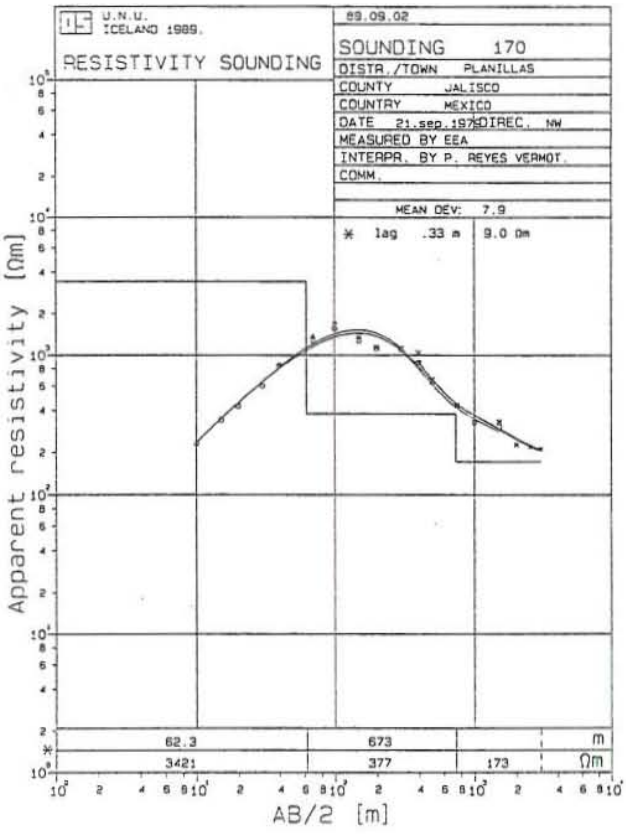
U.N.U.
ICELAND 1989.
RESISTIVITY SOUNDING
89.09.02
SOUNDING 170
DISTR./TOWN PLANILLAS
COUNTY JALISCO
COUNTRY MEXICO
DATE 21.sep.1978 DIREC. NW
MEASURED BY EEA
INTERPR. BY P. REYES VERMOT.
COMM.
MEAN DEV: 7.9
* lag .33 m 9.0 Ωm
Apparent resistivity [Ωm]
AB/2 [m]
62.3 673 m
* 3421 377 173 Ωm

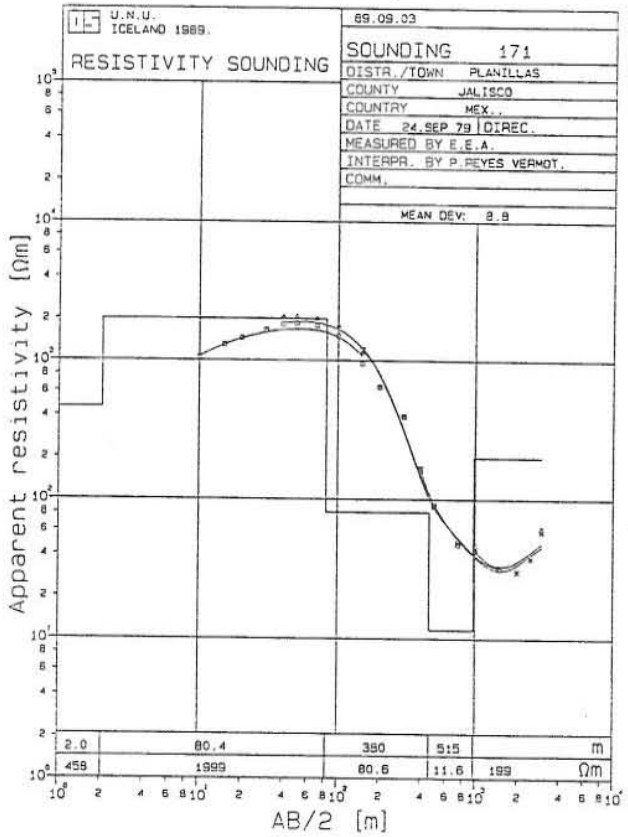
U.N.U.
ICELAND 1989.
RESISTIVITY SOUNDING
89.09.03
SOUNDING 171
DISTR./TOWN PLANILLAS
COUNTY JALISCO
COUNTRY MEX.
DATE 24.SEP.79 | DIREC.
MEASURED BY E.E.A.
INTERPR. BY P.REYES VERMOT.
COMM.
MEAN DEV: 8.9
Apparent resistivity [Ωm]
AB/2 [m]
2.0 80.4 380 515 m
458 1999 80.6 11.6 199 Ωm

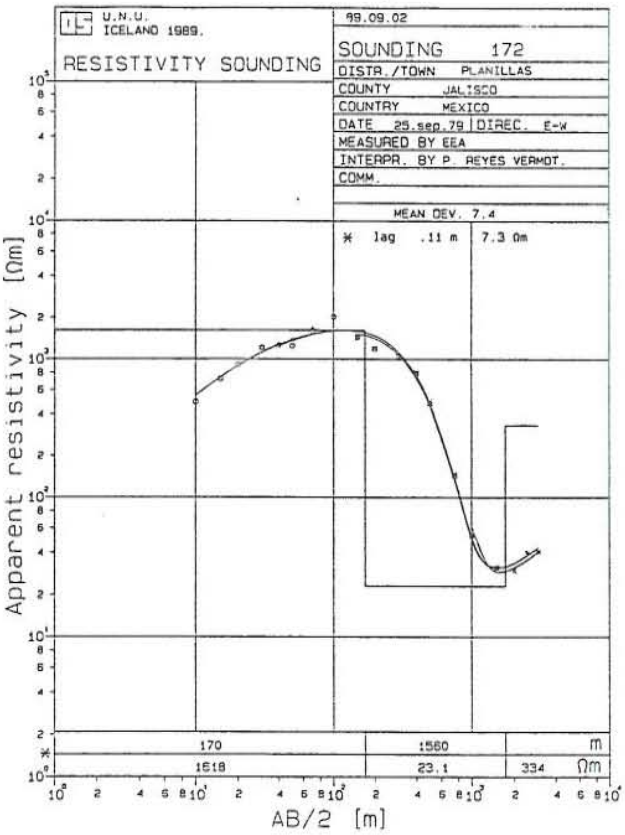
U.N.U.
ICELAND 1989.
RESISTIVITY SOUNDING
89.09.02
SOUNDING 172
DISTR./TOWN PLANILLAS
COUNTY JALISCO
COUNTRY MEXICO
DATE 25.sep.79 | DIREC. E-W
MEASURED BY EEA
INTERPR. BY P. REYES VERMOT.
COMM.
MEAN DEV. 7.4
* lag .11 m 7.3 Ωm
Apparent resistivity [Ωm]
AB/2 [m]
170 1560 m
1618 23.1 334 Ωm

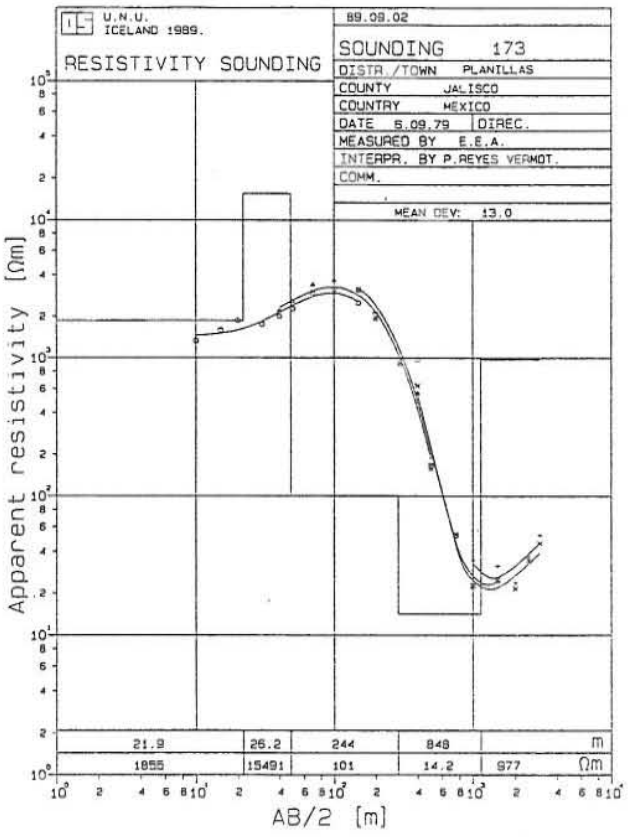
U.N.U.
ICELAND 1989.
RESISTIVITY SOUNDING
89.09.02
SOUNDING 173
DISTR./TOWN PLANILLAS
COUNTY JALISCO
COUNTRY MEXICO
DATE 5.09.79 | DIREC.
MEASURED BY E.E.A.
INTERPR. BY P.REYES VERMOT.
COMM.
MEAN DEV: 13.0
Apparent resistivity [Ωm]
AB/2 [m]
21.9 26.2 244 848 m
1855 15491 101 14.2 977 Ωm

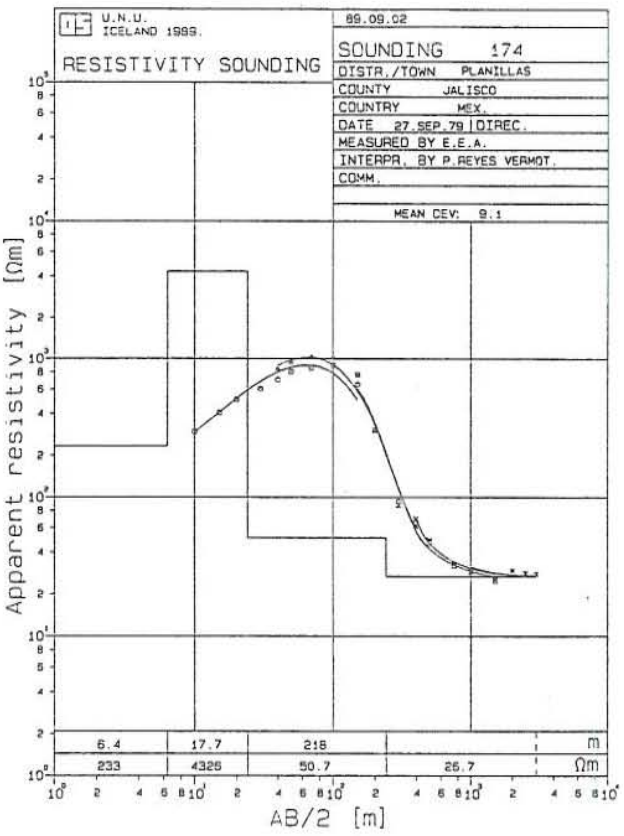
U.N.U.
ICELAND 1989.
RESISTIVITY SOUNDING
89.09.02
SOUNDING 174
DISTR./TOWN PLANILLAS
COUNTY JALISCO
COUNTRY MEX.
DATE 27.SEP.79 | DIREC.
MEASURED BY E.E.A.
INTERPR. BY P.REYES VERMOT.
COMM.
MEAN DEV: 9.1
Apparent resistivity [Ωm]
AB/2 [m]
6.4 17.7 218 m
233 4326 50.7 26.7 Ωm

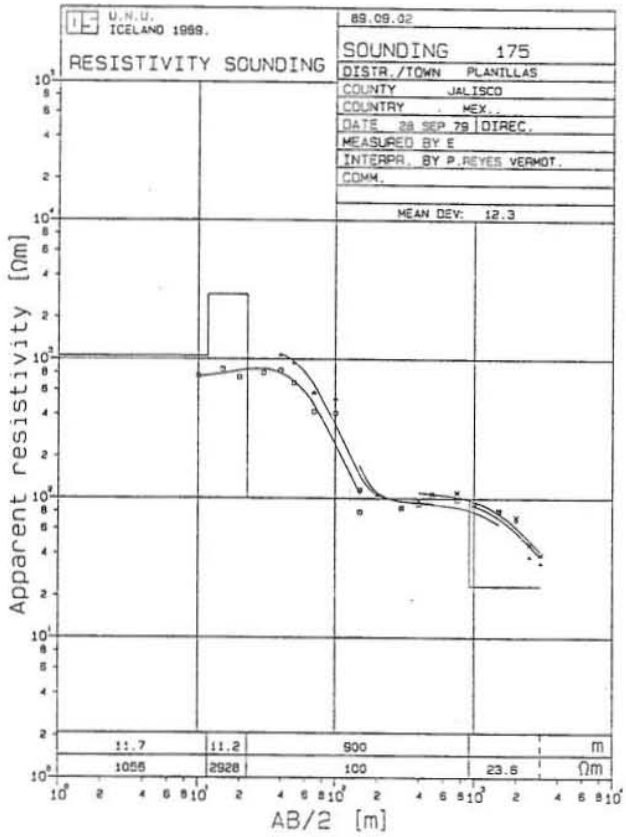
U.N.U.
ICELAND 1989.
RESISTIVITY SOUNDING
89.09.02
SOUNDING 175
DISTR./TOWN PLANILLAS
COUNTY JALISCO
COUNTRY MEX.
DATE 28 SEP 79 DIREC.
MEASURED BY E
INTERPR. BY P.REYES VERMOT.
COMM.
MEAN DEV: 12.3
Apparent resistivity [Ωm]
AB/2 [m]
11.7 | 11.2 | 900 | m
1056 | 2928 | 100 | 23.6 | Ωm

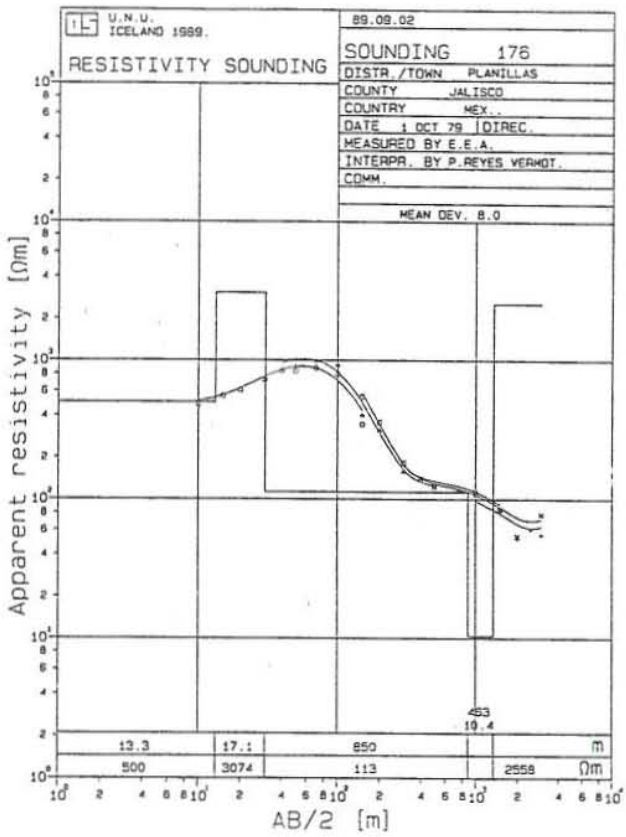
U.N.U.
ICELAND 1989.
RESISTIVITY SOUNDING
89.09.02
SOUNDING 176
DISTR./TOWN PLANILLAS
COUNTY JALISCO
COUNTRY MEX.
DATE 1 OCT 79 DIREC.
MEASURED BY E.E.A.
INTERPR. BY P.REYES VERMOT.
COMM.
MEAN DEV. 8.0
Apparent resistivity [Ωm]
AB/2 [m]
453
10.4
13.3 | 17.1 | 850 | m
500 | 3074 | 113 | 2558 | Ωm

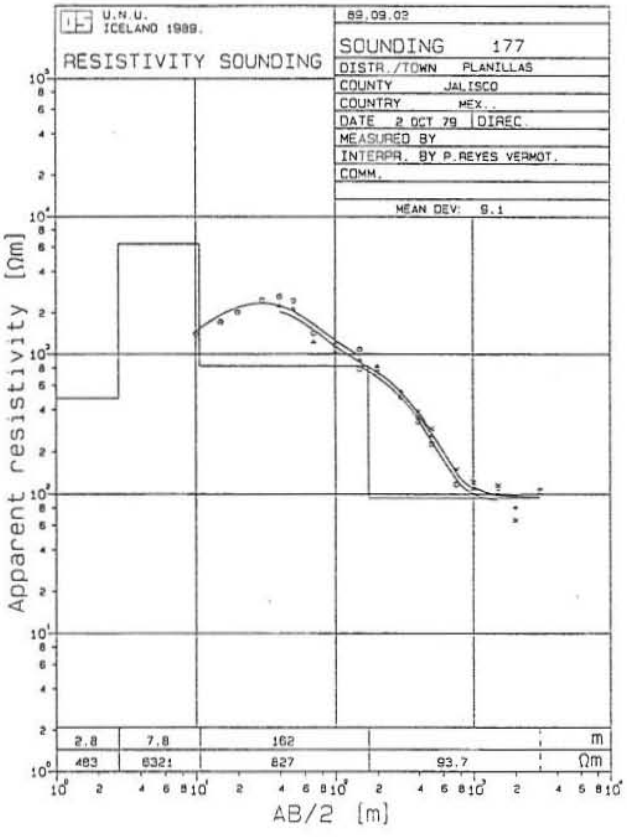
U.N.U.
ICELAND 1989.
RESISTIVITY SOUNDING
89.09.03
SOUNDING 177
DISTR./TOWN PLANILLAS
COUNTY JALISCO
COUNTRY MEX.
DATE 2 OCT 79 DIREC.
MEASURED BY
INTERPR. BY P.REYES VERMOT.
COMM.
MEAN DEV: 9.1
Apparent resistivity [Ωm]
AB/2 [m]
2.8 | 7.8 | 162 | m
483 | 8321 | 827 | 93.7 | Ωm

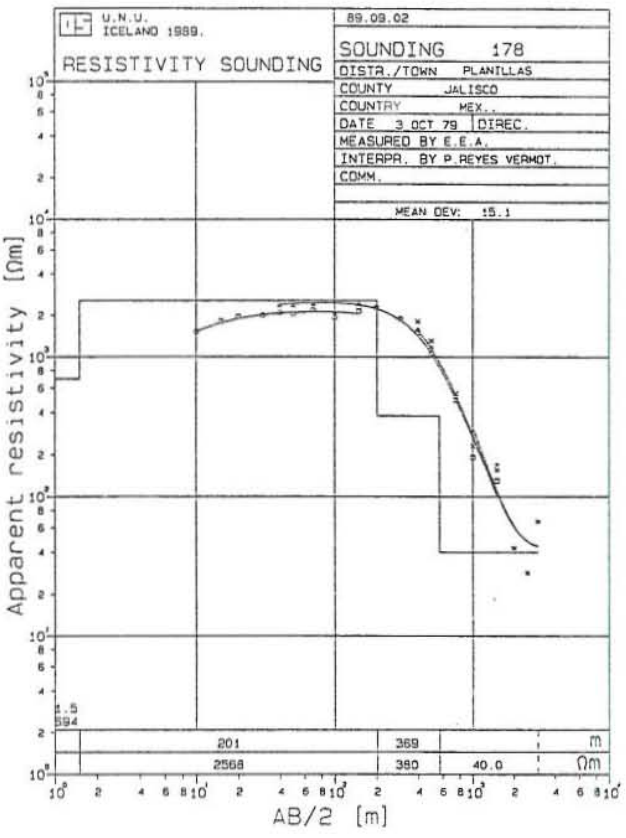
U.N.U.
ICELAND 1989.
RESISTIVITY SOUNDING
89.09.02
SOUNDING 178
DISTR./TOWN PLANILLAS
COUNTY JALISCO
COUNTRY MEX.
DATE 3 OCT 79 DIREC.
MEASURED BY E.E.A.
INTERPR. BY P.REYES VERMOT.
COMM.
MEAN DEV: 15.1
Apparent resistivity [Ωm]
AB/2 [m]
1.5
594
201 | 369 | m
2568 | 380 | 40.0 | Ωm

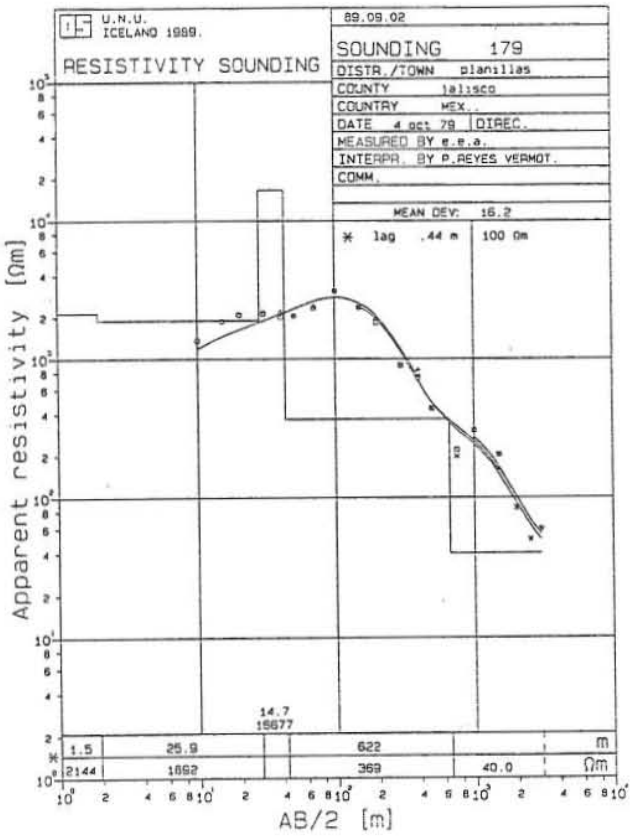
U.N.U.
ICELAND 1989.
RESISTIVITY SOUNDING
89.09.02
SOUNDING 179
DISTR./TOWN planillas
COUNTY Jalisco
COUNTRY MEX.
DATE 4 oct 79 | DIREC.
MEASURED BY e.e.a.
INTERPR. BY P.REYES VERMOT.
COMM.
MEAN DEV: 16.2
lag .44 m 100 Om
14.7
15677
1.5 25.9 622 m
2144 1692 369 40.0 Ωm
Apparent resistivity [Ωm]
AB/2 [m]

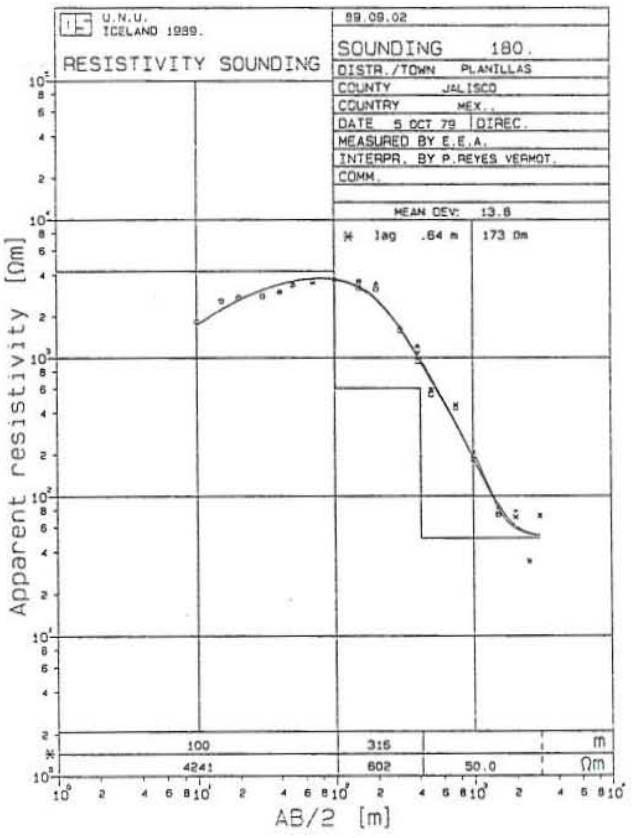
U.N.U.
ICELAND 1989.
RESISTIVITY SOUNDING
89.09.02
SOUNDING 180.
DISTR./TOWN PLANILLAS
COUNTY JALISCO
COUNTRY MEX.
DATE 5 OCT 79 | DIREC.
MEASURED BY E.E.A.
INTERPR. BY P.REYES VERMOT.
COMM.
MEAN DEV: 13.8
lag .64 m 173 Om
100 315 m
4241 602 50.0 Ωm
Apparent resistivity [Ωm]
AB/2 [m]

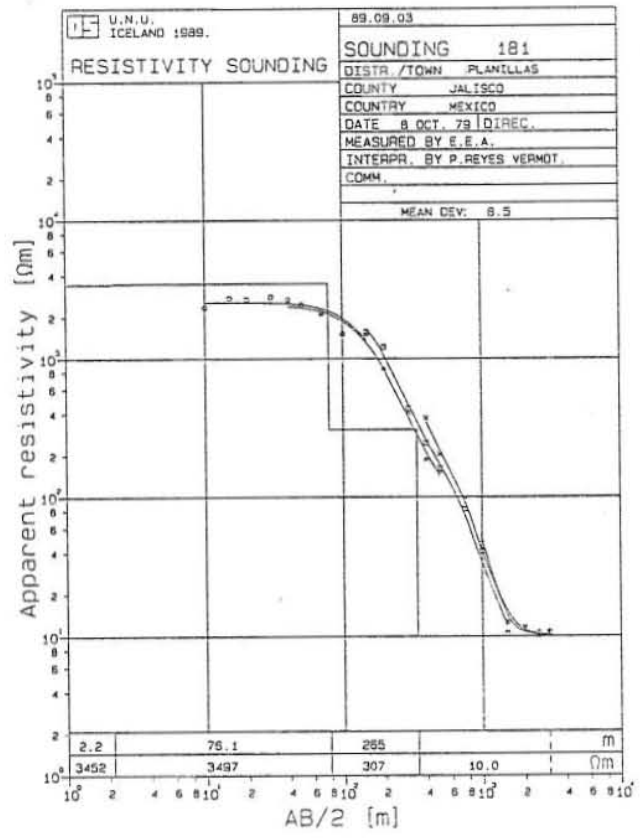
U.N.U.
ICELAND 1989.
RESISTIVITY SOUNDING
89.09.03
SOUNDING 181
DISTR./TOWN PLANILLAS
COUNTY JALISCO
COUNTRY MEXICO
DATE 8 OCT. 79 | DIREC.
MEASURED BY E.E.A.
INTERPR. BY P.REYES VERMOT.
COMM.
MEAN DEV: 8.5
2.2 76.1 265 m
3452 3497 307 10.0 Ωm
Apparent resistivity [Ωm]
AB/2 [m]

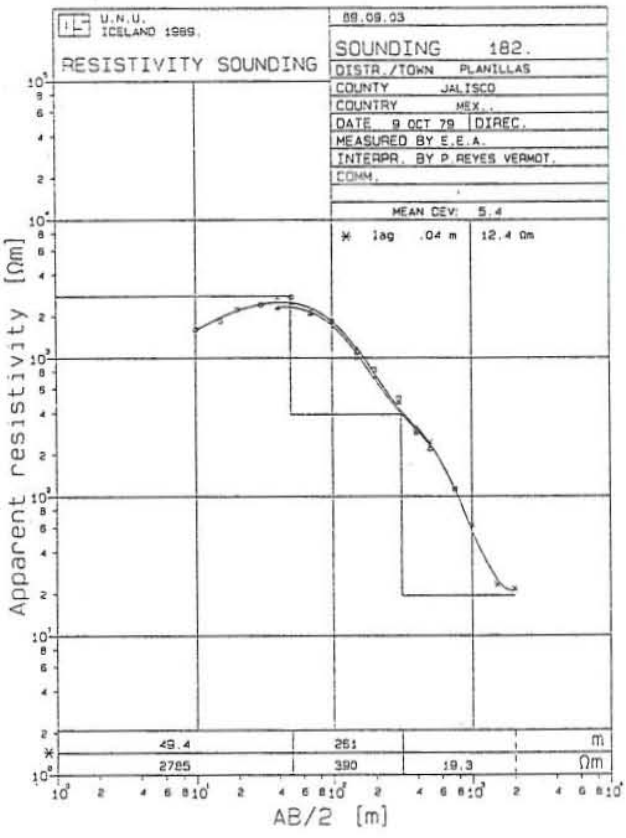
U.N.U.
ICELAND 1989.
RESISTIVITY SOUNDING
89.09.03
SOUNDING 182.
DISTR./TOWN PLANILLAS
COUNTY JALISCO
COUNTRY MEX.
DATE 9 OCT 79 | DIREC.
MEASURED BY E.E.A.
INTERPR. BY P.REYES VERMOT.
COMM.
MEAN DEV: 5.4
lag .04 m 12.4 Om
49.4 251 m
2785 390 19.3 Ωm
Apparent resistivity [Ωm]
AB/2 [m]

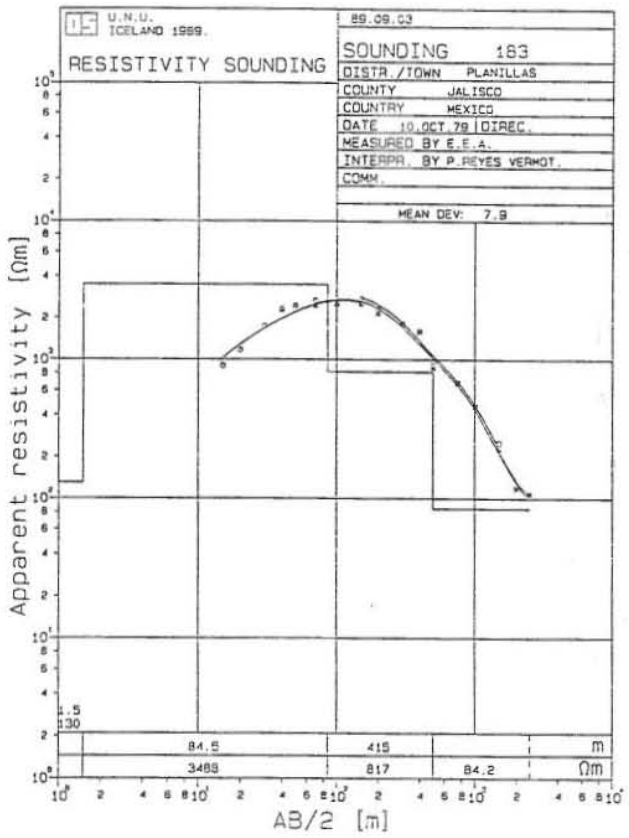
U.N.U.
ICELAND 1989.
RESISTIVITY SOUNDING
89.09.03
SOUNDING 183
DISTR./TOWN PLANILLAS
COUNTY JALISCO
COUNTRY MEXICO
DATE 10.OCT.79 | DIREC.
MEASURED BY E.E.A.
INTERPR. BY P.REYES VERMOT.
COMM.
MEAN DEV: 7.9
Apparent resistivity [Ωm]
AB/2 [m]
1.5
130
84.5 415 m
3469 817 84.2 Ωm

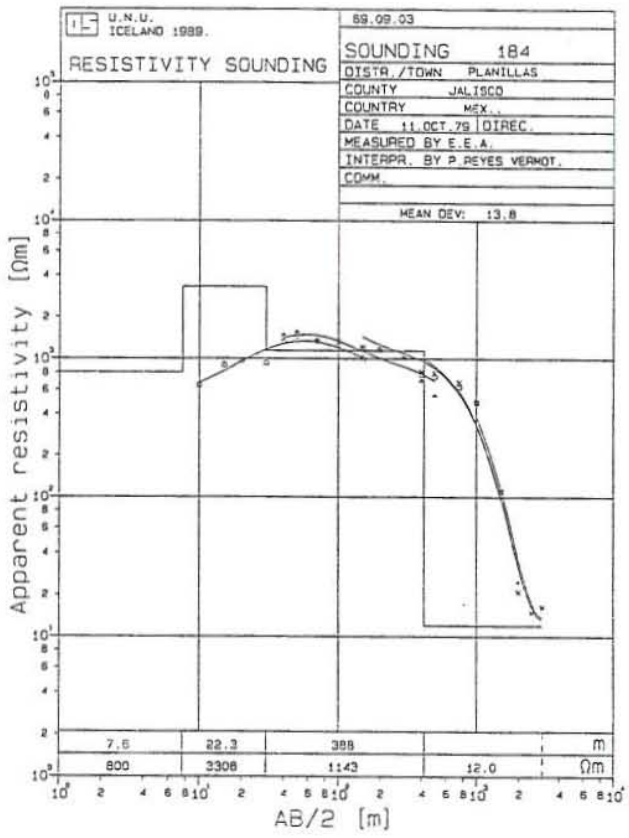
U.N.U.
ICELAND 1989.
RESISTIVITY SOUNDING
89.09.03
SOUNDING 184
DISTR./TOWN PLANILLAS
COUNTY JALISCO
COUNTRY MEX.
DATE 11.OCT.79 | DIREC.
MEASURED BY E.E.A.
INTERPR. BY P.REYES VERMOT.
COMM.
MEAN DEV: 13.8
Apparent resistivity [Ωm]
AB/2 [m]
7.6 22.3 388 m
800 3308 1143 12.0 Ωm

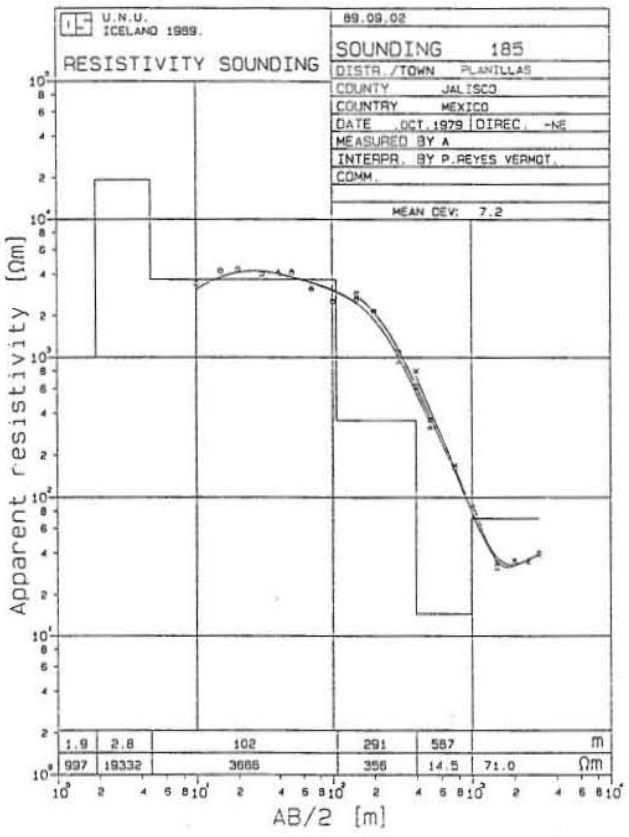
U.N.U.
ICELAND 1989.
RESISTIVITY SOUNDING
89.09.02
SOUNDING 185
DISTR./TOWN PLANILLAS
COUNTY JALISCO
COUNTRY MEXICO
DATE OCT.1979 | DIREC. -NE
MEASURED BY A
INTERPR. BY P.REYES VERMOT.
COMM.
MEAN DEV: 7.2
Apparent resistivity [Ωm]
AB/2 [m]
1.9 2.8 102 291 587 m
997 19332 3666 356 14.5 71.0 Ωm

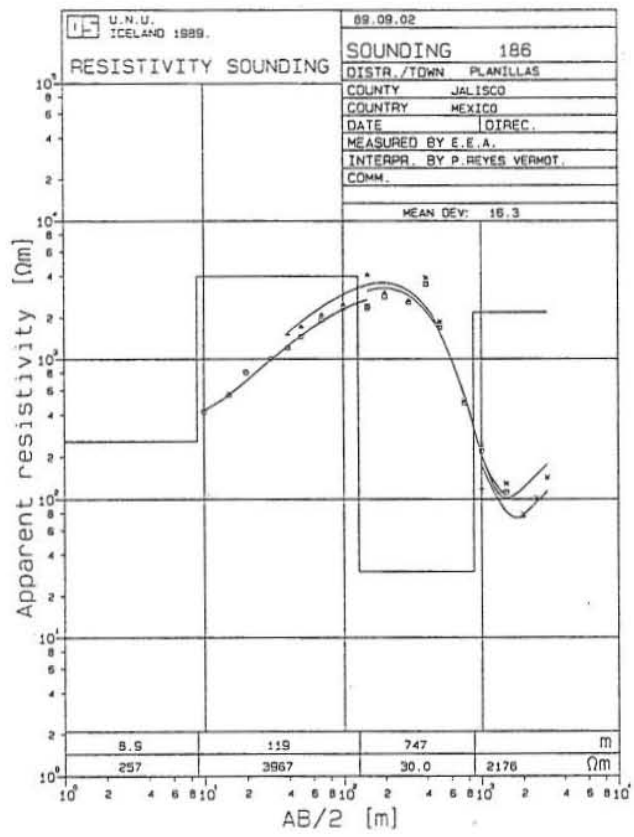
U.N.U.
ICELAND 1989.
RESISTIVITY SOUNDING
89.09.02
SOUNDING 186
DISTR./TOWN PLANILLAS
COUNTY JALISCO
COUNTRY MEXICO
DATE DIREC.
MEASURED BY E.E.A.
INTERPR. BY P.REYES VERMOT.
COMM.
MEAN DEV: 16.3
Apparent resistivity [Ωm]
AB/2 [m]
8.9 119 747 m
257 3967 30.0 2176 Ωm

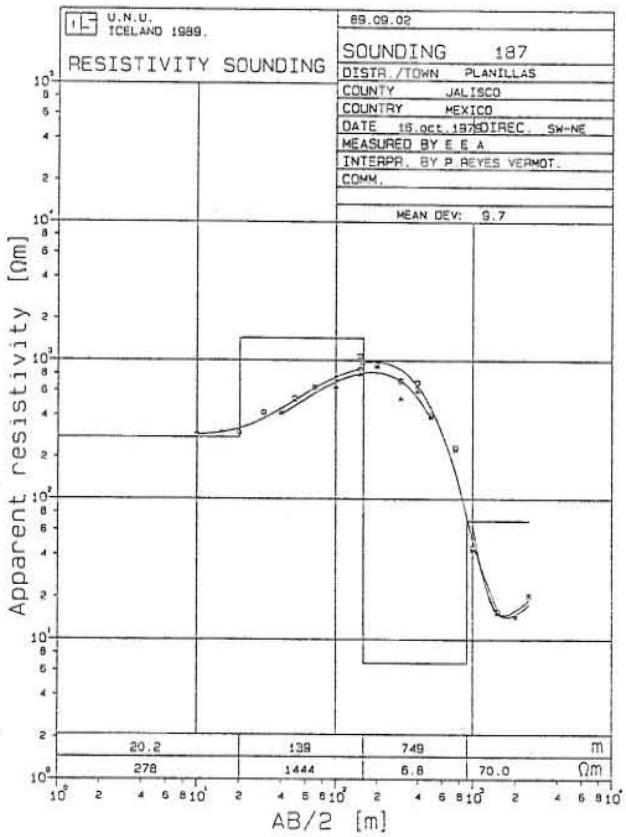
U.N.U.
ICELAND 1989.
RESISTIVITY SOUNDING
89.09.02
SOUNDING 187
DISTR./TOWN PLANILLAS
COUNTY JALISCO
COUNTRY MEXICO
DATE 16.oct.1979 DIREC. SW-NE
MEASURED BY E.E.A.
INTERPR. BY P.REYES VERMOT.
COMM.
MEAN DEV: 9.7
Apparent resistivity [Ωm]
AB/2 [m]
20.2 | 138 | 749 | m
278 | 1444 | 6.8 | 70.0 | Ωm

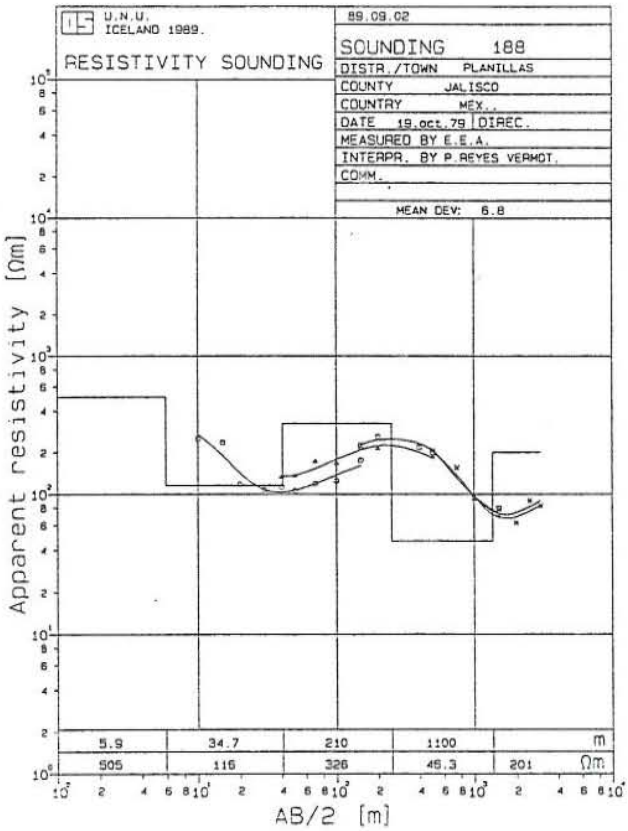
U.N.U.
ICELAND 1989.
RESISTIVITY SOUNDING
89.09.02
SOUNDING 188
DISTR./TOWN PLANILLAS
COUNTY JALISCO
COUNTRY MEX.
DATE 19.oct.79 DIREC.
MEASURED BY E.E.A.
INTERPR. BY P.REYES VERMOT.
COMM.
MEAN DEV: 6.8
Apparent resistivity [Ωm]
AB/2 [m]
5.9 | 34.7 | 210 | 1100 | m
505 | 116 | 326 | 46.3 | 201 | Ωm

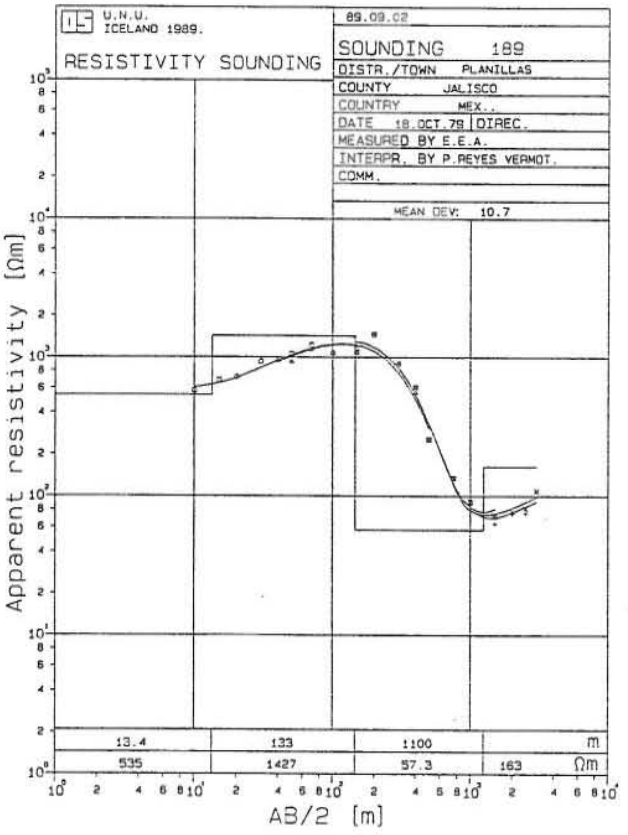
U.N.U.
ICELAND 1989.
RESISTIVITY SOUNDING
89.09.02
SOUNDING 189
DISTR./TOWN PLANILLAS
COUNTY JALISCO
COUNTRY MEX.
DATE 18.OCT.79 DIREC.
MEASURED BY E.E.A.
INTERPR. BY P.REYES VERMOT.
COMM.
MEAN DEV: 10.7
Apparent resistivity [Ωm]
AB/2 [m]
13.4 | 133 | 1100 | m
535 | 1427 | 57.3 | 163 | Ωm

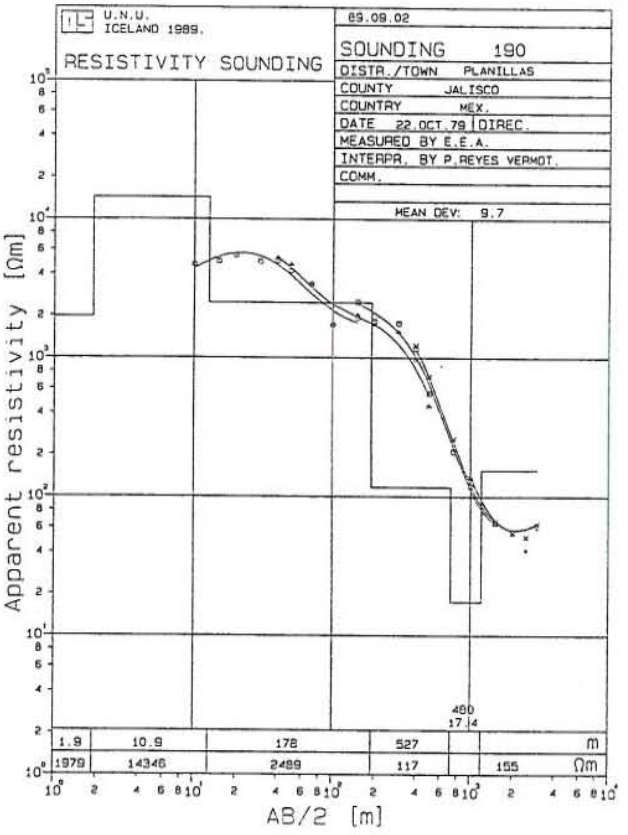
U.N.U.
ICELAND 1989.
RESISTIVITY SOUNDING
89.09.02
SOUNDING 190
DISTR./TOWN PLANILLAS
COUNTY JALISCO
COUNTRY MEX.
DATE 22.OCT.79 DIREC.
MEASURED BY E.E.A.
INTERPR. BY P.REYES VERMOT.
COMM.
MEAN DEV: 9.7
Apparent resistivity [Ωm]
AB/2 [m]
480
17.4
1.9 | 10.9 | 178 | 527 | m
1979 | 14346 | 2489 | 117 | 155 | Ωm

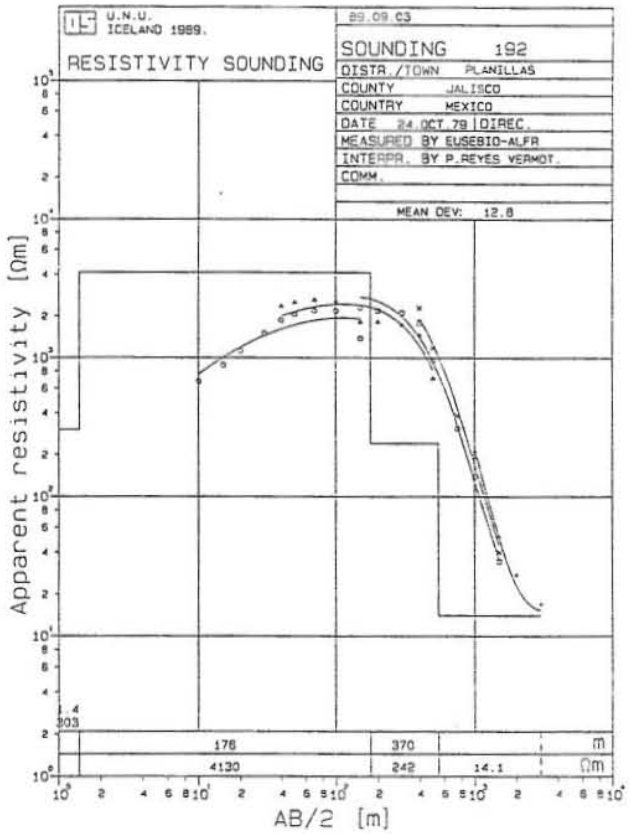
U.N.U.
ICELAND 1989.
RESISTIVITY SOUNDING
89.09.03
SOUNDING 192
DISTR./TOWN PLANILLAS
COUNTY JALISCO
COUNTRY MEXICO
DATE 24.OCT.79 | DIREC.
MEASURED BY EUSEBIO-ALFR
INTERPR. BY P.REYES VERMOT.
COMM.
MEAN DEV: 12.8
Apparent resistivity [Ωm]
AB/2 [m]
1.4 303
176 370 m
4130 242 14.1 Ωm

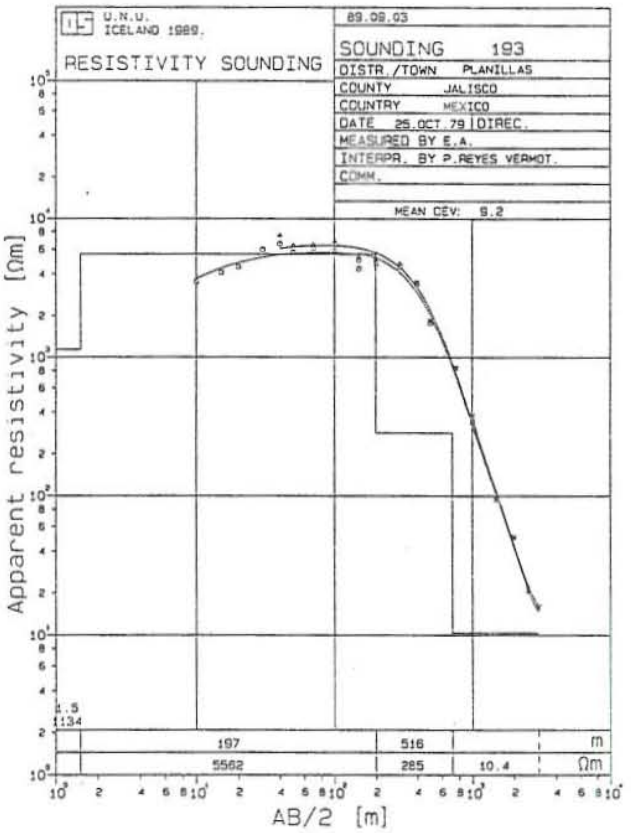
U.N.U.
ICELAND 1989.
RESISTIVITY SOUNDING
89.09.03
SOUNDING 193
DISTR./TOWN PLANILLAS
COUNTY JALISCO
COUNTRY MEXICO
DATE 25.OCT.79 | DIREC.
MEASURED BY E.A.
INTERPR. BY P.REYES VERMOT.
COMM.
MEAN DEV: 9.2
Apparent resistivity [Ωm]
AB/2 [m]
1.5 1134
197 516 m
5562 285 10.4 Ωm

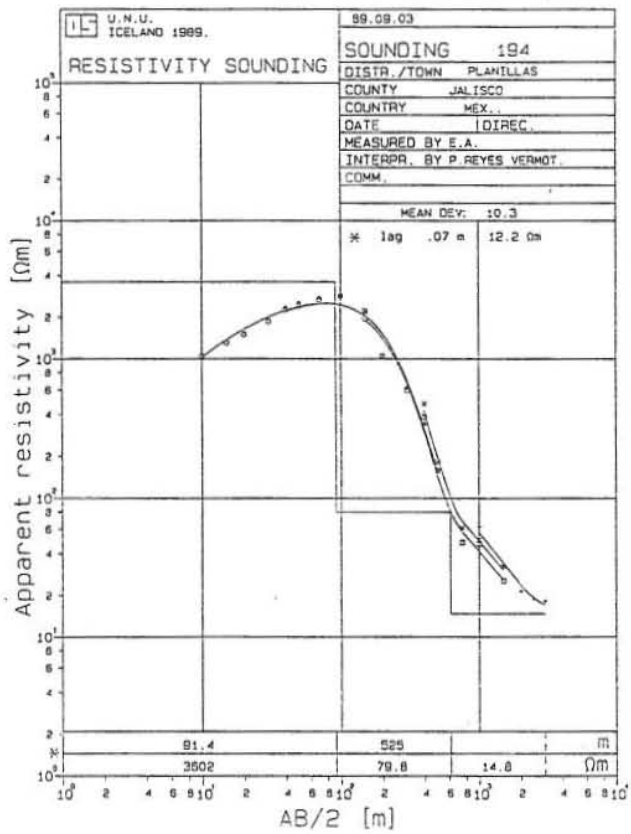
U.N.U.
ICELAND 1989.
RESISTIVITY SOUNDING
89.09.03
SOUNDING 194
DISTR./TOWN PLANILLAS
COUNTY JALISCO
COUNTRY MEX.
DATE | DIREC.
MEASURED BY E.A.
INTERPR. BY P.REYES VERMOT.
COMM.
MEAN DEV: 10.3
* lag .07 m 12.2 Ωm
Apparent resistivity [Ωm]
AB/2 [m]
91.4 525 m
* 3602 79.8 14.8 Ωm

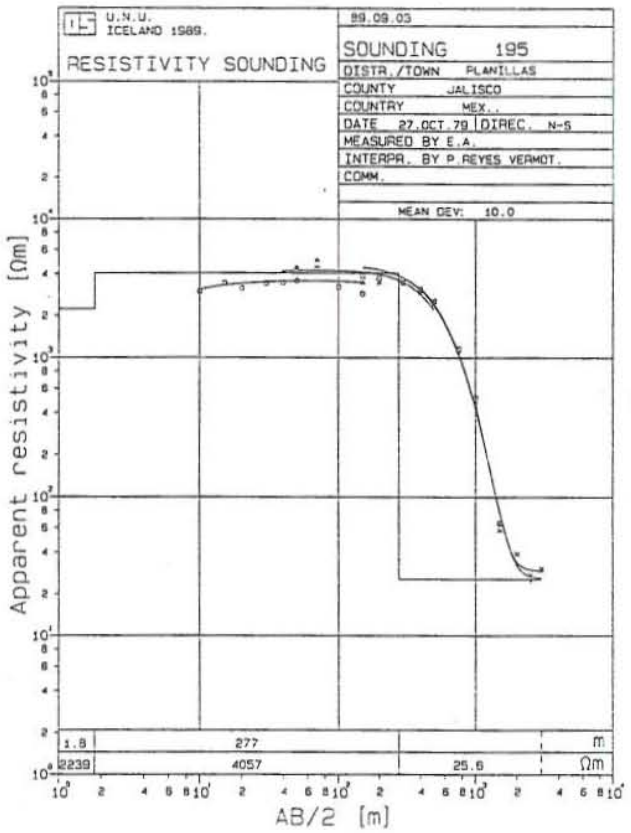
U.N.U.
ICELAND 1989.
RESISTIVITY SOUNDING
89.09.03
SOUNDING 195
DISTR./TOWN PLANILLAS
COUNTY JALISCO
COUNTRY MEX.
DATE 27.OCT.79 | DIREC. N-S
MEASURED BY E.A.
INTERPR. BY P.REYES VERMOT.
COMM.
MEAN DEV: 10.0
Apparent resistivity [Ωm]
AB/2 [m]
1.8 277 m
2239 4057 25.6 Ωm

APPENDIX III

Two dimensional interpretation of Schlumberger soundings. FELIX-program:

Measured apparent resistivity curves (shown as points) and calculated apparent resistivity curves (shown as continuous curves). The two dimensional model is shown in figure 12 in the main report.

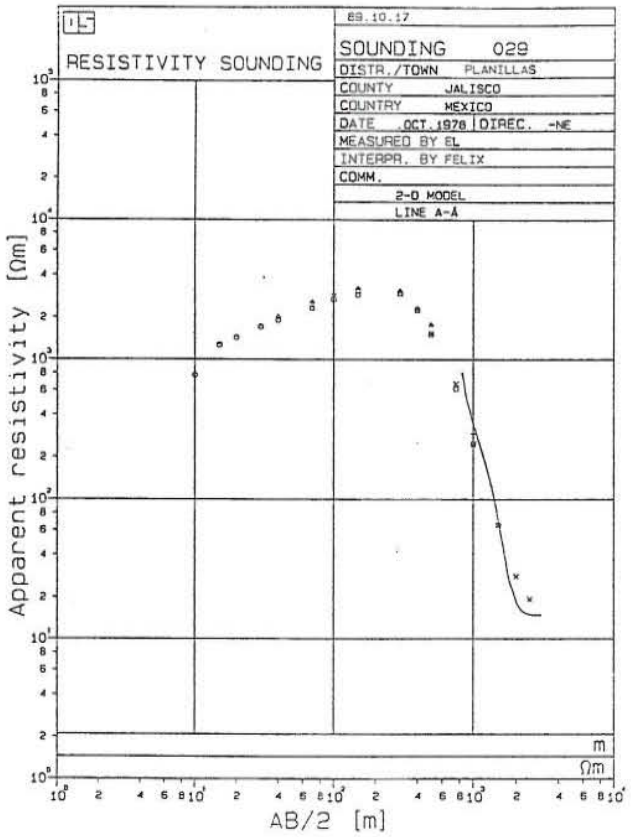
89.10.17
RESISTIVITY SOUNDING
SOUNDING 029
DISTR./TOWN PLANILLAS
COUNTY JALISCO
COUNTRY MEXICO
DATE OCT.1976 DIREC. -NE
MEASURED BY EL
INTERPR. BY FELIX
COMM.
2-D MODEL
LINE A-Á
Apparent resistivity [Ωm]
AB/2 [m]
m
Ωm

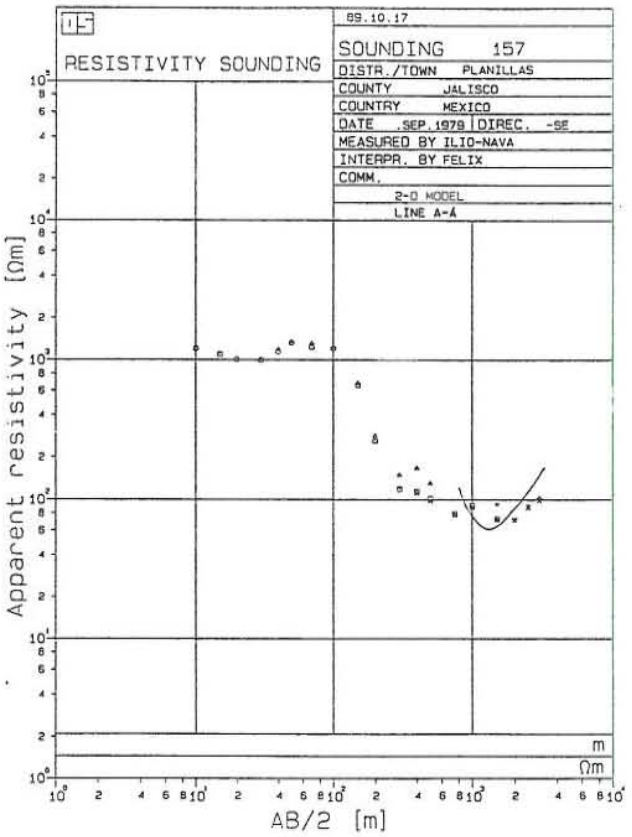
89.10.17
RESISTIVITY SOUNDING
SOUNDING 157
DISTR./TOWN PLANILLAS
COUNTY JALISCO
COUNTRY MEXICO
DATE SEP.1979 DIREC. -SE
MEASURED BY ILIO-NAVA
INTERPR. BY FELIX
COMM.
2-D MODEL
LINE A-Á
Apparent resistivity [Ωm]
AB/2 [m]
m
Ωm

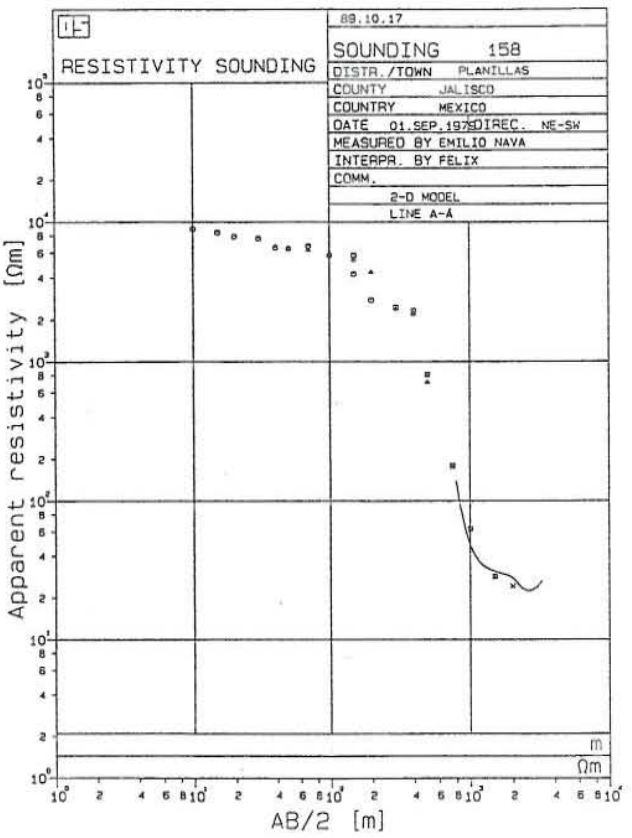
89.10.17
RESISTIVITY SOUNDING
SOUNDING 158
DISTR./TOWN PLANILLAS
COUNTY JALISCO
COUNTRY MEXICO
DATE 01.SEP.1979 DIREC. NE-SW
MEASURED BY EMILIO NAVA
INTERPR. BY FELIX
COMM.
2-D MODEL
LINE A-Á
Apparent resistivity [Ωm]
AB/2 [m]
m
Ωm

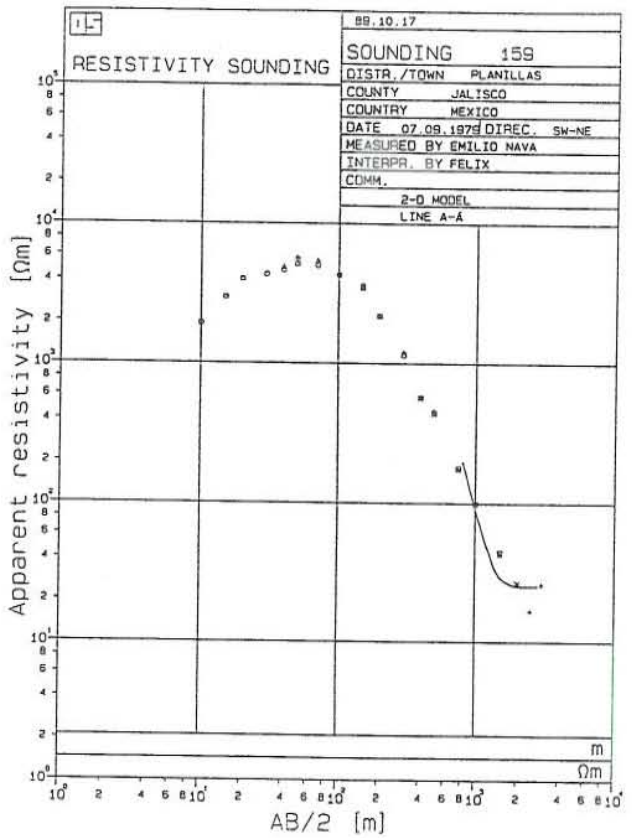
89.10.17
RESISTIVITY SOUNDING
SOUNDING 159
DISTR./TOWN PLANILLAS
COUNTY JALISCO
COUNTRY MEXICO
DATE 07.09.1979 DIREC. SW-NE
MEASURED BY EMILIO NAVA
INTERPR. BY FELIX
COMM.
2-D MODEL
LINE A-Á
Apparent resistivity [Ωm]
AB/2 [m]
m
Ωm

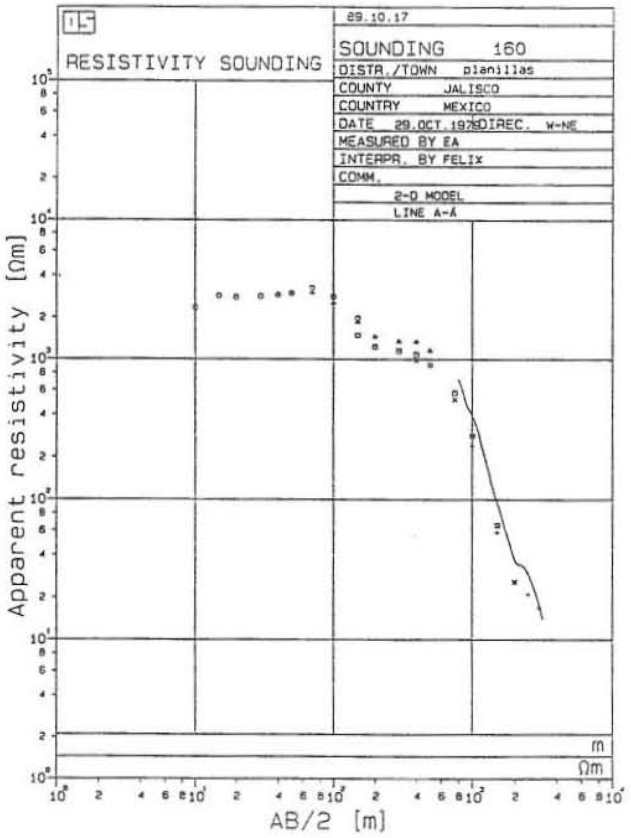
RESISTIVITY SOUNDING
89.10.17
SOUNDING 160
DISTR./TOWN planillas
COUNTY JALISCO
COUNTRY MEXICO
DATE 29.OCT.1979 DIREC. W-NE
MEASURED BY EA
INTERPR. BY FELIX
COMM.
2-D MODEL
LINE A-Á
Apparent resistivity [Ωm]
AB/2 [m]
m
Ωm

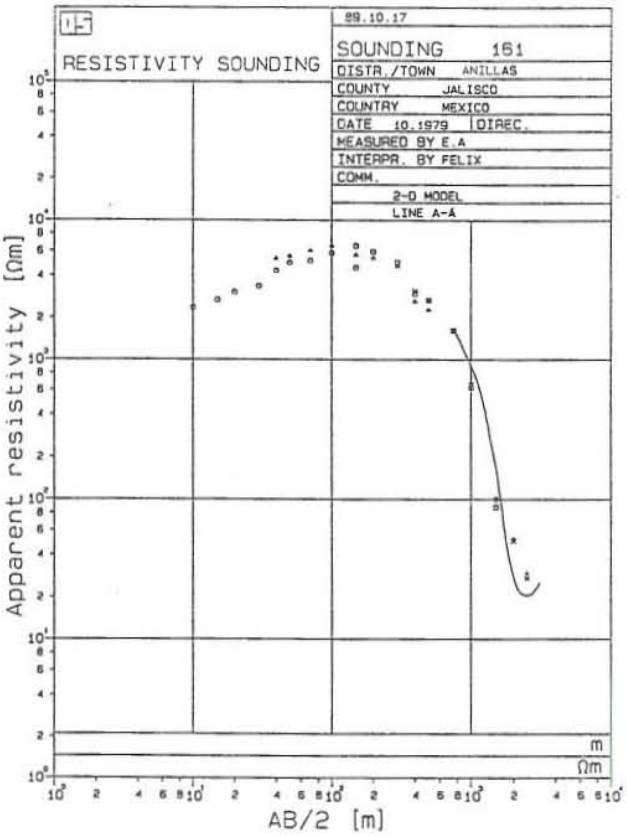
RESISTIVITY SOUNDING
89.10.17
SOUNDING 161
DISTR./TOWN ANILLAS
COUNTY JALISCO
COUNTRY MEXICO
DATE 10.1979 DIREC.
MEASURED BY E.A
INTERPR. BY FELIX
COMM.
2-D MODEL
LINE A-Á
Apparent resistivity [Ωm]
AB/2 [m]
m
Ωm

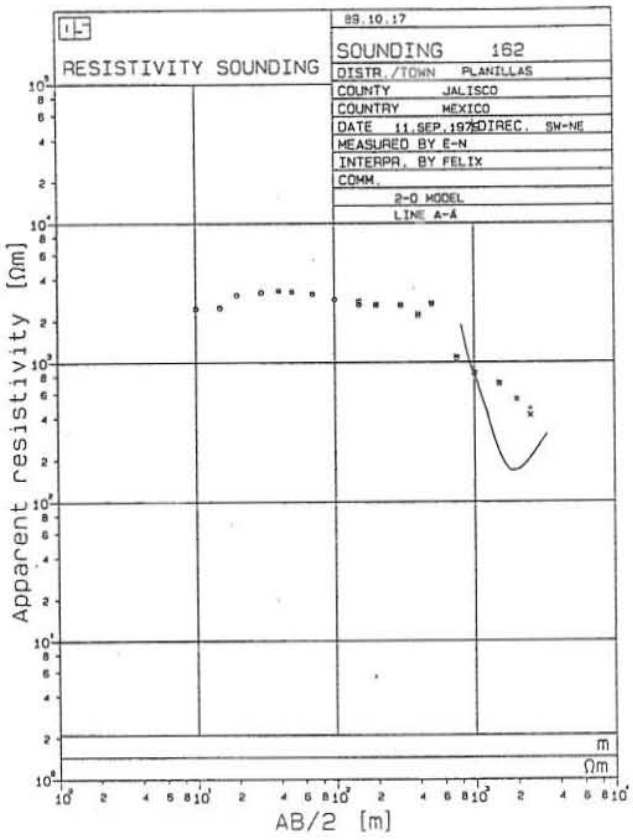
RESISTIVITY SOUNDING
89.10.17
SOUNDING 162
DISTR./TOWN PLANILLAS
COUNTY JALISCO
COUNTRY MEXICO
DATE 11.SEP.1979 DIREC. SW-NE
MEASURED BY E-N
INTERPR. BY FELIX
COMM.
2-D MODEL
LINE A-Á
Apparent resistivity [Ωm]
AB/2 [m]
m
Ωm

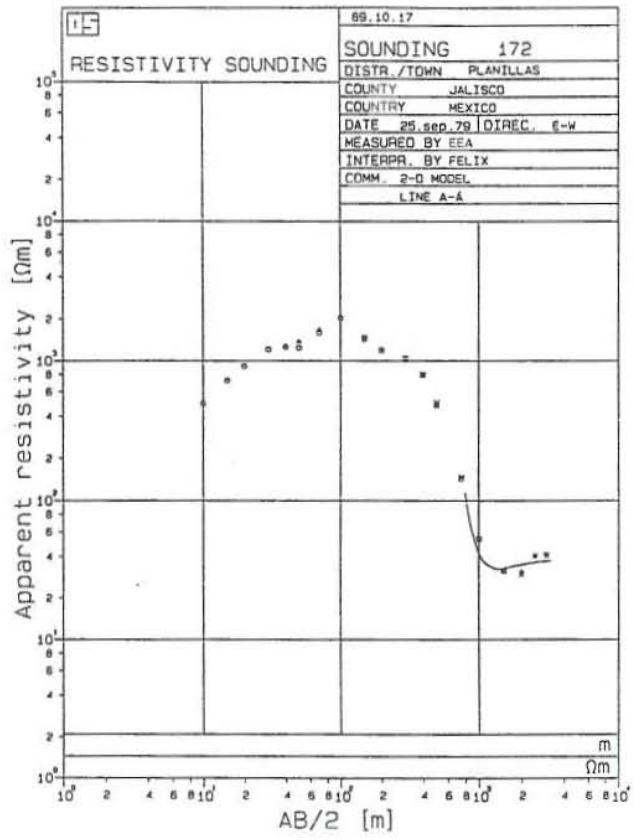
RESISTIVITY SOUNDING
89.10.17
SOUNDING 172
DISTR./TOWN PLANILLAS
COUNTY JALISCO
COUNTRY MEXICO
DATE 25.sep.79 DIREC. E-W
MEASURED BY EEA
INTERPR. BY FELIX
COMM. 2-D MODEL
LINE A-Á
Apparent resistivity [Ωm]
AB/2 [m]
m
Ωm

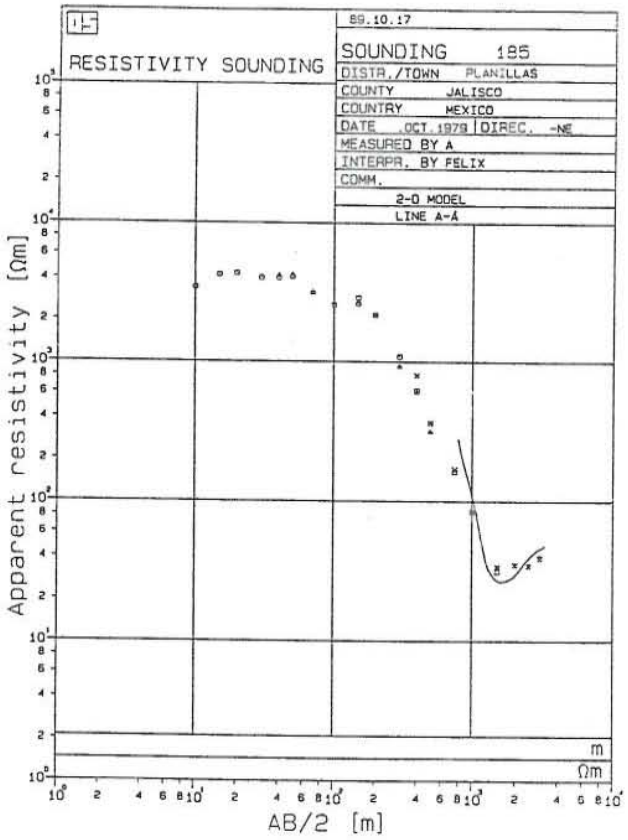
RESISTIVITY SOUNDING
89.10.17
SOUNDING 185
DISTR./TOWN PLANILLAS
COUNTY JALISCO
COUNTRY MEXICO
DATE OCT.1979 DIREC. -NE
MEASURED BY A
INTERPR. BY FELIX
COMM.
2-D MODEL
LINE A-Á
Apparent resistivity [Ωm]
AB/2 [m]
m
Ωm

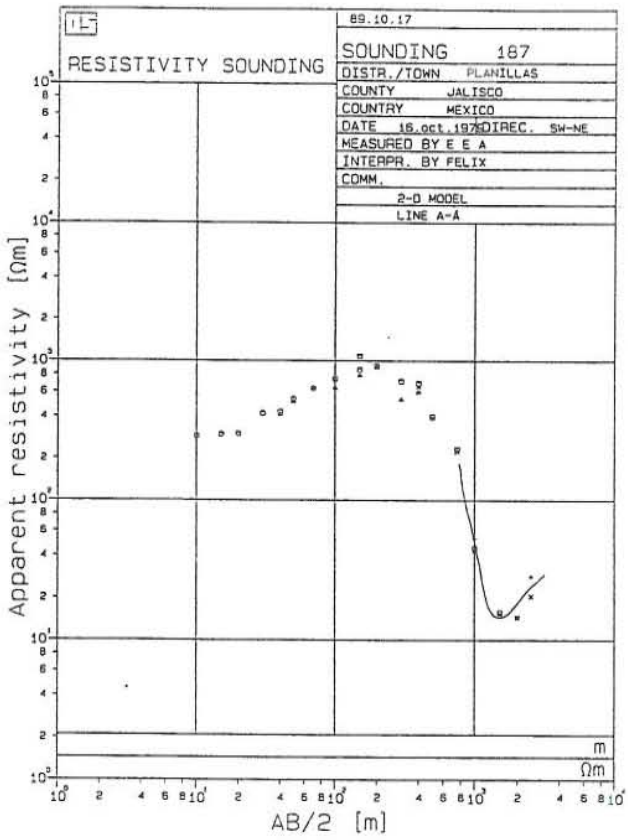
RESISTIVITY SOUNDING
89.10.17
SOUNDING 187
DISTR./TOWN PLANILLAS
COUNTY JALISCO
COUNTRY MEXICO
DATE 16.oct.197? DIREC. SW-NE
MEASURED BY E E A
INTERPR. BY FELIX
COMM.
2-D MODEL
LINE A-Á
Apparent resistivity [Ωm]
AB/2 [m]
m
Ωm